CHALMERS
UNIVERSITY OF TECHNOLOGY

Technical Concept Study of an Electric Motorcycle Powertrain

Product Development and Initial Design

Master's thesis in Mobility Engineering

Carl Thunberg & Herman Wäpling

DEPARTMENT OF INDUSTRIAL AND MATERIAL SCIENCE
CHALMERS UNIVERSITY OF TECHNOLOGY
Gothenburg, Sweden 2023
www.chalmers.se

Master's thesis 2023

Technical Concept Study of an Electric Motorcycle Powertrain

Product Development and Initial Design

CARL THUNBERG & HERMAN WÄPLING

CHALMERS
UNIVERSITY OF TECHNOLOGY

Department of Industrial and Materials Science
Division of Product Development
Chalmers University of Technology
Gothenburg, Sweden 2023

Technical Concept Study of an Electric Motorcycle Powertrain
Product Development and Initial Design
CARL THUNBERG & HERMAN WÄPLING

Supervisor: Henrik Hellström, RGNT Electric AB
Examiner: Magnus Evertsson, Department of Industrial and Materials Science

Master's Thesis 2023
Department of Industrial and Materials
Chalmers University of Technology
SE-412 96 Gothenburg
Telephone +46 31 772 1000

Cover: SICKAS POWERTRAIN.

Typeset in LaTeX
Printed by Chalmers Reproservice
Gothenburg, Sweden 2023

Technical Concept Study of an Electric Motorcycle Powertrain
Product Development and Initial Design
CARL THUNBERG & HERMAN WÄPLING
Department of Industrial and Materials Science
Chalmers University of Technology

Abstract

During the last few years, the market for electric motorcycles has expanded and many new manufacturers have entered the market. The Swedish motorcycle producer RGNT Motorcycle is currently producing A1 motorcycles and would like to investigate powertrain options for a more powerful electric motorcycle with comparable performance to a conventional internal combustion engine motorcycle.

This master's thesis aims to provide RGNT with a technical concept study of an electric motorcycle powertrain based on the principles of product development and mechanical engineering.

The thesis work began with defining the problem, benchmarking competitors and making a functional analysis to gain better knowledge and understanding of electric motorcycle powertrains. The initial design targets and requirements were then set together with engineers at RGNT Motorcycles and compiled into a requirement specification sheet.

Calculations and simulations were made in order to define the specifications of the powertrain based on the performance targets from the requirement specification sheet. Overall dimensions and motorcycle parameters that were needed for evaluations were compiled from existing motorcycles and relevant literature.

Different types of motors, primary- and final transmissions were combined to generate feasible concepts. The concepts were evaluated using elimination and Kesselring matrices as well as packaging models in CAD. The number of concepts was gradually reduced until three remained.

It was concluded that a PMSM (Permanent Magnet Synchronous Machine) axial flux motor with a belt drive would fit the motorcycle best. Initial mechanical design and CAD modelling of the final transmission and swingarm were made.

It was also found that the most suitable powertrain configuration is largely dependent on the motor and inverter used and further work with souring these components was recommended.

Keywords: Electric Motorcycle, Powertrain, Drive Cycle Simulation,
Product Development.

Acknowledgements

This master thesis was carried out by two students with a background in mobility engineering. The project had a time span of 20 weeks, beginning in January of 2023. The thesis has been carried out at Chalmers University of Technology in collaboration with RGNT Motorcycles.

Firstly we would like to thank RGNT Motorcycle for giving us the opportunity to work on this both interesting and challenging project on a topic that lies close to our hearts. We were greeted with open arms and treated as a part of the team from day one.

We would also like to thank Henrik Hellstrom who was our supervisor during the project. His knowledge and support during both good and more challenging times were invaluable.

Lastly, a special thanks to our examiner Magnus Evertsson who shares our passion for all things mechanical and who has supported us through the project.

Carl Thunberg & Herman Wäpling, Gothenburg, June 2023

Contents

List of Figures **xv**

1 Introduction **1**
1.1 Background . . . 1
1.2 Purpose and Goals . . . 1
1.3 Scope . . . 2

2 Theory **3**
2.1 Performance and Drivability . . . 3
2.1.1 Top Speed . . . 3
2.1.2 Acceleration . . . 3
2.1.2.1 Equivalent Inertia Mass . . . 4
2.1.3 Power Demand . . . 5
2.1.4 Resistance Forces . . . 5
2.1.5 Negative Torque . . . 6
2.2 Energy Consumption and Range . . . 7
2.2.1 Quasi-Static Simulation . . . 7
2.2.2 EU Homologation Range Test . . . 7
2.3 Motorcycle Design and Geometry . . . 8
2.3.1 Wheelbase . . . 8
2.3.2 Center of Gravity Location . . . 8
2.3.2.1 CoG Height . . . 8
2.3.2.2 CoG Longitudinal Location . . . 8
2.3.3 Anti Squat . . . 9
2.4 Sound and Noise Emissions . . . 10
2.4.1 A-sounds . . . 10
2.4.2 B-sounds . . . 11
2.5 Complexity . . . 11
2.5.1 Manufacturing and Assembly . . . 11
2.5.2 Production Cost . . . 12
2.5.3 Maintenance and Reliability . . . 13
2.6 Electric Motors . . . 14
2.6.1 Motor Configurations . . . 15
2.6.2 Radial Flux Permanent Magnet Synchronous Motor . . . 15
2.6.3 Axial Flux Permanent Magnet Synchronous Motor . . . 15
2.6.4 Synchronous Reluctance Motor . . . 16

2.7 Transmission . . . 16
2.8 Gear Trains . . . 17
2.8.1 Straight Spur Gears . . . 17
2.8.2 Helical Gears . . . 17
2.8.3 Bevel Gears . . . 18
2.8.4 Planetary Reduction . . . 18
2.8.5 Multistage Transmission . . . 19
2.8.5.1 Conventional Transmissions . . . 19
2.8.5.2 Power-shifting Transmissions . . . 19
2.8.5.3 Continuously Variable Transmissions . . . 20
2.8.5.4 Dual Motor . . . 20
2.9 Belt . . . 20
2.9.1 Synchronous Belts . . . 21
2.9.1.1 Geometry and Function of Tooth Belts . . . 21
2.10 Chain Drives . . . 23
2.10.1 Roller Chain . . . 23
2.10.1.1 The Polygon Problem . . . 23
2.10.2 Silent Chain . . . 24
2.11 Hub Motor . . . 24

3 Methods **25**
3.1 Product Development . . . 25
3.1.1 Problem Definition . . . 25
3.1.2 Benchmarking . . . 25
3.1.3 Function Analysis . . . 25
3.1.4 Requirement Specification . . . 26
3.2 Concept Generation . . . 26
3.2.1 Morphological Matrix . . . 26
3.3 Concept Elimination . . . 26
3.3.1 Elimination Matrix . . . 26
3.3.2 Kesselring Matrix . . . 26
3.4 Motorcycle Design . . . 27
3.4.1 Motorcycle Dimensions and Geometry . . . 27
3.4.2 Calculations and Simlations . . . 27
3.4.3 Mechanical Design and CAD Modelling . . . 27

4 Implementations **29**
4.1 Problem Definition . . . 29
4.1.1 Evaluation of Competing Motorcycles . . . 29
4.1.2 Electric Motorcycles . . . 29
4.1.3 Function Analysis . . . 30
4.1.4 Requirements . . . 30
4.1.5 Environmental, Ethical and Social Aspects . . . 31
4.2 Motorcycle Dimensions and Parameters . . . 31
4.2.1 Wheelbase . . . 31
4.2.2 Mass . . . 32
4.2.3 Center of Gravity location . . . 32

4.2.4 Tyre Sizes . . . 32
4.2.5 Wheel inertia and Equivalent Mass . . . 32
4.3 Resistance Forces . . . 34
4.4 Power and Torque . . . 34
4.4.1 Torque and Power Demand for Acceleration . . . 34
4.4.2 Power Demand for Top Speed . . . 37
4.4.3 Continuous Power Demand . . . 38
4.4.4 Power Demand for Gradients . . . 38
4.4.5 Negative Torque . . . 39
4.5 Range and Battery Capacity . . . 40
4.5.1 Constant Speed Range . . . 40
4.5.2 Range Calculation . . . 40
4.5.3 QSS Toolbox Simulink Model . . . 42
4.5.3.1 The Driving cycle . . . 42
4.5.3.2 Vehicle . . . 42
4.5.3.3 The Wheel . . . 43
4.5.3.4 Transmission . . . 43
4.5.3.5 Motor . . . 44
4.5.3.6 Battery . . . 44
4.5.4 Battery Capacity . . . 45
4.6 Hub Motor Handling Evaluation in BikeSim . . . 45
4.6.1 Onboard Motor Model . . . 45
4.6.1.1 Onboard Motor Unsprung Mass Model . . . 46
4.6.1.2 Rider Mass Model . . . 46
4.6.1.3 Wheel Models . . . 47
4.6.2 Hub Motor Model . . . 47
4.6.2.1 Hub Motor Rear Wheel Mass . . . 47
4.6.2.2 Hub Motor Rear Wheel Inertia . . . 48
4.6.2.3 Hub Motor Sprung Mass model . . . 48
4.6.3 BikeSim Simulations . . . 49
4.6.3.1 Double Lane Change at 140 km/h . . . 49
4.6.3.2 Double Lane Change at 100 km/h . . . 50
4.6.3.3 Sharp Bump Simulation . . . 50
4.7 Electric Motors . . . 51
4.8 Cost Estimation . . . 51
4.8.1 Manufacturing and Reliability - Primary Transmission . . . 52
4.8.1.1 Direct Drive . . . 52
4.8.1.2 Spur Gear Train . . . 52
4.8.1.3 Planetary Gear Train . . . 52
4.8.1.4 Multi Stage Transmission . . . 53
4.8.1.5 Silent Chain . . . 53
4.8.2 Manufacturing and Reliability - Final Drive . . . 53
4.8.2.1 Shaft Drive . . . 54
4.8.2.2 Tooth Belt . . . 56
4.8.2.3 Roller Chain . . . 56
4.8.2.4 Hub Motor . . . 56

4.9 Concept Generation . . . 56
4.9.1 Morphological Matrix . . . 58
4.10 Patent Search . . . 58
4.11 Concept Elimination . . . 58
4.11.1 Elimination Matrix . . . 58
4.11.2 Kesselring Matrix . . . 59
4.12 Mechanical Design . . . 60
4.12.1 CAD Packaging Models . . . 61
4.12.2 Ergonomics . . . 61
4.12.3 Belt Drive Design . . . 63
4.12.3.1 Speed Ratio and Geometrical Limitations . . . 64
4.12.3.2 Swing Arm Length . . . 65
4.12.3.3 Wrap Angles, Span Length and Teeth in Engagement 66
4.12.3.4 Belt Speed . . . 68
4.12.3.5 Belt Tension and Tension System . . . 68
4.12.3.6 Belt Width and Life Span . . . 71
4.12.3.7 Belt Alignment and Pulley Flanges . . . 71
4.12.3.8 Noise and Frequency Calculations . . . 72
4.12.4 Anti Squat and Swing Arm Pivot Location . . . 74

5 Final Concept and Initial Design 77
5.1 Final Concept . . . 77
5.2 Swing Arm and Final Drive . . . 78
5.2.1 Belt Drive . . . 79
5.2.2 Belt tension and alignment . . . 80
5.3 Alternative Concepts . . . 81

6 Conclusions and Recommendations 83
6.1 Performance Target . . . 83
6.2 Motorcycle Dimensions . . . 83
6.3 Multistage Transmission . . . 83
6.4 Motor and Inverter . . . 84
6.5 Heat management and cooling . . . 84
6.6 Mechanical Design . . . 84
6.7 Prototype and Testing . . . 84

Bibliography 85

A Vehicle Requirements I

B Pre Study - Competing Models III
B.1 Pre-study - belt drive layouts . . . V

C Concept generation VII
C.1 Morphological matrix hub motors . . . VIII
C.2 Morphological matrix drive shaft . . . IX
C.3 Morphological matrix tooth belt . . . X

C.4 Morphological matrix chain XI

D Primary transmission complexity analysis XIII
D.1 Spur gear transmission complexity XIV
D.2 Planetary transmission complexity analysis XV
D.3 tooth belt transmission complexity analysis XVI
D.4 Silent chain transmission complexity analysis XVII

E Final drive complexity analysis XIX
E.1 Driveshaft complexity analysis XX
E.2 Tooth belt complexity analysis XXI
E.3 Roller chain complexity analysis XXII
E.4 Hub motor complexity analysis XXIII

F Elimination XXV
F.1 Initial Elimination Matrix XXV
F.2 Initial Elimination Matrix XXVI

List of Figures

2.1 Forces Acting on a Vehicle 4
2.2 World Motorcycle Test Cycle 7
2.3 Shaft Drive Anti Squat 9
2.4 Chain Drive Anti Squat 10
2.5 Electric Motor Efficiency Map 14
2.6 Transmission Types and Efficiency 16
2.7 Planetary Gear Set 18
2.8 Harley Davidson Belt Drive 21
2.9 Stress in Tooth Belts 22
2.10 The Polygon Problem 23
2.11 BMW Transfer Case 24

4.1 System Function Model 30
4.2 Motorcycles and Their Wheelbases 31
4.3 Front Tyre Weights 33
4.4 Rear Tyre Weights 33
4.5 Free Body Diagram of an Acceleration Motorcycle 35
4.6 Power and Torque 36
4.7 Power versus 0-100 Time 37
4.8 Motor Examples with Gearing and Resulting 0-100 Time 37
4.9 Power Demand Contributions 38
4.10 QSS-Tb BEV model 42
4.11 Motor Efficiency Map 44
4.12 BikeSim Sports Bike 45
4.13 BikeSim Onboard Motor Model 46
4.14 BikeSim Rider Model 47
4.15 Masses of Bodies for different BikeSim Models 48
4.16 BikeSim Graphics of DLC Simulation 49
4.17 Required Steering Angle for a DLC at 140km/h 49
4.18 Required Steering Angle and Steering Torque for a DLC at 110 km/h 50
4.19 Vertical Acceleration from Small Sharp Bump Simulation 50
4.20 Motor Types 57
4.21 Primary Transmission Configurations 57
4.22 Final Drive Configurations 57
4.23 Initial Packaging Models 61
4.24 Rider Posture 62

4.25 Synchronous Belt Geometry 63
4.26 Belt Pitch Comparison 64
4.27 Belt Wrap Angles and Span Length 66
4.28 Belt Speed 68
4.29 Belt Tension Systems 68
4.30 Belt Forces 69
4.31 Belt Meshing Frequency 72
4.32 Belt Harmonics 73
4.33 Motorcycle Kinematic Setup 75
4.34 Anti-squat versus Suspension Travel 75

5.1 Motor, Swing Arm and Final Drive 78
5.2 Swing Arm and Final Drive 79
5.3 Belt Drive Design 79
5.4 Rear Axle and Belt Tension System 80
5.5 Planetary Reduction 81
5.6 Spur Gears with Idler 82

1
Introduction

During the last few years, the market for electric motorcycles has expanded and many new manufacturers have entered the market. To stay relevant, companies must constantly improve the performance of their products. The electric motorcycle market is currently in a state where an electric motorcycle with comparable performance to an internal combustion engine (ICE) motorcycle is desired. This master's thesis within mobility engineering will strive to deliver a high-performing electric motorcycle powertrain concept to meet the manufacturer's performance goals.

1.1 Background

RGNT is a Swedish motorcycle manufacturer that produces electric motorcycles in Kungsbacka. They are currently making and selling modern retro A1 motorcycles (equivalent to 125cc ICE motorcycles). The company would like to investigate a new electric powertrain. This thesis will therefore explore the possibilities for a new A3 (unrestricted) drive train. The focus will be to propose concepts and evaluate different powertrain layouts and their overall specifications to best meet the requirements.

1.2 Purpose and Goals

The powertrain will be designed using data-driven product development methods and performance simulations. The goal of this thesis is to provide RGNT with specifications, a layout, and an initial design of a powertrain concept that will meet the design targets. Requirements and performance goals for this concept will be defined together with RGNT Motorcycles during the initial stage of the thesis. Some of the requirements will be:

- Range
- Top speed
- Acceleration
- NVH, (Noise, Vibrations and Harshness), Perceived quality
- Maintenance/reliability
- Vehicle dynamics and handling
- Brand identity
- DFMA, (Design For Manufacturing and Assembly)
- Cost
- Sustainability

1.3 Scope

The scope will be to evaluate different powertrain configurations on a conceptual level. The work will result in an initial design concept rather than a finalized design. The project will focus on the mechanical aspects of the drive train and not the electrical parts such as power electronics and battery layout/design. The properties of the battery and power electronics that are relevant for evaluating the powertrain will be used. The required battery capacity will be investigated.

2
Theory

2.1 Performance and Drivability

Three commonly used performance quantifiers for determining the drivability of a vehicle are; top speed, maximum uphill gradient in which the vehicle can maintain the speed limit and acceleration, often measured from zero to 100 km/h according to Guzzella, L and Sciarretta A, [1]. With the relatively high power-to-weight ratio of an A3 motorcycle compared to other vehicles, the performance quantifier of a maximum gradient in which the motorcycle can maintain the speed limit is unnecessary. Therefore the top speed and acceleration are better performance quantifiers for a motorcycle.

2.1.1 Top Speed

The top speed of a vehicle is largely determined by the available power and the aerodynamic resistance. Top speed on a flat surface can be approximated by solving the following power balance equation

$$P_{max} \approx \frac{\rho A C_d v_{max}^3}{2} \tag{2.1}$$

according to [1], since at higher speeds, the air resistance is typically one order of magnitude greater than the rolling resistance.

2.1.2 Acceleration

Acceleration performance is the most important drivability quantifier. This can be calculated using Newton's second law of motion

$$\sum F = ma \tag{2.2}$$

A simple model of the forces acting on a road vehicle can be seen in figure 2.1. The acceleration force can be calculated using equation 2.3 and the acceleration can then be calculated by dividing the force by the mass of the vehicle.

$$F_{acceleration} = F_{tractive} - F_{Drag} - F_{Roll} - F_{Grad} \tag{2.3}$$

$$F_{Acceleration} = m_{vehicle}\, a \tag{2.4}$$

The acceleration of the vehicle can now be calculated by rearranging equation 2.4

$$a = \frac{F_{Acceleration}}{m} \tag{2.5}$$

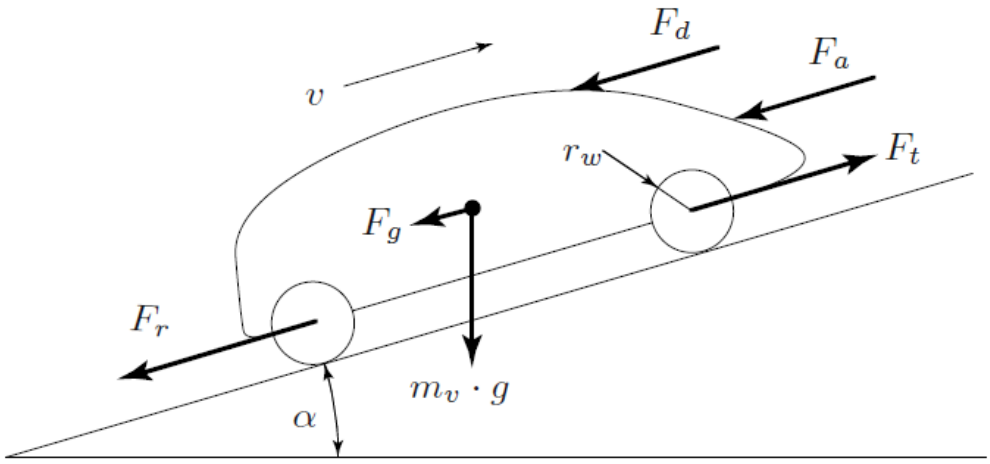

Figure 2.1: A model of the forces acting on a vehicle

2.1.2.1 Equivalent Inertia Mass

When accelerating a motorcycle the effect of rotational inertia of all rotating parts will resist the acceleration. For an ICE motorcycle, the rotating parts will be the wheels and all rotating parts of the engine and transmission. This resisting torque can be calculated for each part as

$$T = \dot{\omega} I \tag{2.6}$$

Where $\dot{\omega}$ is the rotational acceleration of the part and I is the moment of inertia which is a physical property of the part. If all the accelerations and moments of inertia are known these torques can then be calculated for all the rotating parts and summed up into one. Cossalter, [2] describes a simpler way of doing this referred to as equivalent inertia mass, where the effect of rotating inertia is added to the vehicle's mass.

$$m_{eqvivalent} = m_{vehicle} + m_{inertia} \tag{2.7}$$

The mass contribution of the rotating inertia $m_{inertia}$ of the front and rear wheels can be calculated as

$$m_{inertia} = I_f \tau_f^2 + I_r \tau_r^2 \tag{2.8}$$

Where I_f and I_r are the moments of inertia of the front and rear wheel respectively. τ_f and τ_r are the speed ratios for the front and rear wheels. The speed ratio is defined as the relation between the speed of the bike V and the rotational speed of the wheel ω_{wheel}.

$$\tau_{wheel} = \frac{\omega_{wheel}}{V} = \frac{1}{R_{wheel}} \tag{2.9}$$

Likewise, the rotating parts of the drivetrain's contribution to $m_{inertia}$ can be calculated using the same method.
The acceleration of the vehicle can now be described with the added influence of the rotating components's moment of inertia

$$F_{Acceleration} = m_{eqvivalent}\, a \tag{2.10}$$

Equation 2.5 now becomes

$$a = \frac{F_{acceleration}}{m_{eqvivalent}} \tag{2.11}$$

2.1.3 Power Demand

An important specification of a drivetrain is the power output, which can be divided into peak- and continuous power demand. The peak can be calculated from top speed or acceleration requirements. The power that propels a vehicle can be calculated by multiplying the tractive force by the speed of the vehicle as

$$P_{out} = F_{tractive} V_{vehicle} \tag{2.12}$$

Where the tractive force can be calculated by dividing the torque on the driven wheel by the wheel radius

$$F_{tractive} = \frac{T_{wheel}}{R_{wheel}} \tag{2.13}$$

Another way of calculating the power on the rear wheel is

$$P_{wheel} = \omega_{wheel} T_{wheel} \tag{2.14}$$

As described earlier the acceleration of a vehicle is largely determined by the mass of the vehicle and the magnitude of the resistance forces compared to the tractive force. Equation 2.12 shows that for any given speed the higher the force the higher the power output. By equation 2.14 it can be seen that the power output can be limited by the available traction since the maximum torque that the tyre can produce is limited by grip.

2.1.4 Resistance Forces

Resistance forces are the forces that counteract the driving force $F_{tractive}$ and are composed of air resistance F_{Drag}, rolling resistance F_{Roll} and gradients i.e driving up or down slopes. The gradient force will switch signs during a downhill slope and contribute to the driving force.
The aerodynamic drag is usually the largest contribution to the resistance forces and is proportional to the square of the velocity. The physical properties of the motorcycle and rider system that govern the magnitude of the drag force are the

frontal area A_f, and the coefficient of drag C_d which has to be determined through wind tunnel tests or by computational fluid dynamics simulation (CFD). Another method for determining the coefficient of drag is described in EU regulation [3]. This method is described in the implementation chapter of this report. The last parameter that affects the drag force is the air density ρ_{air}. The equation for aerodynamic drag is

$$F_{Aero} = \frac{C_{drag}\, A_{frontal}\, \rho_{air}\, v^2}{2} \tag{2.15}$$

The rolling resistance F_{Roll} is a torque loss due to deformation on the tyre but is often expressed as a force that counteracts the tractive force according to Jacobsson [4] where the magnitude of this force is calculated by multiplying a coefficient of rolling resistance c_{roll} by the vertical or normal force acting on the tyre as equation 2.16. The coefficient of rolling resistance depends on many things such as tyre pressure, slip angle, road surface and vehicle speed. The EU regulation [3] has a standardised method of determining the c_{roll} for a motorcycle and this is described in the implementation part of this report.

$$F_{Roll} = C_{roll}\, m_{vehicle}\, g \tag{2.16}$$

Uphill gradients will naturally cause a resistance force due to the influence of gravity and its magnitude will depend on the mass of the vehicle and the inclination of the slope and can be calculated by equation 2.17. Downhill gradients will likewise assist the tractive force. When driving up or down gradients the vertical load on the tyres will change. Equation 2.16 therefore needs to be modified to equation 2.18

$$F_{Grad} = m_{vehicle}\, g\, sin(\alpha) \tag{2.17}$$

$$F_{Roll} = c_{roll}\, m_{vehicle}\, g \cos(\alpha) \tag{2.18}$$

$$F_{Acceleration} = m_{vehicle}\, a \tag{2.19}$$

Or with the added influence of rotating components inertia

$$F_{Acceleration} = m_{eqvivalent}\, a \tag{2.20}$$

2.1.5 Negative Torque

An electric drivetrain can be designed with the ability to charge the battery using the motor as a generator during braking. This is commonly called regenerative braking. An electric powertrain with this feature must therefore be able to handle negative torque. The maximum negative torque the rear tyre can handle is limited by the grip it can generate. The grip is a function of many things but the most important factor is the normal load acting on the tyre. The forward load transfer that occurs during braking will reduce the normal load in the rear and thereby reduce the grip in the rear. The magnitude of the forward load transfer depends on the location of the CoG, the mass of the bike, and the braking force.

2.2 Energy Consumption and Range

The energy consumption and battery capacity will determine the range of an electric vehicle. The battery capacity needed to achieve a given range can be approximated by calculating the theoretical energy consumption for different riding scenarios and driving cycles.

2.2.1 Quasi-Static Simulation

A quasi-static simulation (QSS) approach can be used for simulating vehicle energy consumption. The QSS approach uses an inverted cause-and-effect relationship compared to what is usually used when calculating dynamic systems, where a resulting acceleration and speed are calculated from a given force. On the other hand, a QSS-based method calculates the force that is required to achieve a given acceleration and speed [1]. The vehicle is assumed to have constant speed, acceleration and gradient in a small time period. The speed for each time step and thus the acceleration is predefined in a so-called driving cycle, which can also include gradients. The energy consumption for a given driving cycle can be calculated by summing the energy consumption for all time steps in the driving cycle.

2.2.2 EU Homologation Range Test

A motorcycle must be approved according to EU regulations in a process called homologation to be sold to and used by the public in the EU. The EU regulation document [3] describes the standardised EU methods for determining the range and other performance specifications of electric motorcycles sold in the EU. The range test is done using the World Motorcycle Test Cycle (WMTC). According to [3] a motorcycle with a top speed of 140 km/h or greater shall use a combination of WMTC parts shown in figure 2.2.

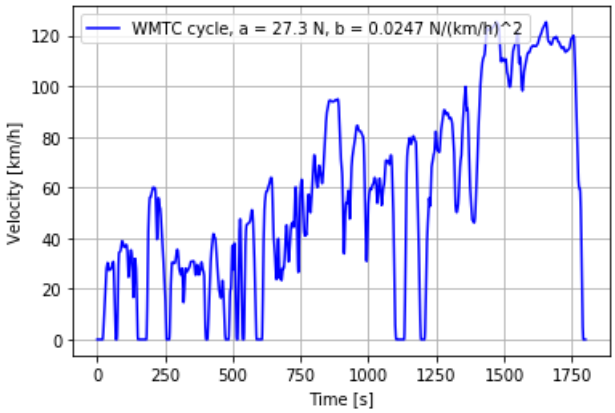

Figure 2.2: WMTC combination for a motorcycle with a top speed greater than 140 km/h

2.3 Motorcycle Design and Geometry

The most suitable powertrain for a given motorcycle is highly dependent on the type and size of the motorcycle. Therefore some physical dimensions and properties of the motorcycle must be known in order to properly evaluate the powertrain.

2.3.1 Wheelbase

The wheelbase (WB) is defined as the centre-to-centre distance between the wheels. A longer WB tends to make the bike more stable but requires more effort to turn. Foyale [5] describes three reasons for this. Firstly a bike with a longer WB needs more steering angle to go around a turn with a given radius. Secondly, for a given sideways deflection of the rear wheel, the displacement angle of the rear wheel relative to the direction of travel will be less for a bike with a longer WB, thus improving directional stability. Lastly, a longer WB gives less longitudinal weight transfer for a given centre of gravity height. The Inertial effects in both roll and yaw are also increased with a longer WB making the bike more sluggish and stable. On trials motorcycles, where low-speed manoeuvrability is important, short wheelbases of around 1250 mm are common while on touring motorcycles, where high-speed stability is desired, wheelbases of more than 1500 mm are not uncommon.

2.3.2 Center of Gravity Location

Where the combined centre of gravity (CoG) of the bike and rider system is located is an important factor that affects the bike's handling and performance. For this project, the location of the CoG will be used to evaluate the performance of different power train concepts and layouts.

2.3.2.1 CoG Height

The height of the CoG will largely determine how much lean angle is required to take a corner with a given centripetal acceleration i.e. radius and speed. The longitudinal weight transfer during braking and accelerating is also determined largely by the height of the CoG relative to the WB. The combined CoG height is usually around 50% of the WB for most bikes [5]. If the CoG is 50% of the WB an acceleration of more than $g = 9.81\ \frac{m}{s^2}$ will result in a wheelie or stoppie. A higher CoG height will also increase the roll inertia making the bike feel heavier.

2.3.2.2 CoG Longitudinal Location

The longitudinal location, or where the CoG is located front to back in the wheelbase, is commonly described as a percentage of weight bias front to rear. Some bikes such as cruisers and motocross machines often have a slight rearward bias of a few per cent. Other types of bikes such as sport bikes tend to have a slight frontward bias according to Bradley [6].

2.3.3 Anti Squat

The following section is based on information found in chapter 9 of [5] regarding motorcycle squat behaviour. The geometry of the rear suspension and final drive can result in a force acting in the z-direction on the sprung mass. This effect is called anti- or pro-squat which lifts (anti-squat) or pulls down (pro-squat) on the sprung mass. Figure 2.3 shows the resulting force, called R, for a shaft-driven motorcycle that acts on the sprung mass. It can be seen that a component of this resultant is acting upwards, in effect lifting the sprung mass and extending the rear suspension. This effect is called anti-squat which counteracts the expected pitching motion caused by forward acceleration.

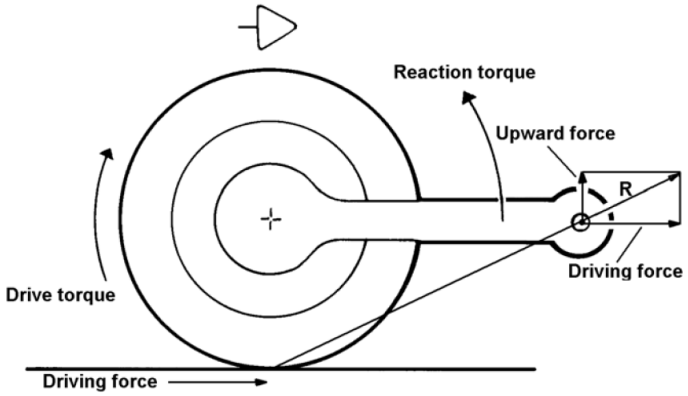

Figure 2.3: Anti squat geometry for a shaft-driven motorcycle, [5].

Figure 2.4 shows the resulting line that can be drawn from the rear tyre contact patch to the resulting instantaneous centre of the swing arm and chain on a chain-driven motorcycle. The chain can have a pro or anti-squat effect depending on the angle of the chain's force line relative to the ground. If the front sprocket is mounted co-axial with the swing arm pivot the change in anti-squat as the suspension moves throughout the stroke will be reduced.

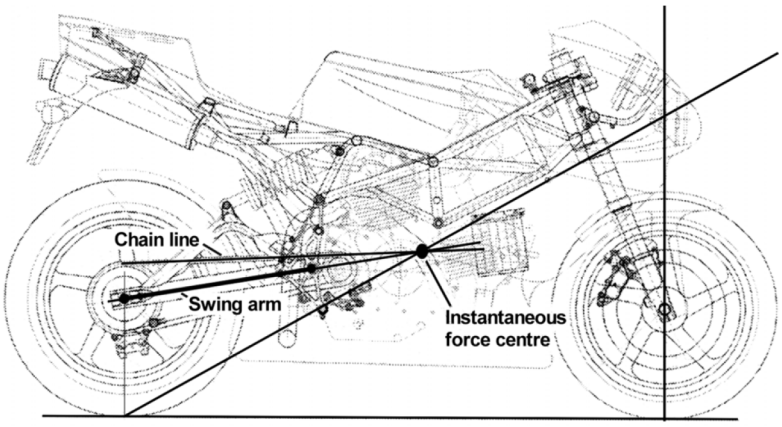

Figure 2.4: Anti squat geometry for a chain-driven motorcycle, [5].

A commonly used measurement of anti-squat is defined as a percentage where 0% anti-squat is defined as having the resultant line at ground level, giving no vertical forces on the sprung mass. 100% anti-squat is defined as when the resultant line intersects a point located at the CoG height in the x-location of the front axle, as in figure 2.4. This will exactly counteract the pitching motion due to acceleration thus resulting in the least possible suspension movement when accelerating. 100% anti-squat is referred to as, "close to ideal" by Foyale [5]. 200% anti-squat is defined as when the resulting line intersects the CoG.

2.4 Sound and Noise Emissions

EV vehicles are generally more silent than their ICE-powered counterpart's since the powertrain inherently is more silent. This does however not necessarily mean that the rider will experience less fatigue due to noise. Sound emissions can be divided into two categories, A-sounds and B-sounds.

2.4.1 A-sounds

A-sounds are sound emissions that positively affect the driving experience. This could be sound emissions from the powertrain that change as speed increases and therefore increase the sense of acceleration and speed. In an ICE-powered motorcycle, this is naturally obtained with the changing speed of the engine and the whine from straight-cut gears in the transmission.

Electric powertrains can be designed to give a similar sense of speed. Two examples of electric motorcycles that have achieved this are the Harley Davidson liveWire s1 [7] and Triumph TE-1 [8]. Both of these vehicles have a notable transmission whine that together with sounds emitted from the motor and inverter adds to the experience.

2.4.2 B-sounds

B-sounds on the other hand are non-desired sounds that is disturbing for the rider and may cause fatigue and decrease the rider's focus. Noise emissions that could be coincided an A-sounds during city and back road riding could be a B-sound while riding on the highway. Other types of noise emissions could be considered B-sounds regardless of the riding conditions for example squeaks and rattles, wind noise, chain noise and high-frequency sound from inverters and high voltage components.

2.5 Complexity

RGNT is a small company with limited development resources and smaller production volumes than big players in the industry. A well-designed and simple drivetrain will be superior to a more complex and rushed through design. The aim should be to design a simple, well-thought trough and robust drivetrain with low complexity. Removing complexity from a design will reduce development, production and maintenance-related problems.

Reducing the complexity of a design is essential to reduce development time, production problems and cost as well as improving reliability. The complexity of the design can be measured in several different ways. The complexity number, K, of a design according to Gustafsson [9], can be determined by analyzing the total part count, the number of different components, and the number of interfaces between components.

$$K = (N_p \; N_{op} \; N_c)^{1/3} \tag{2.21}$$

$N_p = total\ part\ count$
$N_{op} = number\ of\ different\ components$
$N_c = number\ of\ interfaces$

2.5.1 Manufacturing and Assembly

Designing for manufacturing and assembly (DFMA) is essential for developing products intended for series production. The principle of DFMA can be condensed down to 8 cornerstones described according to Six-Sigma [12].

- Simple design: The design philosophy of simplifying the geometries and removing unnecessary features to aid manufacturing is important to improve manufacturability. The need for special tooling and fixtures should be minimized.

- Modular design: By designing with modularity in mind and basing product families on platforms rather than model-specific designs several models can share a majority of the components. By sharing components the development time can be reduced along with part cost and assembly since the same production equipment can be used across the product range.

- Efficient fasteners: The assembly process can be aided by utilising efficient fastening methods. This can be done in several ways including using fasteners that are easy to install, utilize snap in place features and standardising screw sizes and lengths.

- Poka-Yoke: Poka-yoke is an essential part of the Toyota manufacturing method. The aim of Poka-Yoke is to make the assembly process mistake-proof. By designing the components with mechanical interlocks that only enable correct mounting or symmetric components assembly errors can be avoided.

- Reduce the number of parts: Reducing the number of parts in a design is an efficient way of aiding manufacturing and assembly. Combining several functionalities into one component reduces the overall complexity.

- Use standard components: Using commercially available off-the-shelf components is often more cost-effective and more reliable than using custom-made components. Standardized components can be obtained from different manufacturers while fulfilling the same standards, this means that lower risks are involved regarding availability. Components like fasteners, bearings, gaskets and similar components are components where standardized parts absolutely should be considered.

- Know the process limitations: As an R&D engineer, it's essential to have a good insight into the manufacturing and assembly process. By knowing the strengths and weaknesses of different processes the design may be altered to suit a more efficient production method. Production volume, material and geometries directly affect the process requirements.

- Use suitable tolerances: Tolerances should be carefully thought through. Tight tolerances are generally harder to achieve and therefore add labour and tooling costs as well as increased risk of scraping. The tolerances must ensure that the components fit together geometrically and suitable fit between components is obtained. Minimizing the need for adjustment and setup work during assembly by having tighter manufacturing tolerances is an efficient way of reducing assembly time.

2.5.2 Production Cost

The production volume can drastically affect which design concept and manufacturing methods are feasible. For low-scale production, it is usually more cost-effective to utilize more flexible production methods such as machining or sand casting while injection moulding or forging requires more specialized tooling and is more cost and time-efficient for larger batches. By predicting the production volume of the product the design can be altered to suit a more suitable manufacturing method.

2.5.3 Maintenance and Reliability

The design should prioritize simplifying frequently accruing maintenance tasks. This can be done by reducing the number of surrounding components that have to be removed and ensuring that enough space is available to perform the work. Special tools should be avoided if possible.

Failure modes and effects analysis,(FMEA) can be used during the design process to evaluate the reliability risks for different designs according to Factory [13]. FMEA is an iterative seven-step process that can be used as an aid for constant improvements both in manufacturing processes as well as the development of new and existing model families. The seven steps of FMEA are:

- Identify the process or functionality: The processes and functionalities are isolated in order to get a better understanding of each subsystem and be able to quantify the potential problems.

- Evaluate risks and faults: Data collection or brainstorming can be used to evaluate risks and problems that may occur for each process, sub-system or component in the design.

- Determine the effects of the problems: Determine the severity and effects of each fault. The severity of each failure mode is ranked on a scale from 1 to 10 where 10 is the most critical.

- Estimate the occurrence of the fault: The occurrence of the fault is evaluated on a scale from 1 to 10 where 10 is a very frequently occurring problem while 1 is less likely.

- Estimate if the problem can be prevented before it is occurring: The possibility to prevent the fault is ranked on a scale from 1 to 10 where 10 is impossible to prevent while 1 is easy to prevent.

- Calculate Risk Priority Number: Risk priority number (RPN) is used when prioritizing the most critical problems to work with. RPN = Severity x Occurrence x Possibility to prevent.

- Iterate the design to lower the sensitivity, and occurrence and improve the possibility to detect problems: The FMEA work should not be considered done after the first analysis.

2.6 Electric Motors

Modern electric vehicles use several different types of electric motors. Common for all types is that they are operating on alternating current, usually 3-phase. The direct current from the battery pack is modulated with an inverter to form sinusoidal voltage curves.
The power density, kW/kg can be used to evaluate the performance of an electric motor. Generally, a higher power density is achieved by reducing the diameter of the rotor and increasing the operating speeds of the e-machine. With a smaller diameter rotor, the output torque will be reduced and the transmission speed ratio has to be altered to get the desired rear wheel torque.
High torque density, on the other hand, Nm/kg is generally obtained by increasing the diameter of the rotor. The higher inertia of a big rotor limits the rotational speeds that can be obtained and thereby the possibility of having a high power density.

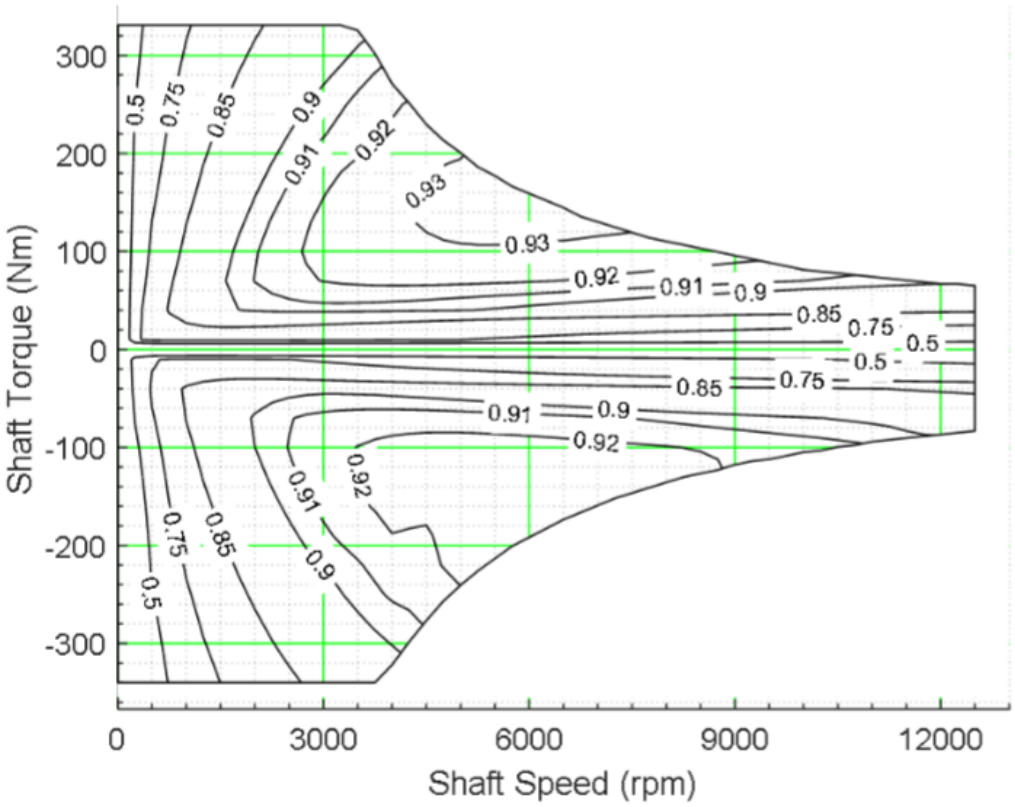

Figure 2.5: Electric motor efficiency map

In figure 2.5 typical torque, speed and efficiency map of an electric motor can be seen. For positive torque the e-machine acts as a motor. For negative torque, it is acting as a generator and can be used for regenerative braking. The typical torque curve of an electric motor can be divided into two regions, constant torque and constant power. For this specific motor, a constant torque of 315 Nm can be obtained from 0rpm to 3150 rpm. From 3150 rpm up to max-rated motor speed the max torque gradually drops off while more or less constant power is available. The motor efficiency is indicated by the iso lines segmenting the graph. To design an efficient powertrain the motor and gearing should be optimized to mainly operate in the more efficient regions while fulfilling the performance requirements.

2.6.1 Motor Configurations

Electric motors can be divided into in-runners and out-runners.
In-runner motors have a stationary housing containing the stator while the rotor is mounted to the output shaft. This configuration is currently the most commonly used within the automotive sector. This type of motor is more suitable for high-speed operations due to the lower rotor inertia.

Out-runners have a rotating motor housing combined with the rotor while the stator is mounted to a shaft or plate. This configuration is commonly seen in applications such as vehicles with hub motors, ultra-light aircraft and P3 hybrids. This type of motor typically has a large rotor diameter, resulting in higher output torque.

2.6.2 Radial Flux Permanent Magnet Synchronous Motor

Radial flux permanent magnet motors have traditionally been the most common motor in EV applications. The stator of a radial flux PMSM motor is commonly constructed out of steel laminates with copper windings or hairpins used to generate the electromagnet field. The rotor core is typically made of steel laminates and houses the permanent magnets. The most common magnet material is neodymium which is a rare earth metal. The radial flux PMSM motor is generally constructed with a smaller rotor diameter. A smaller rotor diameter will produce lower torque but allows for higher operating speeds.

2.6.3 Axial Flux Permanent Magnet Synchronous Motor

Axial flux PMSM are often referred to as pancake motors. Bigger diameter axial flux motors generally operate at lower speeds than radial flux motors while producing higher torque [15] and can therefore be suitable for powertrains without a primary transmission. Axial flux motors are becoming increasingly popular in automotive applications due to their low speeds and high torque density.

2.6.4 Synchronous Reluctance Motor

The reluctance motor has a rotor without permanent magnets and is therefore a more environmentally friendly alternative to the PM machines that relies on neodymium-based magnets. The reluctance motor has a ferromagnetic rotor made out of special steel alloy laminates. The stator is similar in its design and operation to a PMSM radial flux motor. The stator energizes the rotor and the 3-pase waves induce a rotating magnetic field acting on the rotor and allowing the machine to rotate.

The reluctance machine can be a relatively cost-effective alternative to a permanent magnet machine however the power and torque density is less than PM motors. The reluctance machine suffers from significant torque ripple or periodic change of torque during each revolution, this may affect the drivability and ergonomics negatively.

2.7 Transmission

The purpose of a transmission in an electric powertrain is to alter the speed and torque of the electric motor to provide the required tractive torque on the rear wheel. The speed ratio of the transmission depends on the characteristics of the motor and the performance targets for the motorcycle.

Different types of transmissions are more suitable for different applications, speeds and torques. In figure 2.6 some common transmission types and their maximum speed ratio and efficiency found in Maskinelement, [14] are presented.

Transmission type	Max speed ratio	Efficency
Spur gear	15	0.94-0.98
Helical gear	15	0.94-0.98
One stage planetary	10	0.94-0.97
Chain	6	0.97-0.99
Thooth belt	15	0.93-0.98
V-belt	10	0.89-0.94
Hypoid	5	0.95-0.99
Bevel	5	0.98-0.99

Figure 2.6: Transmission types and efficiency

The total speed ratio for a synchronous transmission can be calculated using equation 2.22 using the angular velocity of the input and output shaft. The output torque of a transmission can then be calculated using equation 2.23 using the speed ratio and input torque. Losses in the transmission will result in reduced torque output and the efficiency of the transmission must be taken into account.

$$i = \frac{\omega_1}{\omega_2} \tag{2.22}$$

$$T_2 = \eta \cdot T_1 \cdot i \tag{2.23}$$

i = speed ratio
ω_1 = angular velocity input shaft
ω_2 = angular velocity output shaft
η = efficiency
T_1 = input torque
T_2 = output torque

2.8 Gear Trains

Gear-based transmissions are commonly used in all types of vehicles because of their ability to transfer high power in a relatively small package while maintaining good reliability and efficiency.

2.8.1 Straight Spur Gears

Spur gear transmission uses straight-cut gears. An involute gear tooth profile with gradual tooth engagement is the most prevalent type. The straight cut generates noise for tooth meshing, commonly called gear whine. This type of gear is commonly used in conventional motorcycle transmissions, where gear whine is not problematic due to other sound emissions.

A benefit of straight-cut gears is that they do not generate any axial forces during operation and thereby reduce axial bearing loads in the transmission. Production costs can be reduced compared to helical gears due to simplified manufacturing processes.

2.8.2 Helical Gears

Helical gears are commonly used in all types of transmissions where noise, harshness and vibration (NVH) are important design aspects. Helical gears use similar involute gear tooth geometries as their straight-cut counterparts but by angling the teeth flank, more teeth can be engaged in the gear meshing and thereby a more silent operation can be obtained. The slanted gear cogs result in higher axial forces on bearings and transmission housings.

2.8.3 Bevel Gears

Driveshafts coupled to a 90° bevel gear reduction have been used by motorcycle manufacturers like BMW and Moto Guzzi since the 1920s and later on by Japanese manufacturers like Honda and Yamaha. Given the more complex and costly design, this type of final drive is most commonly used in heavier touring and adventure motorcycles. This type of bike is marketed more towards riders that can afford to pay extra for the convenience and reliability that the oil-lubricated bevel transmission provides. Compared to a final drive using a chain or belt this system contributes to a significantly higher unsprung mass and this is one of the reasons why it's rarely seen on more performance-orientated bikes.

The play and contact patch between the ring and pinion gear is crucial to obtain a silent and long-lasting bevel reduction. Surface properties, tolerances and hardness of the gear flanks are also key aspects. The complexity and cost involved both in terms of design and manufacturing mean that this type of final drive is more suitable for large production runs.

2.8.4 Planetary Reduction

Planetary or epicyclic gear reductions are a common type of gear reduction found in everything from electric power tools to automatic transmissions and industrial machines.

The main advantage of a planetary reduction is its compact format and significant speed reduction capabilities. The input and output shafts are concentric with each other and several stages can therefore be stacked for greater reduction.

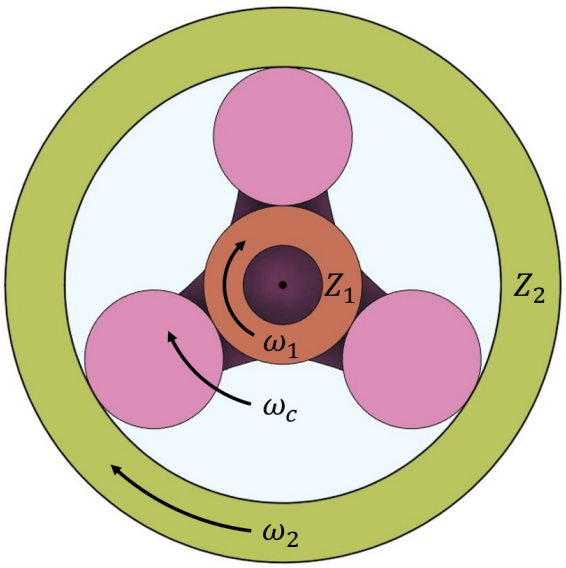

Figure 2.7: Planetary gear set

The speed ratio of a planetary gear set can be calculated using the equation 2.24. The planetary gear set can be used in several different configurations depending on the applications and combined with clutches and brakes to build multi-stage transmissions. In reduction applications, the motor is often coupled to the sun gear while the ring gear is fixed and power output is taken from the planet carrier. It is also possible to have a fixed planet carrier and power output on the ring gear.

Off-the-shelf solutions are available from a number of manufacturers and can relatively easily be integrated as a primary transmission.

$$i = \frac{\omega_1 - \omega_c}{\omega_2 - \omega_c} = -\frac{Z_2}{Z_1} \tag{2.24}$$

ω_1 = angular velocity sun gear
ω_2 = angular velocity ring gear
ω_c = angular velocity planet carrier
Z_1 = number of teeth sun gear
Z_1 = number of teeth ring gear

2.8.5 Multistage Transmission

Just as for ICE powered motorcycles a multi stage transmission could improve the efficiency, range, drivability and top speed of the motorcycle.

The ability to operate the vehicle at optimal efficiency during highway cruising and still have good acceleration can be achieved by having a highway gear with a lower speed ratio and an acceleration gear with a higher speed ratio [15]. The total speed ratio of a given transmission can be calculated using equation 2.25.

$$i_{tot} = \prod_{i=1}^{n} i_i = i_1\, i_2\, i_3 ... i_n \tag{2.25}$$

2.8.5.1 Conventional Transmissions

Conventional layshaft transmissions are the most common type of transmission in ICE motorcycles today. This type of transmission does not have powershifting abilities since two gears cant be engaged at the same time [15].

2.8.5.2 Power-shifting Transmissions

Power shifting transmissions are referring to transmissions that can perform gear changes without significant power interruptions. The two most common types of power-shifting transmissions in automotive applications are automatic planetary transmissions (APT), and dual-clutch transmissions (DCT).

2.8.5.3 Continuously Variable Transmissions

Continuously variable transmission (CVT) is commonly found in applications like mopeds, scooters and cars. The gear ratio can be altered continuously and therefore allowing the motor to operate at the most efficient operating point for every given situation [15].

The most basic form of CVT transmissions consists of a belt and two pulleys that can change their effective rolling diameter. Increasing the effective radius on the drive pulley and reducing the effective radius on the driven pulley results in a low-speed ratio and a high-speed ratio is obtained by decreasing the effective radius of the drive pulley and increasing the effective radius of the driven pulley.

For A1 motorcycles and mopeds, rubber belts are commonly used while more powerful vehicles use a belt composed of steel laminates that are enclosed and oil lubricated.

The efficiency of a traditional CVT is rather poor compared to other types of transmissions and is not suitable for high-torque applications.

2.8.5.4 Dual Motor

The benefits of a multistage transmission can also be obtained by using a twin-motor arrangement. By using one motor for low torque operation high efficiency can be obtained and by engaging the second motor the acceleration and top speed requirements can be reached. The motors can be optimized for different operating conditions to further improve overall vehicle performance.

A similar approach is used in the automotive industry by Tesla [16] and Volvo [17] for their all-wheel-drive models. By using a motor with high torque optimized for lower speeds on the rear axle and a motor optimised for highway driving on the front axle

this arrangement is relatively simple from a mechanical standpoint but the downside is the added cost of two motors and inverters which is a substantial cost to the vehicle. A seamless transition between single and dual motor operation would be preferred in order to have a predictable riding experience.

2.9 Belt

Belts can be divided into synchronous and asynchronous. Synchronous belts are geometrically locked into the pulley to prevent slip. V belts and multi-rib belts on the other hand transmit force via the friction between the belt and pulley and therefore allow for slip i.e. asynchronous [14].

2.9.1 Synchronous Belts

Tooth belts, often called synchronous belts or timing belts are used by Zero, Livewire, and Cake along with other electric motorcycles as their final drive transmissions. Tooth belts are also commonly used as camshaft belts for ICE engines. By changing pulleys the speed ratios can easily be changed. The toothed belt requires well-adjusted tension to have a long operating life. The tension can be done by an automatic tensioner system or by adjusting manually and measuring the deflection or frequency of the belt.

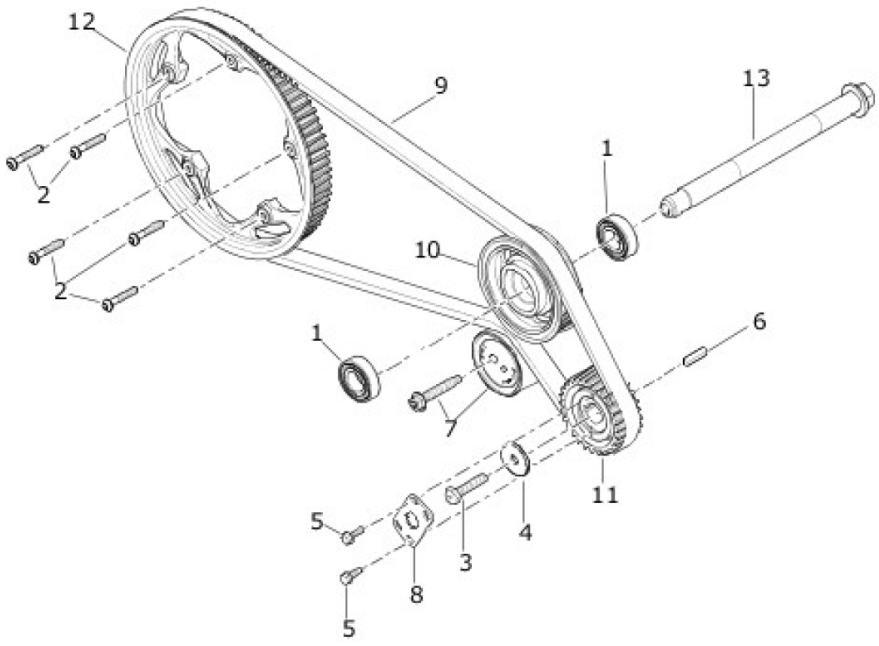

Figure 2.8: Harley Davidson Live Wire S1 belt transmission, Harley Davidson manual [18]

The maximum speed ratio that can be obtained for a tooth belt final drive is limited geometrically by the size of the rear wheel pulley as well as the arc of engagement and bending radius of the belt on the front pulley. Greater speed ratios result in fewer teeth being engaged on the smaller pulley which results in higher stress levels. This can to some extent be improved by using an idler pulley arrangement, Harley Davidson implemented this on the Live Wire S1 seen in Figure 2.8. This also allowed for more design freedom regarding motor placement and anti-squat geometries.

2.9.1.1 Geometry and Function of Tooth Belts

Tooth belts are produced with standardized lengths, widths and profiles. The force acting on the rubber teeth is transferred into the belt cord. Depending on the application different tooth profiles, rubber hardness and cord materials can be chosen.

Tooth belts provide smoother operation and better high-speed properties than a chain. The belt does not use lubrication and tends to require less maintenance than a chain drive. Tooth belts provide a slip-free synchronous power transfer with high efficiency and relatively low cost.

Trapezoidal, curvilinear and modified curvilinear belt profiles are the most commonly used types according to STP/SI [19]. The geometry of the belt greatly affects the stress levels and wear resistance as well as the sound emissions from the belt transmission.

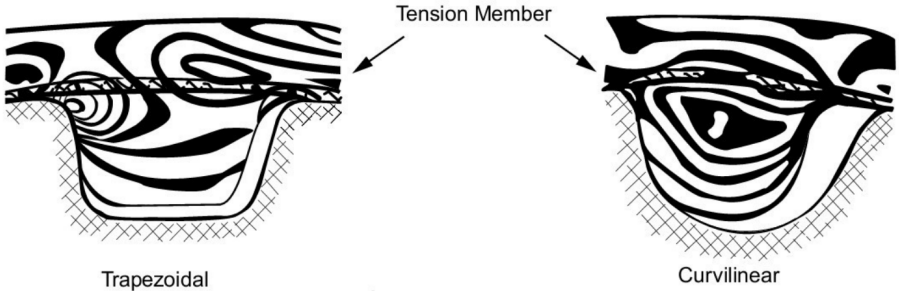

Figure 2.9: Stress pattern in tooth belts [19]

In figure 2.9 the differences in the stress pattern of trapezoidal and curvilinear profiles can be seen.

The trapezoidal belt profile is the most widely used tooth profile both in industrial applications as well as within the automotive sector. This type of belt is often found in applications like timing belts for ICE engines or drive belts for superchargers [15]. This belt type has good force transmitting capabilities but the sharp corners of the tooth flanks result in stress concentrations which can result in increased wear during high-speed and high-torque operations. The teeth engagement of a trapezoidal belt is more rough compared to other profiles due to the angular tooth shape and this results in more noise emissions according to Gates [20].

Curvilinear belts are often referred to as high torque drive (HTD). The main advantage of this type of belt is improved speed and torque transfer capabilities.
Increasing the tooth height and altering the tooth shape can reduce stress concentrations. The geometry of the curvilinear profile results in more even stress levels troughs out the tooth with the highest stress near the centre.
Smoother meshing between the belt and pulley is obtained with this belt geometry which results in a more silent transmission compared to an equivalent trapezoidal belt drive. The Modified curvilinear profile is a slightly modified version of the HTD profile with lower tooth profiles and steeper flank angles to obtain even higher torque transfer capabilities than standard HTD belts. This type of belt is less likely to experience belt ratcheting i.e. when the belt teeth cog over on the pulley under high loading and high speeds according to [19].

2.10 Chain Drives

Chain drives are ubiquitous in the motorcycle world both as final drives as well as for camshaft drives. The traditional roller chain is however not the standard for electric motorcycles.

2.10.1 Roller Chain

Roller chains are by far the most common type of final drive for ICE motorcycles. It is a cost-effective way of transferring a lot of torque to the rear wheel. The speed ratio can be changed to suit different types of bikes by changing the sprockets. A roller chain is less sensitive to correct tension than a toothed belt but requires more maintenance in terms of cleaning and lubrication than a belt drive.

2.10.1.1 The Polygon Problem

The roller chain is composed of hardened steel rollers connected to stamped steel laminates with pins. Engagement between the chain rollers and sprocket results in rattling noise. Each link in the chain is geometrically a straight line with the length of the chain pitch. This results in a speed variation of the chain during the sprocket engagement. This is commonly referred to as the polygon problem or polygon effect according to Kinematics of roller chain drives — Exact and approximate analysis [21].

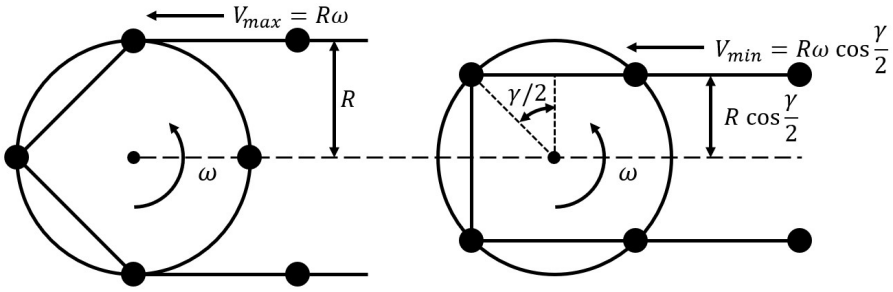

Figure 2.10: Speed variation caused by the polygon effect

V = chain speed, m/s
R = pitch radius of the sprocket, mm
ω = angular velocity of the sprocket, rad/s
γ = pitch angle, °
The speed variation caused by the polygon problem can be calculated using the equations in figure 2.10, in this case for a four-toothed sprocket.

2.10.2 Silent Chain

A silent chain (inverted tooth chain) is built up by steel laminates rather than rollers according to Ramsey Products [22]. A silent chain in an oil bath can have an efficiency of up to 99%. Since a chain transmission usually relies on a tensioner and is less sensitive to variation in shaft spacing. Therefore less tight tolerances on transmission housings can be used. Silent chains are commonly used in transfer cases for 4wd vehicles like BMW xDrive, Audi, Mercedes, Toyota, and GM. Silent chains are also commonly used as cam chains and primary transmissions for motorcycles such as HD and Indian as well as snowmobiles.

Figure 2.11: BMW xDrive transfer case, BMW [23]

A silent chain in an oil bath can be an alternative to a gear-based transmission, see figure 2.11. The steel laminates of the chain form a tooth geometry similar to an involute gear set. The geometry of the laminates and sprockets reduces the sound levels through a gradual engagement.

2.11 Hub Motor

Directly connecting the electric motor to the wheel allows for a drivetrain without any transmission. The current RGNT models are using a PMSM radial flux outrunner as a hub motor. By using a hub motor more space can be freed up in the frame and utilised for example to carry more battery cells.

The lack of a transmission in a hub motor powertrain results in low driveline losses and good regenerative braking performance. The reduced complexity results in a reliable and almost maintenance-free drivetrain with low noise and vibrations.

The hub motor is mounted in the rim which results in high unsprung mass and more wheel inertia. The hub motor layout requires a motor designed to produce the desired wheel torque while operating at relatively low speeds which will result in a heavier motor.

3
Methods

In this chapter, the methods used during the project will be presented. The initial phase of the project relies on the data-driven product development methods described in [9]. To evaluate different concepts and their performance potentials vehicle dynamic and energy consumption simulations using the WMTC cycle were used. Mechanical design was also used to evaluate the feasibility of different concepts.

3.1 Product Development

A data-driven product development process was used. The decisions taken during the product development phase are largely based on the results from simulations, knowledge gathered as well mechanical design and packaging.

3.1.1 Problem Definition

The problem definition was compiled to get a better understanding of the problems and tasks that needed to be solved. The problem definition was finalized together with R&D engineers at RGNT Motorcycles to ensure common expectations for the project.

3.1.2 Benchmarking

The current state of the motorcycle market was investigated to learn from other manufacturers. Technical solutions, performance, dimensions and geometries for both electric and ICE-powered motorcycles were evaluated. In addition to the relatively small motorcycle industry, state-of-the-art solutions from the closely related automotive sector were also evaluated.

3.1.3 Function Analysis

Functional analysis was done to get a more refined picture of how the powertrain system works and break down the problem into partial functions.

3.1.4 Requirement Specification

The requirement specification was used to condense down what the new model should be into measurable and verifiable requirements that are possible to evaluate. The requirement specification was compiled with input from the R&D department at RGNT Motorcycles as well as information gathered in the bench-marking.
The requirement specification consists of "must" and "should" criteria. Each concept must full fill all the "must" criteria to be deemed useable.

3.2 Concept Generation

Solutions to the functions were generated using brainstorming as an unstructured and creative way of concept generation. The goal of a brainstorming session is to encourage the participants to generate all types of concepts and ideas. This method may result in solutions that would otherwise be missed out due to more rational thinking. Partial solutions from the benchmarking were also used to generate concepts in this step.

3.2.1 Morphological Matrix

Ideas and partial solutions found during the benchmarking and brainstorming were categorized into function groups. Concepts were then generated by combining partial solutions from each function group. This method can result in a large number of concepts and therefore a systematic approach was taken where only concepts that were found reasonable and realistic were generated.

3.3 Concept Elimination

Once the concepts were generated the process of gradually eliminating less-suitable concepts were initiated, first by removing all unusable concepts that did not fully meet all "must" criterion in the requirement specification.

3.3.1 Elimination Matrix

The initial reduction of concepts was made using an elimination matrix. Concepts that did not fulfil all requirements in the requirements specification were discarded in this step.

3.3.2 Kesselring Matrix

Further reduction of concepts was done using a Kesselring matrix. In the Kesselring matrix, each concept was evaluated to see how well the criteria from the requirement specification were met. By ranking the importance of the criterions a further reduction of concepts was possible.

3.4 Motorcycle Design

To aid the product development process a preliminary motorcycle concept was designed.

3.4.1 Motorcycle Dimensions and Geometry

Based on the geometries of current motorcycles in production, literature and initial VD (Vehicle Dynamics) calculations an initial motorcycle geometry was set.

3.4.2 Calculations and Simlations

Calculations and simulations were used to define the powertrain specifications needed to meet the requirements. Further calculations/simulations were used to evaluate the performance of powertrain concepts.

3.4.3 Mechanical Design and CAD Modelling

An initial packaging model with the intended motorcycle geometry was modelled in CAD. The packaging model was used to test different packaging concepts and verify that all components could fit in the relatively small space of a motorcycle frame. Further, the model was used to conduct initial ergonomic studies for different rider manikins.

4
Implementations

The implementation chapter will present work carried out during the thesis project. The results needed to continue the evaluations will also be presented, while the final results can be seen in the results and conclusion chapters.

4.1 Problem Definition

The first step in the product development process is to properly define the problem. By doing a proper problem definition prior to looking at solutions a broader solution approach without the risk of eliminating potential solutions can be conducted.

This section will describe the processes used to gain sufficient knowledge about the problem before the actual development work was initiated.

4.1.1 Evaluation of Competing Motorcycles

The first step in the product development process was to evaluate current motorcycle models on the market. This was done both to gain knowledge about the current state of the motorcycle market and collect data from competing manufacturers and models.

4.1.2 Electric Motorcycles

The electric motorcycle market is currently in a state where new models and manufacturers constantly are entering the market with more or less realistic ambition levels, however, relatively few of the startup manufacturers have a homologated model for sale.

Of the electric motorcycles available on the market a majority of manufacturers without experience in producing ICE motorcycles. One early and successful EV motorcycle manufacturer is the Californian-based ZERO Motorcycles [10] founded in 2006 which currently offers a wide range of motorcycles from adventure and touring to more sport-orientated machines. Energica [11] from Italy is focusing on extreme performance and Italian design and has widened its horizon to include an adventure motorcycle.

More established manufacturers such as Harley Davidson (under their sub-brand LiveWire), BMW and KTM are launching models as well. We can still see a gap in high-performance, retro-inspired motorcycles leaving a potential marketplace for bigger RGNT motorcycles available. In Appendix B the powertrain specifications of some models of interest can be seen.

4.1.3 Function Analysis

A function model was made to visualize how the powertrain system works and how it affects different parts of the motorcycle.

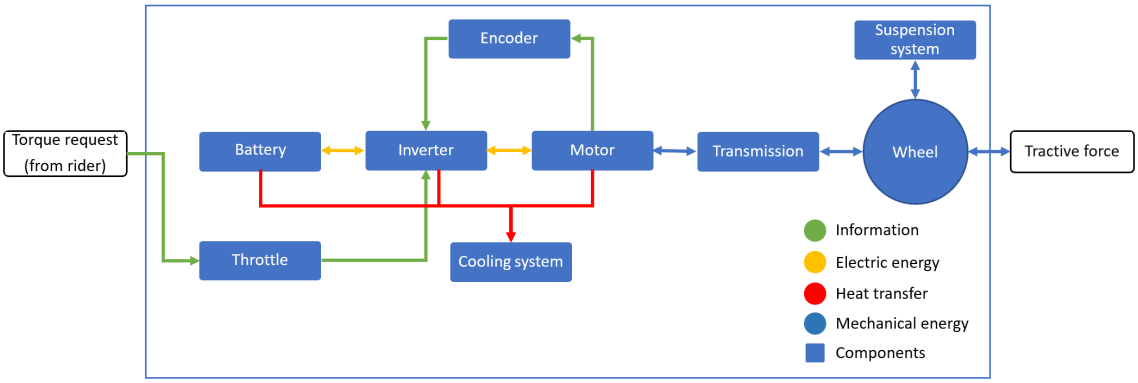

Figure 4.1: Function model

In Figure 4.1 the different components and sub-assemblies of the powertrain system are represented as blocks. Energy and information flow between the components are indicated with coloured arrows. The outline represents the powertrain system limit with torque request as an input and tractive force as the output.

The focus of this thesis work was the mechanical parts of the powertrain and mainly the motor and transmission evaluation. Therefore, the functional model is simplified and does not include all components but subsystems.

4.1.4 Requirements

The requirements on the powertrain were compiled with input from the R&D team at RGNT Motorcycles and results from the evaluation of competing motorcycles. These requirements are presented in appendix A and are divided into six categories:

- Performance
- NHV and perceived quality
- Vehicle dynamics and handling
- Manufacturing
- Reliability and handling
- Life cycle and sustainability

4.1.5 Environmental, Ethical and Social Aspects

RGNT Motorcycles believes in a sustainable society, in terms of production, use and recycling of their products. By designing a vehicle with high efficiency that relies on sustainable materials that are recyclable it's possible to contribute to this goal. By designing a robust and well-dimensioned powertrain the life expectancy of the motorcycle can be increased, thereby reducing the life-cycle environmental impact associated with production. The battery cells are the most environmentally demanding components in an electric motorcycle. By developing the most efficient powertrain that still fulfils the requirements, fewer battery cells can be used. Noise emissions have proven to reduce human health and well-being [24]. The aim should therefore be to reduce noise emissions from the powertrain as much as possible to reduce the motorcycles' contribution to urban sound pollution.

4.2 Motorcycle Dimensions and Parameters

When designing a motorcycle powertrain the complete vehicle needs to be considered since the type and size of the motorcycle will determine which powertrain layout and specifications are best suited. Hence the overall dimensions and parameters of the motorcycle needed to be determined for the packaging and further evaluation of different powertrain concepts.

4.2.1 Wheelbase

The wheelbase of a motorcycle is an important parameter that affects the overall size, handling and performance of the motorcycle. For the scope of this thesis, the wheelbase was chosen by evaluating the wheelbases of motorcycles with similar performance specifications as described in appendix A. These motorcycles and their respective wheelbases are presented in figure 4.2. The wheelbase used was 1450 mm.

Motorcycle Wheelbase Benchmark		
Make	**Model**	**Wheelbase [mm]**
Yamaha	MT07	1400
Yamaha	MT09	1440
Honda	CB650F	1450
Honda	Hornet 600	1425
Honda	CB750	1430
Ducati	Monster	1474
Suzuki	SV650	1445
Triumph	trident 660	1401
Kawasaki	ER6	1410
Triumph	Bonneville T120	1450
Triumph	Scrambler	1500
KTM	Duke 790	1475
KTM	Duke 890	1481
Moto Guzzi	V7	1450
Aprilia	Shiver 750	1440
Average		1444,73

Figure 4.2: Motorcycles and their respective wheelbase

4.2.2 Mass

The total mass of the motorcycle and rider was needed for evaluating the performance of the powertrain. The mass of the motorcycle was set to the maximum allowed weight of 240 kg as defined in the requirements, appendix A, and the mass of the rider was set to 75 kg in accordance with EU regulation [3].

$$m_{total} = m_{motorcycle} + m_{rider} = 315\,kg \tag{4.1}$$

4.2.3 Center of Gravity location

The height of the CoG was set to be half of the wheelbase since this is common according to Foyale [5] and the longitudinal position was set to be centred front to back giving a 50/50 weight bias front to rear.

4.2.4 Tyre Sizes

Choosing tyre sizes and compounds is very important for the handling of the motorcycle and requires testing, [5]. This was however outside the scope of this project other than for the purpose of packaging, performance simulations and determining gearing. Therefore the rear tyre size was chosen to be 180/55-r17 which is a typical rear tyre size for bikes that have similar specifications/performance to the performance requirements found in appendix A. The rear tire size was then used to calculate the rolling radius of the rear wheel

$$R_{wheel} = \frac{Rim\ diameter + 2\ Sidewall\ height}{2} = 0.315\,m \tag{4.2}$$

The front tyre size was chosen to be 120/70-r17 since this is the most common size for motorcycles of this type. This was then used for inertia calculations and packaging.

4.2.5 Wheel inertia and Equivalent Mass

The wheel's moment of inertia (MoI) was needed for performance calculations and simulations. The general formula for MoI is

$$J = mr^2 \tag{4.3}$$

The radius is the dominating term since it's squared. Therefore the mass of the tyre will have the largest contribution to the wheel's MoI followed by the wheel rim. The influence of the brake discs is likewise small and for this project, only the influence of the tyre and rim will be used. The online calculator [25] was used to approximate the tyre's MoI based on the size and weight of the tyres. The sizes of the front and the rear tyre were already determined however the mass of a generic tyre in these sizes needed to be found. This was done by finding the weights of seven different models of tyres in the front and rear sizes and calculating the average weight. All the tyres are of similar category - street/sport tyres. The different tyres makes and

models and the resulting average weights are presented in tables 4.3 and 4.4. These average weights gave a MoI of 0.35 kgm^2 for the front tyre and 0.57 kgm^2 for the rear using [25].

120/70-17 Front Tyre Weight		
Make	**Model**	**weight [kg]**
Michelin	Road 6 gt	4,5
Michelin	Power Cup	4,28
Michelin	Pilot Power 2CT	4,08
Pirelli	Corsa 2	4,3
Pirelli	Angel	4,3
Bridgestone	Battlax S22	4,35
Bridgestone	Battlax Bt-021	4,26
Average weight		**4,3**

Figure 4.3: Front Tyres

180/55-17 Rear Tyre Weight		
Make	**Model**	**weight [kg]**
Michelin	Road 6 GT	6,25
Michelin	Road 5	6,07
Michelin	Pilot Road 4	6,26
Metzeler	Racetec RR	5,76
Metzeler	Sportec	6,16
Bridge stone	Battlax	6,63
Kingtyre	K902	6,67
Average weight		**6,26**

Figure 4.4: Rear Tyres

The MoI of the wheels needed to be determined. These values were taken directly from Brockes Performance [26] which states that the stock cast wheel on a Suzuki GSX-R 1000 is 0.15 kgm^2 for the front and 0.26 kgm^2 for the rear. The combined MoI for the front and rear wheel/tyre combination was then calculated

$$J_{front} = 0.35 + 0.15 = 0.50 kgm^2 \tag{4.4}$$

$$J_{rear} = 0.57 + 0.26 = 0.83\, kgm^2 \tag{4.5}$$

The equivalent inertia mass could now be calculated as

$$m_{eqv} = m_{total} + \frac{J_{front}}{R^2_{wheel}} + \frac{J_{rear}}{R^2_{wheel}} = 328.4kg \tag{4.6}$$

These values were then used for performance evaluations.

4.3 Resistance Forces

The resistance forces were needed for performance and range evaluations. This section describes how the drag- and rolling resistance forces were determined. The EU regulation document [3] describes how the resistance forces can be determined using a standardised on-road coast-down test or taken directly from a predefined running resistance table based on vehicle total mass. Performing on-road coast-down tests were out of the scope of this thesis and therefore the running resistance table in appendix 5 of document [3] was used. This table is based on vehicle total mass and the rolling resistance is given as a force called a.

$$F_{roll} = a \tag{4.7}$$

The aerodynamic drag is not given as a force but instead, as a coefficient called b. This coefficient is in the unit newtons per kilometre per hour squared.

$$b = \frac{N}{(km/h)^2} \tag{4.8}$$

The drag force can then be calculated as

$$F_{drag} = b\,(\frac{v}{3.6})^2 \tag{4.9}$$

4.4 Power and Torque

The power and torque specifications are basic defining properties of a powertrain to which all other aspects of the powertrain can be developed. This section describes the process used to determine the power and torque specifications needed to fulfil the performance requirements.

4.4.1 Torque and Power Demand for Acceleration

The maximum acceleration of a motorcycle is ultimately limited by 2 things, (even with unlimited power). The first is the available grip and the second is the maximum longitudinal load transfer i.e. when the front wheel lifts off the ground, commonly called wheeling. To calculate the acceleration performance of the bike the first thing that needed to be determined was the maximum tractive force, which can be calculated as

$$F_{tractive} = F_{zr}\mu = ma \tag{4.10}$$

Where F_{zr} is the vertical force on the rear wheel and μ is the coefficient of friction. F_{zr} will depend on the mass of the bike and the longitudinal load transfer.

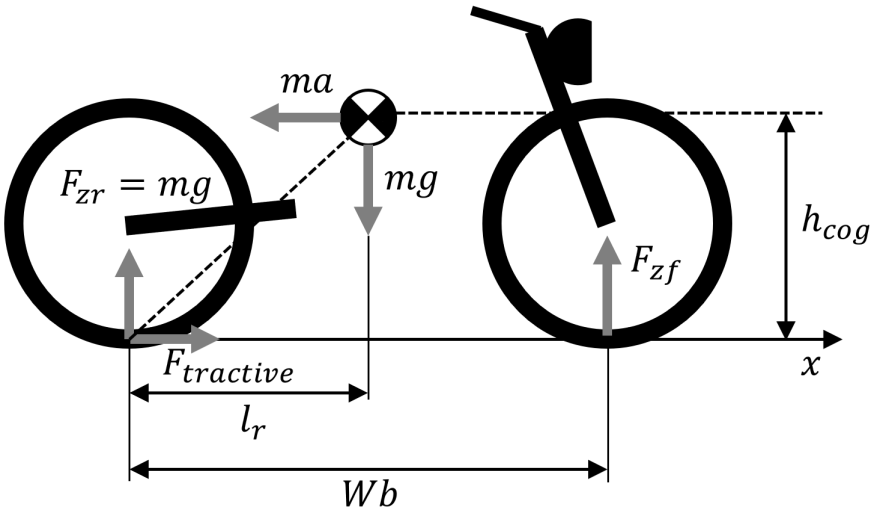

Figure 4.5: A free body diagram of an accelerating motorcycle, ma is a fictive inertial force

The vertical force on the rear tire during acceleration seen in figure 4.5 can be calculated as

$$F_{zr} = mg\frac{Wb - l_r}{Wb} + ma\frac{h_{cog}}{Wb} \tag{4.11}$$

It can be seen from equation 4.11 that a motorcycle with a CoG height of half the WB and a 50/50 weight distribution i.e. $l_r = \frac{WB}{2}$, 100% load transfer will occur at an acceleration of $a = g$. This is close to the highest acceleration commonly achieved by racing bikes according to [27]. 100% load transfer means that all of the motorcycle's weight will be on the rear wheel. The maximum tractive force and wheel torque can now be calculated as

$$F_{tractive-max} = mg\mu \tag{4.12}$$

$$T_{max} = F_{tractive-max}R_{wheel} \tag{4.13}$$

The maximum wheel torque will limit the acceleration until peak power output is reached. After which the constant power line of peak power will reduce the torque as the speed increases since $P = T\omega$. An example of this ideal wheel torque versus wheel rpm can be seen in figure 4.6. A model like this of rear wheel torque and power was then used as the basis for determining the required torque and power needed to achieve a certain 0-100 time. This model also coincides with a typical torque versus speed curve of an electric motor seen in figure 2.5.
The tractive force model $F_{tractive}(v)$ along with a model of the resistance forces $F_{drag}(v)$ and F_{roll} was implemented in a Python script as

$$F_{tractive}(v) = \begin{cases} \frac{T_{max}}{R_{wheel}} & \text{if } T_{max}\omega(v) < P_{max} \\ \frac{P_{max}}{R_{wheel}\omega(v)} & \text{if } T_{max}\omega(v) \geq P_{max} \end{cases} \tag{4.14}$$

where

$$\omega(v) = \frac{v}{R_{wheel}} \tag{4.15}$$

F_{drag} and F_{roll} was determined using the EU homologation method described previously

$$F_{drag}(v) = b(\frac{v}{3.6})^2 \tag{4.16}$$

$$F_{roll} = a \tag{4.17}$$

The resulting acceleration force for a given speed on flat ground could then be calculated

$$F_{acceleration}(v) = F_{tractive}(v) - F_{drag}(v) - F_{roll} \tag{4.18}$$

The velocity was then calculated numerically with a timestep $h = 0.001s$

$$v(t+h) = v(t) + \frac{F_{acceleration}v(t)}{m_{equivalent}}h \tag{4.19}$$

This was then used to evaluate the 0-100 acceleration time for different torque and power output levels. Figure 4.7 shows an example graph of resulting 0-100 acceleration times as a function of different rear wheel peak power levels.

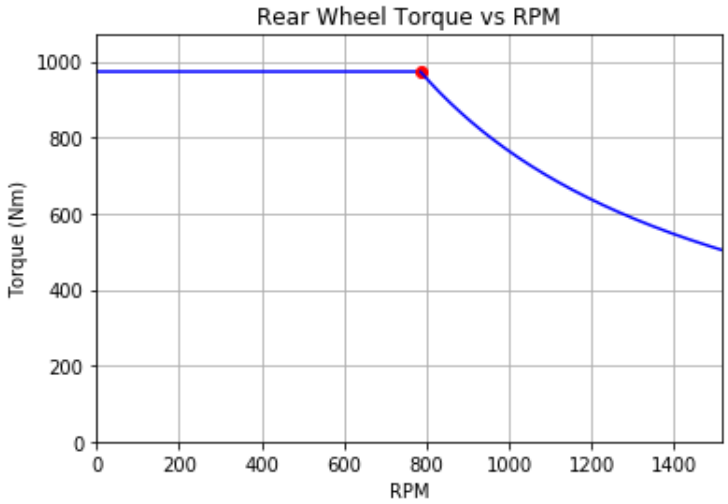

Figure 4.6: Power and torque needed at the rear wheel

The required rear wheel power and torque needed to fulfill all of the performance requirements was found to be 80 kW of peak power and 973 Nm of torque at the rear wheel. A rotational speed of at least 1500 rpm is also needed to reach a top speed of 180 km/h. The resulting torque versus speed graph is presented in Figure 4.6

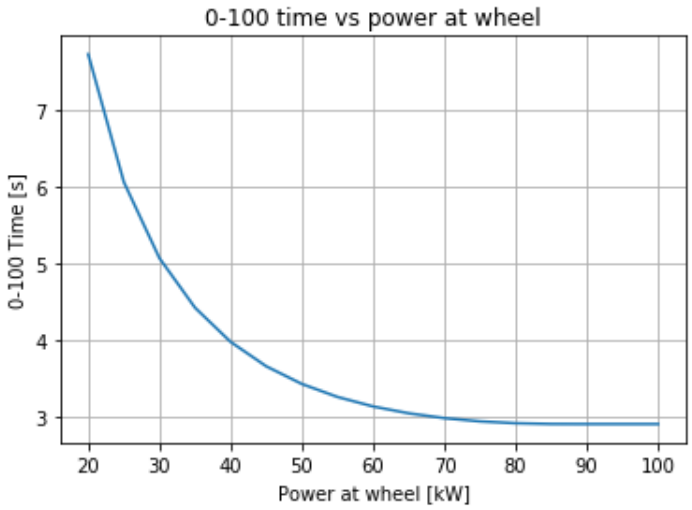

Figure 4.7: Power required at the rear wheel for given 0-100 time

The performance requirements could be difficult to fulfill at the stated maximum cost. Therefore a summary of acceleration simulation results for three different example motors was made. The three motors with required gearing and resulting top speeds for six different 0-100 acceleration times are presented in figure 4.8

Resulting; 0-100 Times, Top speed and Gearing																
0-100 TIME:				3s		3,5s		4s		4,5s		5s		5,5s	
MOTOR	POWER [kW]	TORQUE [Nm]	MAX RPM	Top Speed	Gearing	Top Speed	Gearing	Top Speed	Gearing	Top Speed	Gearing	Top Speed	Gearing	Top Speed	Gearing
Example 1	60	100	8000	-	-	105,5	9	124,5	7,63	140	6,68	147,3	6,45	169,6	5,6
Example 2	86	150	7000	125	6,6	144,8	5,74	164,6	5,05	**184,3**	**4,51**	**203,7**	**4,08**	**222**	**3,74**
Example 3	124	230	6500	**181,6**	**4,25**	**206,4**	**3,74**	**234,6**	**3,29**	**262,5**	**2,94**	**270**	**2,66**	**270**	**2,44**

Figure 4.8: Three different motor examples and gearing for 0-100 times

4.4.2 Power Demand for Top Speed

The top speed of a vehicle will occur when the tractive force equals the resistance forces. For a motorcycle on level ground, the top speed will be reached when

$$F_{tractive}(v_{max}) - F_{drag}(v_{max}) - F_{roll} = 0 \tag{4.20}$$

This will most likely occur when the tractive force is limited by the peak power and not the maximum torque.

$$F_{tractive}(v_{max}) = \frac{P_{max}}{R_{wheel}\,\omega(v_{max})} \tag{4.21}$$

$$\frac{P_{max}}{R_{wheel}\,\omega(v_{max})} - b(\frac{v_{max}}{3.6})^2 - F_{roll} = 0 \tag{4.22}$$

$$\frac{P_{max}}{v_{max}} - b(\frac{v_{max}}{3.6})^2 - F_{roll} = 0 \tag{4.23}$$

This equation was then solved numerically using Python.
If the top speed is known the required power can be calculated as

$$P_{max} = \frac{25\, b\, v^3}{324} + F_{roll}\, v \tag{4.24}$$

With the power of 80 kW needed for the 0-100 acceleration time the requirement of a 180 km/h top speed was found to not be power limited.

4.4.3 Continuous Power Demand

The continuous power output that the powertrain needed to deliver was set by the requirement of continuous riding on a level road without overheating at a certain speed. The required power for this was calculated as

$$P_{countinous} = F_{tractive}(v_{countinous})v_{continous} \tag{4.25}$$

The power demand when riding the motorcycle at a constant speed of 140 km/h on a level road, as stated in the requirements, is 19.9 kW at the rear wheel. The components of the power demand for this riding scenario are presented in figure 4.9.

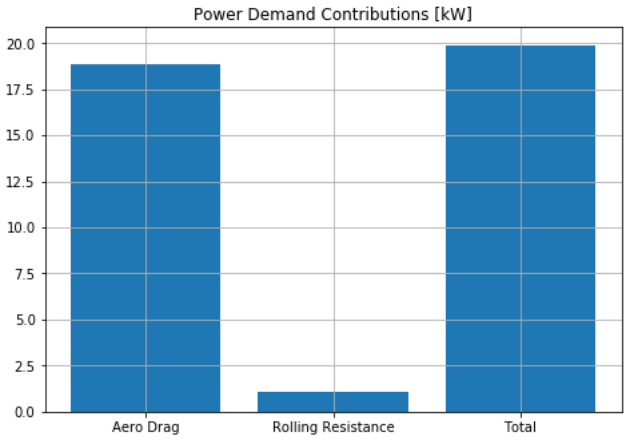

Figure 4.9: Power demand contributions when driving on a level road at 140 km/h

4.4.4 Power Demand for Gradients

Another requirement was stated as "Capable of riding in the Alps without overheating". This is a loosely defined requirement and the first step was therefore to redefine this as a requirement of riding at a constant speed up an uphill gradient.
The road called Grossglockner Road in the Austrian Alps was used. Google Maps was then used to find the distance travelled and the change in altitude when driving from Ferliten in the valley to Fucher Törl, which is close to the highest point of the road. The average gradient could then be calculated

$$Gradient = \arctan(\frac{Distance}{\Delta_{Altitude}}) \approx 5.4^\circ \tag{4.26}$$

The tractive force needed to maintain a constant speed when driving up a gradient with a constant speed

$$F_{tractive}(v_{alps}) = F_{drag}(v_{alps}) + F_{roll} + F_{gradient} \tag{4.27}$$

Where $F_{gradient} = mg\sin(5.4°)$ and the speed was set to be $v_{alps} = 100km/h$ since this is the speed limit in Austria. The required power was calculated

$$P_{gradient} = F_{tractive}(v_{alps})v_{apls} \tag{4.28}$$

The required power when driving up a 5.4° gradient at 100 km/h is 15.7 kW at the rear wheel which is lower than in the case of riding on a level road at 140 km/h. This gradient case could thus be ignored when designing the drive train.

4.4.5 Negative Torque

An early requirement was given to be 'able to handle negative torque during regenerative braking'. An estimation of how much regenerative braking torque the rear tyre/wheel could generate was needed to redefine this requirement. This was calculated in the same way as the maximum tractive force during acceleration using equation 4.11, with the only difference being the change of sign of the acceleration.

$$F_{zr} = mg\frac{Wb - l_r}{Wb} - ma\frac{h_{cog}}{Wb} \tag{4.29}$$

If $\mu = 1$ then $F_{zr} = F_{xr} = -ma$, thus

$$F_{xr} = mg\frac{Wb - l_r}{Wb} - F_{xr}\frac{h_{cog}}{Wb} \tag{4.30}$$

Solved for F_{xr}

$$F_{xr} = \frac{mg\frac{Wb-l_r}{Wb}}{1 + \frac{h_{cog}}{Wb}} = 324\ N \tag{4.31}$$

4.5 Range and Battery Capacity

The range of an electric motorcycle is one of the most important performance aspects for the end user and is largely determined by battery capacity, drivetrain efficiency, riding style, resistance forces and more. The required battery capacity needed to achieve the required range specified in appendix A was calculated using three methods. The first was a simple calculation using constant speed and the other two use a QSS-based approach with driving cycles. The first of the two is a range calculation Python script and the second is a Simulink model built using the Simulink toolbox called QSS-Tb.

4.5.1 Constant Speed Range

A range requirement of 230-250 km when driving at a constant speed of 110 km/h on a flat road was stated in the requirements, see appendix A. The range and thus required battery capacity were approximated by first assuming a drivetrain efficiency and a usable battery capacity and then calculating the resulting range. Firstly the constant power draw was calculated using equation 4.25

$$P_{110} = F_{tractive}(v_{110})v_{110} \tag{4.32}$$

The time needed to discharge the battery is then

$$t_{discharge} = \frac{P_{110}}{Capacity\,\eta_{drivetrain}} \tag{4.33}$$

Lastly, the range when riding at a constant speed was calculated

$$Range = t_{discharge}v_{110} \tag{4.34}$$

The energy consumption while riding at a constant 110 km/h on a flat road is 113 Wh/km. For this case, a usable battery capacity of 28.5 kW is needed to achieve a range of 250 km

4.5.2 Range Calculation

A Python script was made based on the QSS method where the needed force is calculated from the speed in a pre-defined driving cycle. The vehicle is assumed to have a constant speed and acceleration for each time step. The time step in most driving cycles aswell as the WMTC is one second, $h = 1$. The average acceleration for each time step was calculated as

$$\bar{a}(t) = \frac{v(t) - v(t-h)}{h} \tag{4.35}$$

The acceleration force could then be calculated as

$$F_{acceleration}(t) = m_{eqv}\,\bar{a}(t) \tag{4.36}$$

The tractive force is then

$$F_{tractive} = \begin{cases} F_{acceleration} + F_{drag} + F_{roll} & \text{if } F_{acceleration} + F_{drag} + F_{roll} > 0 \\ 0 & \text{if } F_{acceleration} + F_{drag} + F_{roll} \leq 0 \end{cases} \tag{4.37}$$

This model does not include regenerative braking and therefore the tractive force is 0 when the negative acceleration is greater than the resistance forces. Meaning that the normal hydraulic brakes are being used. This is how the range test is performed during homologation testing.
The power and the energy have the same value for each step since the step size is one second. The energy and power is calculated as

$$E(t) = F_{tractive}\, v(t)\, h = F_{tractive}\, v(t)\, 1 \tag{4.38}$$

$$P(t) = F_{tractive}\, v(t) \tag{4.39}$$

The drivetrain energy delivered to the wheel/ground during the cycle

$$E_{cycle} = \sum_{t=0}^{t_{end}} E(t) \tag{4.40}$$

The total energy used during the cycle will be the drivetrain energy plus the energy used by the low voltage and accessory systems called E_{draw}. The average energy consumption for the drive cycle can then be calculated using the efficiency $\eta_{drivetrain}$ for the complete drive train from the battery to the wheel/ground.

$$Consumption = \frac{(E_{cycle} + E_{draw})}{Total\ distance}\ \frac{1}{\eta_{drivetrain}} \tag{4.41}$$

Lastly, the range for a motorcycle with a given capacity was calculated as

$$Range = \frac{Capacity}{Consumtion} \tag{4.42}$$

4.5.3 QSS Toolbox Simulink Model

A motorcycle model was also made in Simulink using the QSS-TB, an abbreviation of Quasi-Static Simulation Toolbox. This was done to verify the results of the Python simulation but also made implementing motor efficiency maps require less work. An example of a battery electric vehicle (BEV) with a single-stage transmission can be seen in figure 4.10. The blocks of the model are, from left to right; the driving cycle, the vehicle, the wheel, the transmission, the motor and the battery. All of these blocks need their respective input parameters relevant to the specific vehicle to be simulated. The input parameters required for the model are;

- Vehicle total mass
- Coefficients of drag, C_d and rolling resistance C_r
- Effective wheel rolling radius
- Equivalent inertia mass
- Transmission efficiency and gear ratio
- Motor torque, speed, efficiency map and inertia
- Battery capacity, state of charge and configuration

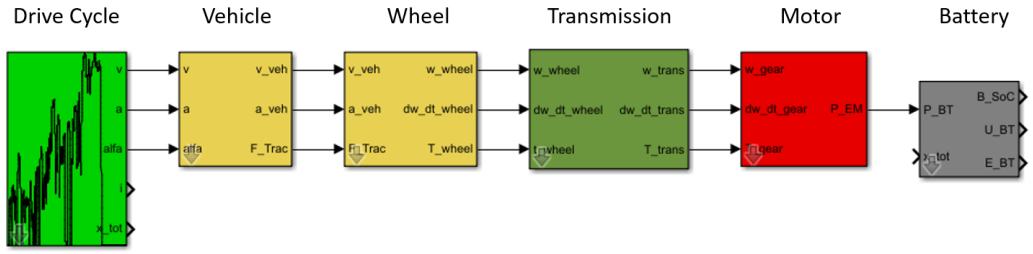

Figure 4.10: An example of a BEV with a single-stage transmission model in QSS-TB

4.5.3.1 The Driving cycle

This simulation uses a QSS-based approach where the resulting forces are calculated from an average speed, acceleration and gradient for a discrete-time period. QSS-TB uses a time step of one second. The driving cycle block is defined as three vectors of speed, acceleration and gradient. The WMTC cycle and modified versions of the WMTC cycle were used.

4.5.3.2 Vehicle

The Vehicle block of the QSS-TB model takes the velocity, acceleration and gradient as inputs from the driving cycle block and has the parameters; vehicle mass, coefficients of drag- and roll, frontal area and mass increase due to inertia. Converting the EU coefficients a and b to C_r and C_d

$$C_r = \frac{a}{m_{tot}\, g} = 0.0088 \tag{4.43}$$

$$C_d\, A_{frontal} = \frac{2\, b\, 3.6^2}{\rho_{air}} = 0.5230 \tag{4.44}$$

The frontal area was set to $A_{frontal} = 1.5\ m^2$ and the coefficient of drag was calcualted

$$Cd = \frac{0.523}{A_{frontal}} = 0.3487 \tag{4.45}$$

The mass increase due to inertia was calculated

$$Mass_{increace} = \frac{m_{eqv} - m_{tot}}{m_{tot}} = 4.254\% \tag{4.46}$$

4.5.3.3 The Wheel

The wheel block only has the wheel diameter as an input parameter.

4.5.3.4 Transmission

The transmission block of the model receives wheel speed, acceleration and torque from the wheel block as inputs and sends the resulting motor speed, acceleration and torque as outputs to the motor block. The transmission parameters are gear ratio and efficiency. The gear ratio was determined for each simulated motor from the 0-100 acceleration requirement. The efficiency of the transmission was set to values found in the book Maskinelement [14] for different types of transmissions. Transmission concepts/layouts that use two stages were modelled as one transmission block with the resulting total gear ratio and the total efficiency calculated as

$$ratio_{total} = ratio_{stage\ one}\, ratio_{stage\ two} \tag{4.47}$$

$$\eta_{total} = \eta_{stage\ one}\, \eta_{stage\ two} \tag{4.48}$$

4.5.3.5 Motor

The motor block receives the required speed, acceleration and torque from the transmission block and the output is the power needed from the battery. The motor parameters are; the efficiency map, motor speed range, motor torque range, maximum motor speed and maximum motor torque. All of these parameters needed to be acquired from motor manufacturers/suppliers. Figure 4.11 shows a motor efficiency map for a specific motor. This map was made by approximating the manufacturer-provided efficiency map found in the data sheet.

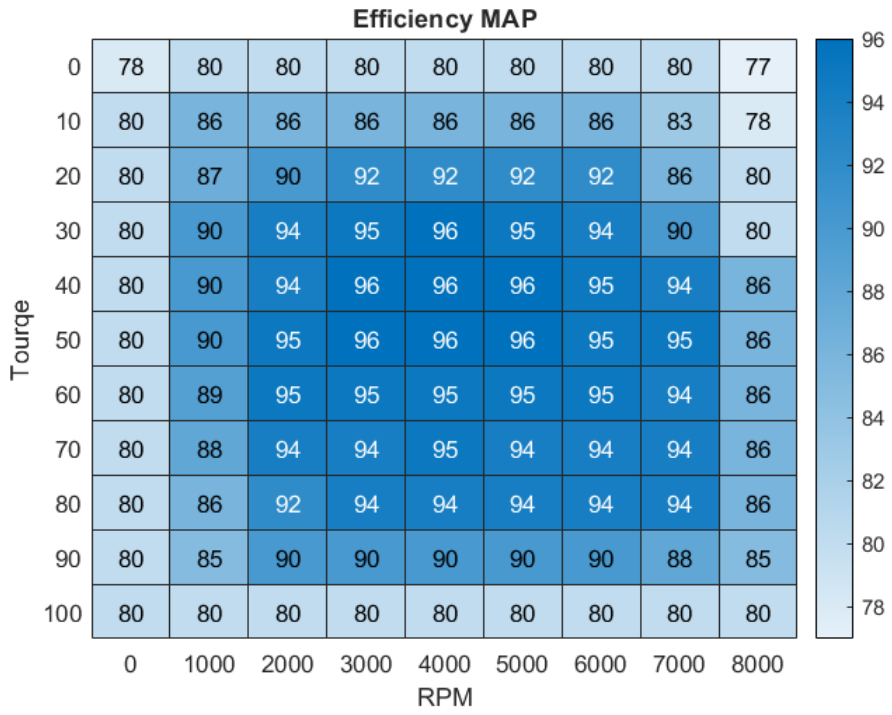

Figure 4.11: A motor efficiency map

4.5.3.6 Battery

The battery model input parameters are; the number of cells in series, the number of cells in parallel and the intital state of charge (SOC). QSS-TB uses a cell model where each cell has a capacity of 96 Ah and an open circuit voltage of 3.8 V. The number of cells in series was set to match the nominal voltage specified in the requirements, see Appendix A. The number of parallel cells was set to achieve enough capacity to run the driving cycles without draining the SOC too much since the QSS-TB manual [29] recommends not running a SOC lower than 10% or more than 90%.

4.5.4 Battery Capacity

The resulting energy consumption from the Python script calculation and QSS-TB model simulation was then used to calculate the required battery capacity needed to fulfil the range requirements. Both of the Qss-based simulation methods showed an energy consumption of around 85 Wh/km for the WMTC driving cycle. This means that 21.5 kWh of usable battery capacity is needed to achieve a range of 250 km.

4.6 Hub Motor Handling Evaluation in BikeSim

The Hub motor concept will affect the performance and handling of the motorcycle negatively in three ways; more rotational inertia of the wheel, added yaw inertia for the whole bike and a drastic increase in un-sprung mass of the rear wheel.
Two models of the motorcycle were made in the vehicle dynamics simulation software called BikeSim in order to evaluate the negative handling properties of a motorcycle with a hub motor. One with a hub motor and the other with an onboard motor. The two models were then run in two different driving scenarios; a double lane change manoeuvre and hitting a small sharp bump. In figure 4.12 the BikeSim graphical model of a sports bike can be seen

Figure 4.12: BikeSim graphical model for a Sports bike

4.6.1 Onboard Motor Model

The onboard motor model was made using the predefined model in BikeSim called Sports, Big: Chain Drive as a starting point. The parts of the model that were modified are;

- Vehicle unsprung mass
- Rider
- Wheels

The following sections will describe how these parts were changed in order to model the motorcycle with an onboard motor.

4.6.1.1 Onboard Motor Unsprung Mass Model

Firstly the sprung mass was increased from 165 kg to 193.05 kg so the total mass of the motorcycle would be 240 kg. Secondly, the wheelbase was increased from 1370 to 1450 mm and the height of the sprung mass CoG was also increased by the same amount of 5.8%. Then the CoG x-location of the sprung mass was moved from 560 to 640 mm in order to achieve a 50/50 weight bias front to rear (for motorcycle and rider system). For the inertia of the sprung mass, the radii of gyration was increased by the same amount as the WB change, that is 5.8%. The onboard motor sprung mass model can be seen in figure 4.13.

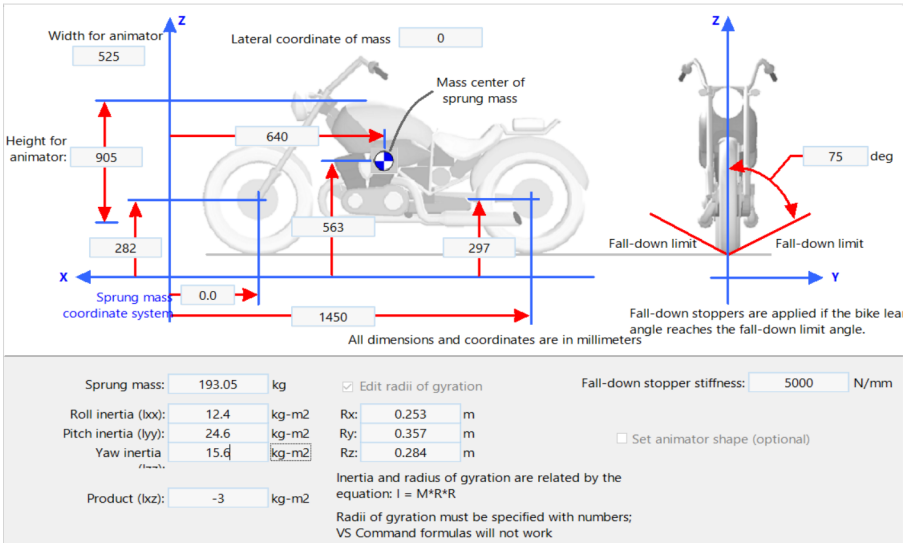

Figure 4.13: Onboard motor sprung mass model

4.6.1.2 Rider Mass Model

The starting point's rider model mass was only 69 kg. To address this both the upper body and lower body mass of the rider were increased by 9.7% to reach the target rider mass of 75 kg. The rider's upper and lower body CoG location was changed in the x-direction by the ratio of the WB change in order to get the same rider-to-bike longitudinal weight bias as the starting point. The rider mass CoG location was also changed in the z-direction by 5.8%, which is the same as the change in z for the CoG of the sprung mass. The rider inertia was also increased by 9.7% by assuming that the proportions of the rider's mass remain the same, i.e. the same radii of gyration but an increase in mass. The rider model can be seen in figure 4.14

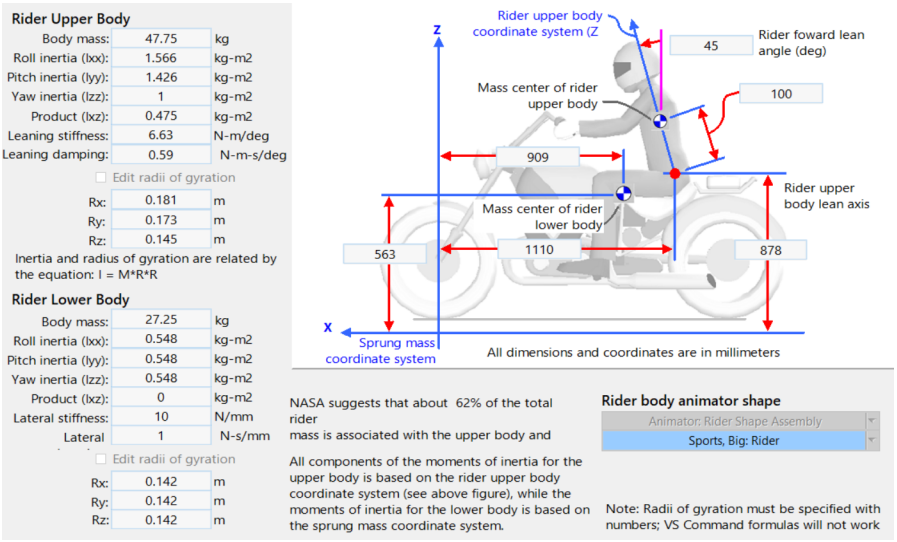

Figure 4.14: 75kg rider model

4.6.1.3 Wheel Models

For the wheel models, the only modification to the starting points wheel models was the rotating inertia's.

4.6.2 Hub Motor Model

The onboard motor model was then modified to represent a motorcycle with a hub motor. The parts of the model that were modified to make the hub motor model are covered in this section. They were the rear wheel and sprung mass.

4.6.2.1 Hub Motor Rear Wheel Mass

The hub motor's mass was determined using the best motor torque density found in the paper [30] and the previously determined peak wheel torque. Assuming that the hub motor has no gearing i.e. direct drive the mass can be calculated as

$$m_{hub\,motor} = \frac{T_{peak}}{Torque\ density} \approx 56\ kg \tag{4.49}$$

For this mass, the power requirement can still be fulfilled with the stated power density of the same motor. The mass of the hub motor wheel was assumed to be the hub motor mass and the tyre

$$m_{hub\,motor\,wheel} = m_{hub\,motor} + m_{rear\,tyre} \approx 62.26\ kg \tag{4.50}$$

4.6.2.2 Hub Motor Rear Wheel Inertia

The rotational inertia of the motor was approximated by assuming that half of the motor mass is rotating and calculating the MoI of a cylinder with that mass and a diameter of 17". This resulted in $J_{hub\,motor} = 0.65\ kgm^2$. The total MoI of the hub motor wheel was assumed to be that of the motor and tyre but not the cast wheel.

$$J_{hub\,motor\,wheel} = J_{hub\,motor} + J_{rear\,tyre} - J_{rear\,wheel} = 1.22\ kgm^2 \tag{4.51}$$

4.6.2.3 Hub Motor Sprung Mass model

This model was made by modifying the onboard motor sprung mass model by reducing the sprung mass by the weight of the onboard motor. An onboard motor's mass was calculated using the same method and torque density as the hub motor but implementing a 4.5:1 gear ratio.

$$m_{onboard\,motor} = \frac{T_{peak}\ gear\ ratio}{Torque\ density} \approx 12.5\ kg \tag{4.52}$$

This mass was then reduced from the sprung mass of the Hub motor model. A further 35 kg had to be removed from the hub motor sprung mass in order to meet the requirement of a maximum total weight of the motorcycle of 240 kg. A summary of the masses can be seen in figure 4.16. The x-location of the CoG was also changed in order to again get a 50/50 weight bias front to rear.

SPORTS BIG (Baseline)		ONOARD MOTOR		HUB MOTOR	
sprung mass	165	sprung mass	193,05	sprung mass	145,49
steering head	10	steering head	10	steering head	10
front unsprung	7,25	front unsprung	7,25	front unsprung	7,25
rear unsprung	8	rear unsprung	8	rear unsprung	8
front wheel	7	front wheel	7	front wheel	7
rear wheel	14,7	rear wheel	14,7	rear wheel	62,26
TOTAL MASS	211,95	**TOTAL MASS**	240	**TOTAL MASS**	240

Figure 4.15: Masses of bodies for the different models

4.6.3 BikeSim Simulations

Two scenarios were simulated; a double lane change manoeuvre, (DLC), where the steering angle and torque were compared. The second scenario that was simulated was hitting a small sharp bump at 40 km/h, here the acceleration of the sprung mass i.e. (how much the rider will feel the bump) was compared. The results of these simulations are presented in this section.

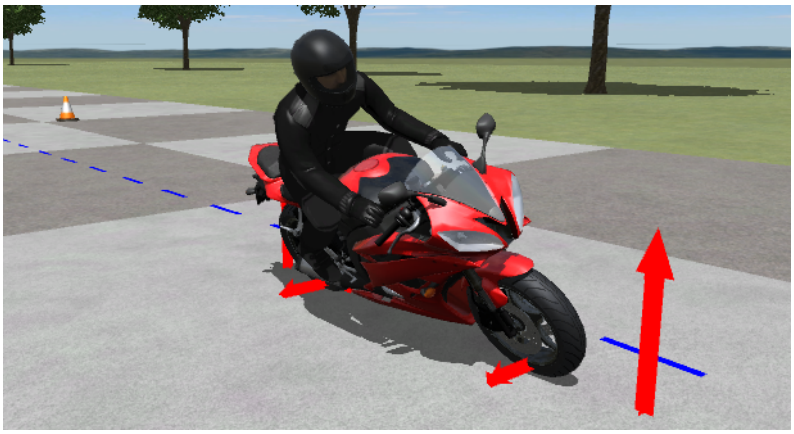

Figure 4.16: BikeSim DLC simulation video graphic

4.6.3.1 Double Lane Change at 140 km/h

The required steering angle was the biggest difference between the two models in the double lane change manoeuvre at 140 km/h. The hub motor model required 0.1587° more steering angle for the same path which is a difference of 21.8% more compared to the baseline. The required steering torque was however roughly the same. The required steering angle can be seen in figure 4.17.

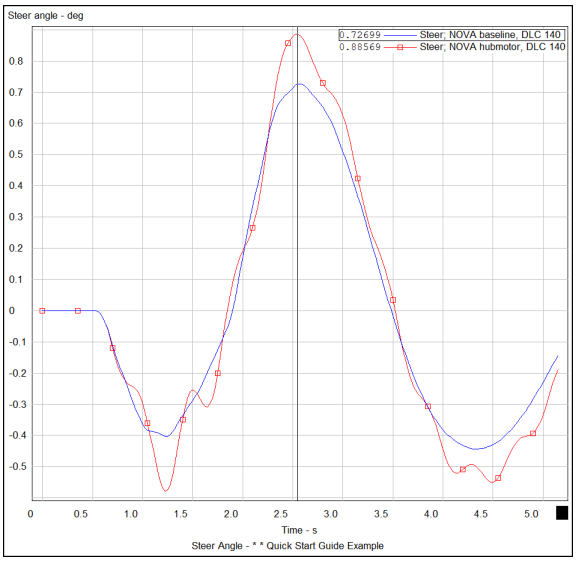

Figure 4.17: DLC 140 steering angle

4.6.3.2 Double Lane Change at 100 km/h

The hub motor model required 22.8% more steering angle and 6.2% more steering torque in the double lane change manoeuvre at 100 km/h compared to the onboard motor model. The resulting graphs for steering angle and torque can be seen in figure 4.18

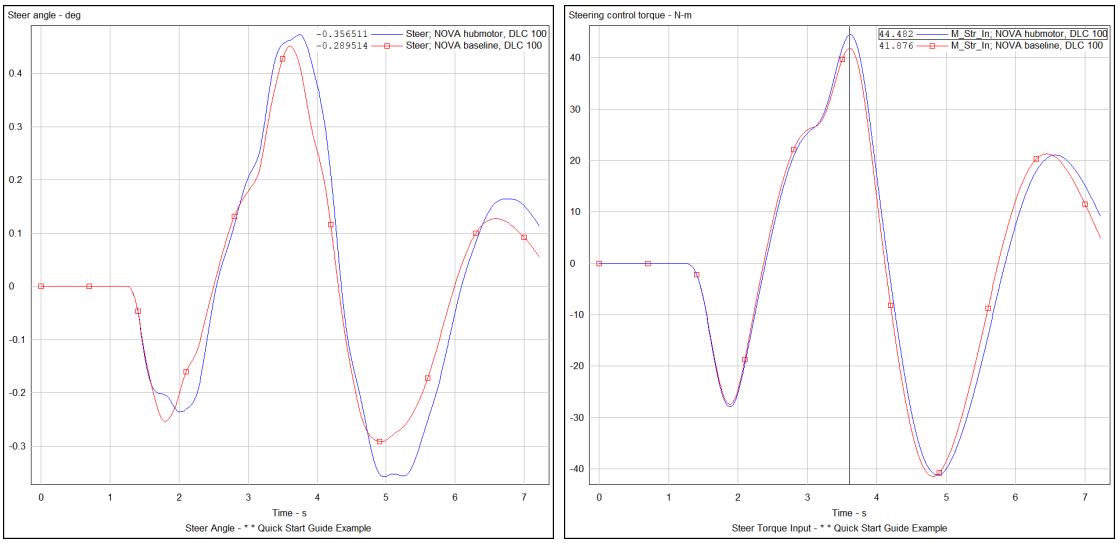

Figure 4.18: DLC 110 steering angle and torque

4.6.3.3 Sharp Bump Simulation

The hub motor model had 31.4% more maximum vertical acceleration of the sprung mass compared to the onboard motor model when hitting a small sharp bump at 40 km/h. The accelerations of the sprung masses when hitting a small sharp bump can be seen in figure 4.19.

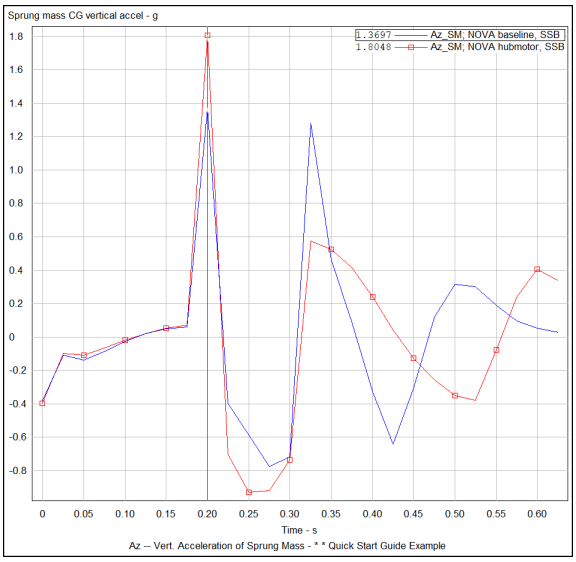

Figure 4.19: Vertical acceleration when hitting a small sharp bump

4.7 Electric Motors

The characteristics and geometries of axial and radial flux motors make them suitable for different powertrain configurations.

Benefits of using axial flux motors:

- Torque density: One of the main benefits of using axial flux motors is the high torque density. This enables a powertrain without a primary transmission and thereby drastically reduces the complexity.
- Geometry: The geometry of axial flux motors makes them well suited to be placed concentrically with the swing arm centre. Motors with hollow shafts are available, making it possible to use a conventional swing arm shaft.

Drawbacks of axial flux motors:

- Diameter: The diameter of an axial flux motor can be a problem for the overall vehicle packaging, especially for fitting the battery cells. A large motor diameter will also result in a longer swing arm.
- Rotor inertia: The larger diameter of an axial flux motor increases the rotational inertia. This can affect the vehicle dynamics and agility of the motorcycle negatively.
- Power density: The high torque density of axial flux motors comes at the expense of lower power density than a radial flux motor.
- Cost: Axial flux motors are gaining popularity within the automotive sector but are still relatively costly.

Benefits of using radial flux motors.

- Power density: The radial flux motors typically have higher operating speeds and thereby a higher power output.
- Availability: More of the shelf options of radial flux motors are available.

Drawbacks of radial flux motors:

- Low torque density: Radial flux motors typically operate at high speeds and therefore a primary transmission is needed. The primary transmission is typically one of the most complex mechanical components in an electrical motorcycle powertrain.
- Dimensions: Radial flux motors in this power range tend to be longer than their axial flux counterparts. This together with the addition of a primary transmission makes it harder to fit the motor in the swing arm centre.

4.8 Cost Estimation

Cost estimations were conducted to ensure that the intended powertrain cost could be met. This was done by requesting quotations on components and systems from suppliers as well as investigating how different manufacturing methods could be used to lower production costs depending on the production volume.

4.8.1 Manufacturing and Reliability - Primary Transmission

The primary transmission of an electric motorcycle can be one of the most complex systems to design, manufacture and assemble. Due to this, the aim was to utilize reliable and proven transmission types. Transmission type was ranked with regard to manufacturability and reliability.

4.8.1.1 Direct Drive

The motorcycle manufacturer ZERO Motorcycles has proven that a powertrain without a primary transmission can be utilised. The complexity in terms of design manufacturing and maintenance is significantly lower for a transmission layout without primary transmission.
For this configuration to work a motor with high torque is required since the speed ratio of the final drive is geometrically limited. It was found that motors with the required power and torque tend to be relatively costly.

4.8.1.2 Spur Gear Train

Transmissions relying on spur gears are the most common type of transmission in ICE motorcycles together with many other sectors of the industry. ICE motorcycles are often using straight cut gears, this has benefits in terms of easier manufacturing processes and low axial thrust. In an electrical powertrain, the higher meshing noise of the straight-cut gear set will be far more noticeable and therefore a helical set is more suitable.

A gear train requires good surface properties, hardness and tolerances as well as well-aligned shafts and flank plays to ensure silent operation and long service life of the transmission. This puts high demands on dimensional accuracy not only for the shafts and gears but also for the gearbox housings. A spur gear transmission is by nature bigger and the transmission housing is more complex than a planetary gearbox due to the offset shafts.

4.8.1.3 Planetary Gear Train

Standardized planetary gear trains are available from several suppliers and they are relatively simple to package in a mid-ship powertrain configuration due to the compact format. Both straight-cut and helical planetary gear sets are available.

The compact format of the planetary gear set would also make the design and manufacturing of the transmission housing less complex and more cost-effective compared to the other types of primary transmissions.

A planetary gear set will always have more tooth engagement than a conventional spur/helical gear set due to the planet gears and therefore more narrow gear can be used. The planet gears also reduce the stress on the transmission housing.

4.8.1.4 Multi Stage Transmission

A multistage transmission could have performance benefits. The two types of power shifting transmissions considered were automatic planetary transmissions (APT) and dual-clutch (DCT). Both types would require significantly more resources for design and testing while adding complexity and more failure points. The transmission control system must be tuned to reduce clutch wear and ensure predictable shifts for good drivability.

Both APT and DCT are traditionally relying on multi-disc wet clutches to enable high torque transfer and controllable clutch slip. By sharing the same fluid between the clutches, bearings and gears the risk of contaminating sensitive components with friction material particles increases and thereby the failure risk.

4.8.1.5 Silent Chain

Silent chain transmissions are becoming more frequently used within the automotive sector in all-wheel drive systems, cam chains as well as primary transmissions for motorcycles and snowmobiles.

The silent chain is an interesting mashup between an involute spur gear and a chain transmission. The biggest benefits in terms of manufacturing are that more standardized components could be used and that the tolerances of shaft placement could be bigger. Long shaft distances can be achieved without idler gears and the motor placement is therefor more free compared to planetary transmissions of spur gears.

Lower speed ratios are possible to achieve than with conventional gear-based transmissions and a chain capable of transferring the desired power will be relatively wide. The system also needs a tension system capable of both positive and negative (regenerative) torque.

4.8.2 Manufacturing and Reliability - Final Drive

A big part of the company's DNA lay in the design of the motorcycles and the looks of the final drive are essential for the overall stance of the bike. The final drive can also be the biggest contributor to noise emissions from the powertrain system and a silent operating and efficient system is required. The final drive must ensure low maintenance.

4.8.2.1 Shaft Drive

Motorcycle producers like Moto Guzzi and BMW Motorrad have a tradition of producing motorcycles with shaft drive systems. In essence, the system consists of a splined drive shaft, two universal joints and a pinion and ring gear set. Due to the expense involved during the design and manufacturing of this type of final drive, the design tends to stay the same for a long time and is used for several models. BMW Motorrad currently have two types of shaft drive systems in production:

- The bigger design is used for all 1250 cc models and has been in production since 2011

- The smaller design was used for all 1200 cc models between 2003 and 2011 and is currently used in the R NineT.

Furthermore, the model range of shaft-driven BMW motorcycles has been gradually reduced from spanning across the entire model range to only including the top-of-the-line flagship models. Two BMW models with similar performance are the BMW R1250R with a two-cylinder boxer engine and shaft drive which is a classic BMW layout and the more conventional F900R with a parallel twin and chain drive proves that the shaft drive is significantly more expensive. The R1250R is around 50000 SEK more expensive than the F900R.

Bevel gears require tight dimensional tolerances, high surface hardness and excellent surface properties. In order to function properly, operate silently and be reliable the flank play and contact patch between the crown gear and pinion gear has to be adjusted and verified. The production of the bevel gears requires the following production methods according to Krajnik, P and Hashimoto, F and Karpuschewski, B and Jannone da Silva, E and Axinte, D [31]:

- Forging: The gear blank is traditionally hot forged to a rough shape using two dies in a press in order to reduce material consumption and improve material properties. The die tooling will make up for a substantial initial investment before production can start.

- Turning: The forging is turned in a multi-axis CNC lathe to profile the blank, machine bearing and races and bolt circles.

- Gleason machining: The gear cogs are traditionally machined using specialized gear-cutting machines. Gleason machines are commonly used to machine the ring and pinions. The setup time and specialised tooling used makes this type of machine less flexible than conventional CNC mills and are there for more suitable for larger production runs.

- Spline shaping: Splines are commonly used to transfer power to the pinion. The production methods for splines are closely related to those used for straight-cut spur gears. Splines can be machined with form mills using conventional CNC machines or more specialized machines such as hobbing, broaching and shaper machines.

- Case hardening: The surface of the gear is hardened to ensure sufficient hardness while preventing the gears from being too brittle. This is commonly done using an induction heating process followed by oil or water quenching.

- Profile grinding: The tooth flanks are ground using a grinding wheel dressed to the specific cog profile to ensure a good surface finish and dimensional accuracy.

- Superfinishing: The final step of the bevel gear production for EV applications is generally super finishing. Superfinishing serves two important functions, the surface finish can be optimized to ensure good tribological properties and reduce the noise.

- Swing arm/bevel housing: The swing arm and bevel housing are generally pressure cast and machined for aluminium to ensure good material properties. Large components like the swing arm require large tooling and are therefor high initial cost and long payoff time. Additionally, the large size and complexity of the components may need several setups in a VMC CNC or 5-axis machining to perform all operations.

All the steps above require rigours quality control and testing to ensure a reliable powertrain. Hardness, surface finish and dimensional measurements are essential. The challenges of manufacturing a drive shaft system does not stop once the gears, housings and drive shaft are machined, the assembly process comes with a number of challenges.

- Pressing of bearings and seals: The system consists of several bearings and shaft seals. These are components that are sensitive to foreign particles and faulty installations. Contamination of the bearings can drastically reduce the operating life and damaged seals may cause oil leakage.

- Adjusting contact patch and flank play: The contact patch and flank play must be adjusted accurately to ensure durability and reduce wear of the gears.

- Risk of oil leaks due to bad castings or assembly faults: The aluminium castings could have porosity and assembly faults may result in oil leaks.

4.8.2.2 Tooth Belt

Tooth belts are a simple and proven form of final drive that is becoming more and more popular as the demand for silent, efficient and reliable electric powertrains increases. Several established manufacturers are producing belts and pulleys for the motorcycle sector.

The belts are preferably bought in standard lengths and widths to reduce cost while the pulleys can be bought from the belt manufacturer or produced.

- Forging: Pulley blanks are commonly forged from steel or aluminium alloys.
- Machining: Flanges and tooths are machined to ensure good dimensional accuracy and surface finish.
- Surface finishing: The wear resistance of the sprocket can be improved by hard anodizing or other forms of surface treatments

4.8.2.3 Roller Chain

Roller chains are by far the most common type of final drive for ICE motorcycles due to their high reliability and low cost. The roller chain has high noise emissions caused by the meshing of the rollers and sprockets. Roller chains are relatively maintenance intense and require frequent cleaning, lubrication and tensioning.

4.8.2.4 Hub Motor

Hub motors tend to be a reliable powertrain system for lighter EV applications such as mopeds and A1 motorcycles. The hub motor is a part of the unsprung mass and will therefore experience all the forces and vibrations transferred from the road through the tyre. This can cause fatigue of the electrical cables and other components.

4.9 Concept Generation

The initial step of concept generation was to compile a list of partial solutions that later would be used as building blocks in the morphological matrix.
This was done by brainstorming and looking at existing electric motorcycles.

The partial solutions for the powertrain were divided into motors, primary transmission and final drive. These are presented in figures 4.20, 4.21 and 4.22.

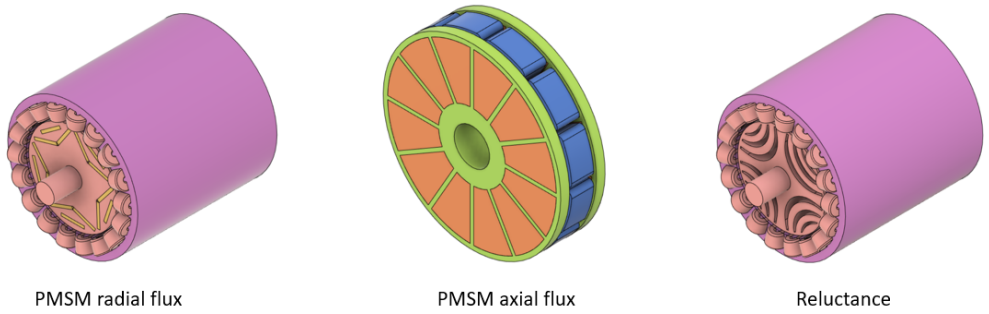

Figure 4.20: Motor types

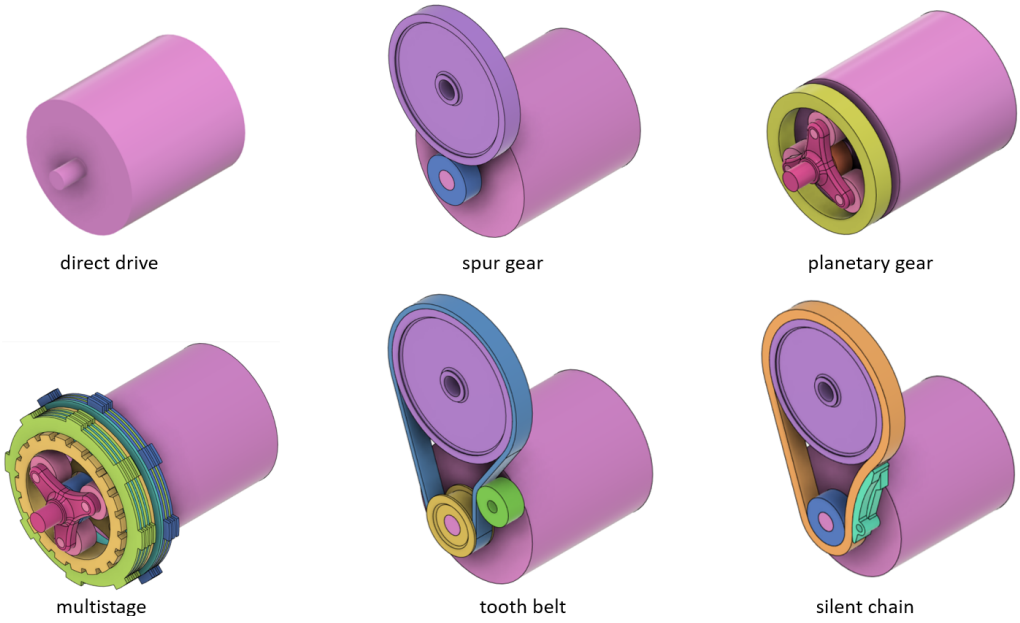

Figure 4.21: Primary transmission configurations

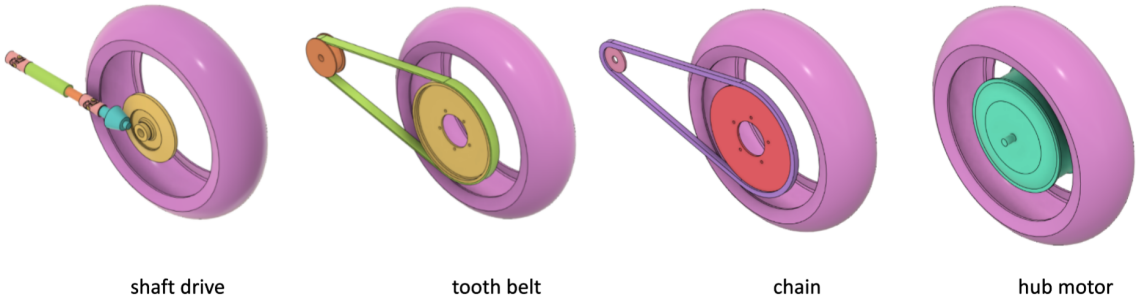

Figure 4.22: Final drive configurations

4.9.1 Morphological Matrix

The morphological matrix was used to combine the partial solutions into concepts. In total 66 individual concepts were generated consisting of different motor, primary transmission and final drive combinations. The morphological matrix can be seen in Appendix C.

4.10 Patent Search

A brief patent search was made using the database Espacenet. 'Electric Motorcycle Transmission' was searched which gave over 36 thousand results and patents for specific drivetrain layouts. One of these patents [32] describes a layout similar to concepts 51, 58 and 65. Another patent [33] describes a layout similar to concepts 47, 54 and 61. A more thorough patent search would be needed but this was deemed to be out of the scope of this thesis.

4.11 Concept Elimination

The concepts were gradually eliminated using an elimination matrix followed by a Kesselring matrix. The information gathered during the project up until this point was used to do a data-driven and objective elimination.

4.11.1 Elimination Matrix

The initial eliminations of the concepts were done using an elimination matrix. In this step, all the concepts that did not meet the requirements were discarded. The elimination matrix can be seen in Appendix F.1.

The geometrical constraints for a motorcycle powertrain require a small, efficient and power-dense motor to physically fit the battery pack, onboard charger and inverter while maintaining good ergonomics and looks. Reluctance motors were not deemed suitable for this application due to the low power density, all concepts using this motor type were therefore eliminated.

The complexity and cost analysis proved that using a shaft drive as the final drive would be too complex to design, manufacture and assemble, and the vehicle dynamics would also be negatively affected by the increased unsprung mass. All the drive shaft concepts were therefore eliminated.

RGNT Motorcycles aim to produce motorcycles that are silent and due to the noise emissions caused by the sprocket engagement, all concepts with roller chains as a final drive were eliminated. Roller chains were also the most maintenance-intense solution considered, requiring cleaning, lubrication and tensioning on a regular basis.

4.11.2 Kesselring Matrix

A Kesselring matrix was used to further reduce the number of concepts. A Kesselring matrix is a systematic way of evaluating concepts by assigning each category of criterion from the requirement spec sheet a weight and then determining how well each concept would fulfill the criteria.

Each category of requirements was weighted by comparing them to each other and then creating a matrix. Both categories were assigned 0.5 when they were considered equally important. Categories considered more important were assigned 1 while less important categories were assigned 0. The relative sum for each criterion was then used in the Kesselring matrix.

By ranking how well each concept fulfils each criterion on a scale from 0-5, where 0 is bad and 5 is excellent, and then multiplying with the weight of the corresponding criterion a comparison number could be obtained. The best-performing concepts get a high number while worse solutions obtain a lower number. The Kesselring matrix reduced the number of concepts to eight remaining.

While being the simplest and possibly the most reliable powertrain configuration the two remaining hub motor concepts were eliminated, mainly due to lack of performance and handling as a consequence of high unsprung mass. Both the remaining concepts using a toothed belt as a primary transmission were eliminated due to the reliability, manufacturing and NHV issues. A reliable system with high belt speeds and short drive centre distance and long intervals between services would be hard to achieve.

The 3 remaining concepts all used a toothed belt as the final drive, PMSM axial or radial flux motors. The most suitable motor and primary transmission configuration are dependent on the overall packaging of the motorcycle as well as what motor and inverter package can be obtained in large enough volume in a good price range.

The remaining concepts are presented in the order as ranked in the Kesselring matrix with the most desired first.

- Concept 32:
  -PMSM axial flux
  -No primary transmission
  -Motor shaft co-centric to swing arm pivot
  -Synchronous belt drive

  The best ranking concept in the Kesselring matrix was based on a PMSM axial flux motor without primary transmission coupled to a synchronous belt drive. The high torque density of the axial flux motors makes them well-suited for this application. The axial flux layout makes for a short motor that is easily integrated into the swinging arm pivot axis.

- Concept 27:
  -PMSM radial flux
  -Planetary gear set
  -Motor and output shaft co-centric with swing arm pivot
  -Synchronous belt drive

  The second best ranking concept in the Kesselring matrix was based on a PMSM radial flux motor coupled to a planetary gear set and a synchronous belt drive. The radial flux motors can have high power density but are generally operating at higher speeds. A planetary gear set was determined to be the most compact option, which is needed in order to fit the powertrain concentric to the swing arm pivot.

- Concept 26:
  -PMSM radial flux
  -Spur/helical gear set
  -Output shaft co-centric with swing arm pivot
  -Synchronous belt drive

  The last remaining concept is based on a PMSM radial flux motor with a gear train to transfer the power to a synchronous belt drive. By using spur or helical gears in the primary transmission the motor can be moved away from the swing arm pivot and therefore a longer motor can be used. With additional idler gears the motor can be moved even further away from the output shaft.

The most suitable placement of the drive pulley was determined to be coaxial with the swingarm pivot in order to reduce the change in belt tension and anti-squat behaviour as the rear suspension moves throughout the stroke. This results in that the motor, primary transmission and drive pulley must fit in this region. The most simplistic powertrain would be a motor mounted concentrically to the swing arm axle without a primary transmission. This would however require a motor with a relatively high torque output since the belt transmission is limited to a max speed ratio of around 4.5:1. For motors with less torque and higher operating speeds a planetary reduction would be the most suitable form of primary transmission with off-the-shelf options for the geartrain available. A planetary gear set has a very small form factor while being relatively easy to package. Motors too long to fit within the swing arm width constraint require a primary transmission using a silent chain or spur gears in order to place the motor in front or above the drive pulley, this would however result in increased complexity and bulkier design.

4.12 Mechanical Design

The remaining concepts were visualised in CAD and initial mechanical design work was conducted. The main focus was to ensure that the powertrain could fit in the desired position in the frame and not to finalize a complete powertrain design.

4.12.1 CAD Packaging Models

CAD models for the remaining concepts were done to evaluate how the remaining concepts could be packaged. The overall dimensions such as seat height, wheelbase, suspension geometry and battery capacity from the calculations were used to create realistic models. CAD models from different potential motor suppliers were used to test different motor and transmission combinations.

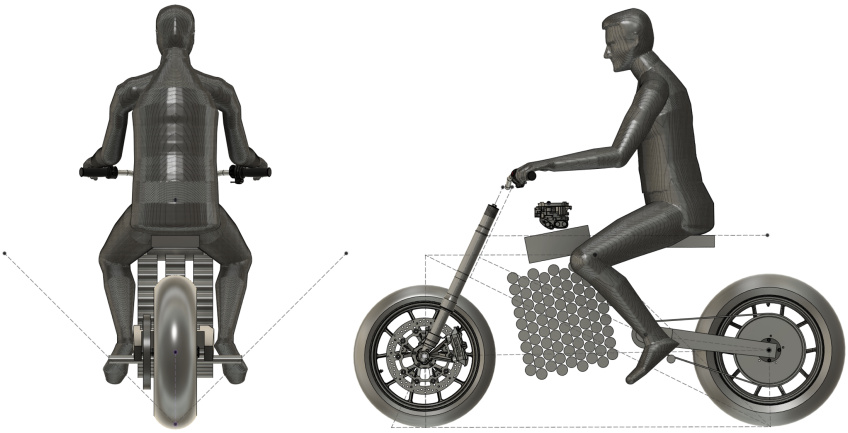

Figure 4.23: Initial Packaging model without motor and inverter

In Figure 4.23 the packaging model can be seen without a motor, inverter and primary transmission. The packaging model was based on the following specifications.

- Seat height: 800 mm
- Tyre dimensions: Front 120/70 R17, Rear 180/55 R17
- Wheelbase: 1450 mm
- Rake angle: 25°
- Swing arm length: 520 mm
- Max lean angle: 45°
- Battery capacity and voltage: 27 kWh, 310 V
- Charging: 6 kW onboard charger with type 2 connector

4.12.2 Ergonomics

Rider ergonomics are important for the overall vehicle packaging. The bike should be a good compromise to suit a broad spectrum of riders. The human builder workbench in CATIA v5 was used to generate anthropology-correct manikins that represent the intended customers.

The manikins were used both to determine suitable positions for the handlebars, foot pegs and seat in order to achieve good riding positions for the rider models but also as a tool to determine where components could be placed and how wide the battery pack could be without interfering with the comfort of the rider.

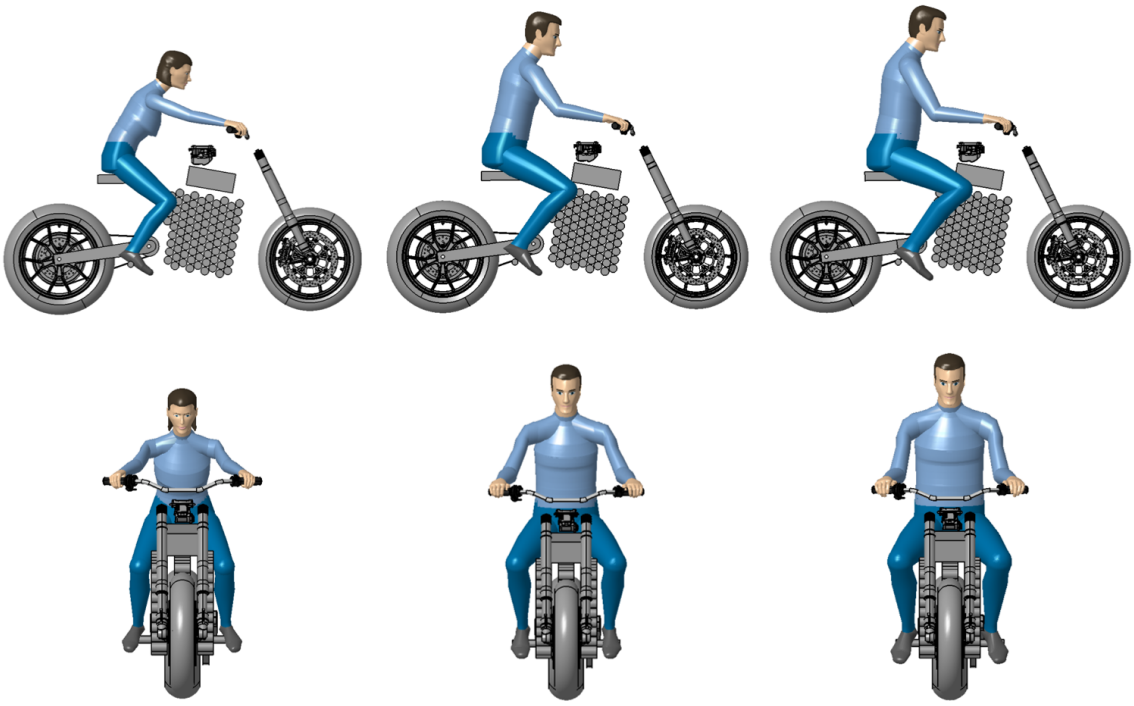

Figure 4.24: Rider posture during straight-line riding

Three different rider models were used to ensure that this motorcycle concept could be operated by a majority of the potential riders. In figure 4.24 the manikins can be seen in a straight-line riding posture on the space claim model for the motorcycle. The 5^{th} percentile female rider can ride the bike but suffers from slightly too short arms and could risk rider fatigue while the rest of the riders have fairly good and relaxed riding positions.

- 5^{th} percentile German female: The smallest manikin represents a female with a length of 1530 mm. This manikin acted as the lower tolerance limit in terms of riders for this motorcycle concept. The distance between the seat and handlebars results in a forward-angled riding position which could cause rider fatigue during longer riding stints and difficulties to manoeuvre the motorcycle at lower speeds. Additionally, the seat height will not allow the rider to have both feet on the ground simultaneously.

- 50^{th} percentile German male: The most likely rider was determined to be a male with a length of 1750 mm. By ensuring that the ergonomics are good for this manikin a majority of the riders should be riding the bike comfortably.

- 95^{th} percentile German male: The biggest manikin represents a male with a length of 1860 mm. The ergonomics for this rider were determined to be good without access to knee or elbow angle.

4.12.3 Belt Drive Design

All three remaining concepts use a synchronous belt drive as their final drive. It was therefore decided to continue the project with the initial design of a synchronous belt final drive. The belt calculations presented in this chapter are based on Optibelt DELTA chain design manual [28], Gates motorcycle and scooter belt drive design manual [20] and Makinelement [14]. Different belt suppliers and belt types were considered during the design process. The tooth profile, cord material, drive centre distance, sprocket diameters, tension system and belt width are parameters that drastically affect the belt life power transfer capabilities of the drive system.

A belt drive typically experiences three main types of failure modes.

- Wear: The tooth flanks will wear over time as a result of the meshing with the pulleys together with the introduction of abrasive particles from the road.

- Stress: High stresses may lead to overloaded teeths and ratcheting when the belt is cogged over on the pulley. High stresses may also lead to belt fractures.

- Fatigue: Bending stress and changing in belt forces cause fatigue in the cord fibres that may lead to fracture.

- Material degradation: The material in the belt will age over time, the process can be faster if the belt is exposed to chemicals of direct UV light.

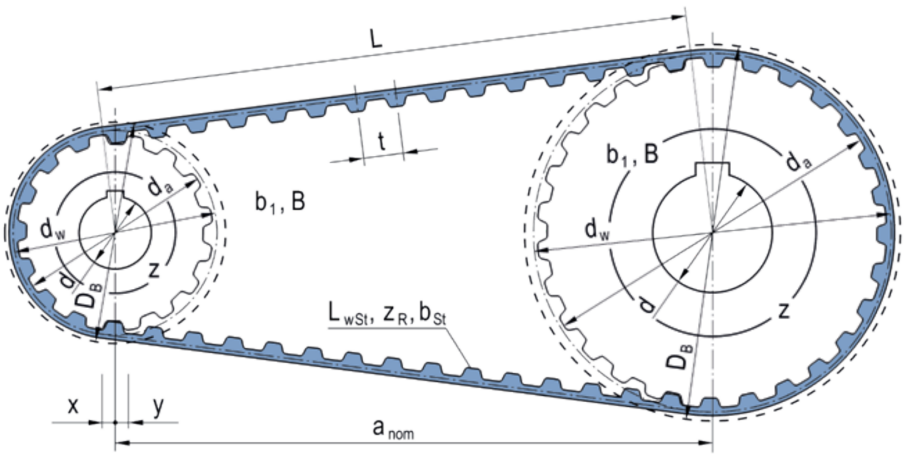

Figure 4.25: Synchronous belt geometry

In figure 4.29 the schematics of the simplest type of synchronous belt transmission consisting of two pulleys and a belt. Depending on the shaft distance and size of each pulley the envelope angles for each pulley will change and thereby the number of teeth engaged will change according to Optibelt [28]

4.12.3.1 Speed Ratio and Geometrical Limitations

The following calculations are done for a speed ratio of 4.5:1. The design considerations affecting the final drive system on top of performance and operation life are the geometrical limitations of the pulleys along with noise emissions. The size of the rear pulley is geometrically limited by the rim and tyre size as well the design language of the vehicle.

Three belt pitches (8 mm, 11 mm, 14 mm) were initially considered. Belts with a large pitch have high torque transfer capabilities but require big pulleys. The maximum belt velocity is lower for a belt with a larger pitch. A more narrow belt can be used with a longer swing arm and bigger pulleys.

Standardized belt profiles for belts and pulleys with 8 mm and 14 mm pitch are available from several suppliers while Gates currently is the only supplier for belts with 11 mm pitch.

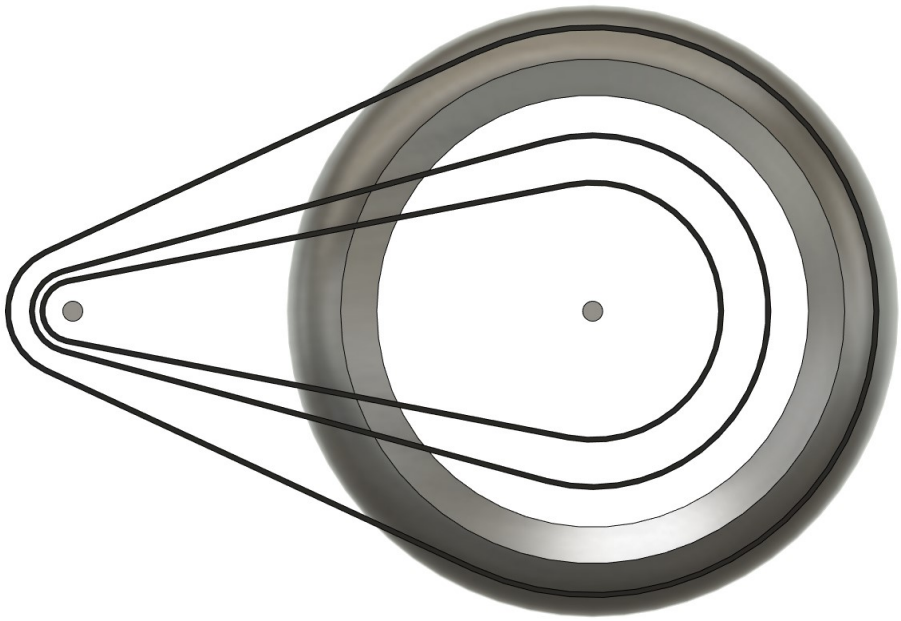

Figure 4.26: Comparison of 8 mm, 11 mm and 14 mm belt pitch

In figure 4.26 a comparison between the smallest possible final drives with a speed ratio of 4.5:1 for each belt pitch can be seen. The minimum amount of teeth for the 8 mm and 11 mm pitch is 22 while the 14 mm belt requires 28 teeth on the drive pulley resulting in a driven pulley almost the size of the rear wheel. The 11 mm pitch was considered to be the best compromise for this application with a relatively compact format and higher power transfer capacity and resistance to tooth ratcheting than a belt with 8 mm pitch. It was therefore concluded that Gates belts with 11mm pitch would be the best compromise between torque transfer capabilities, max belt speed and pulley sizes.

$$a > 0.5 \cdot (d_{w1} + d_{dw2}) + 15\,mm \tag{4.53}$$

$$a < 2 \cdot (d_{w1} + d_{dw2})\,mm \tag{4.54}$$

d_{w1} =Pitch diameter of drive pulley [mm]

d_{w2} =Pitch diameter of driven pulley mm

According to [28] a synchronous tooth belt arrangement without idler pulleys should have a drive centre distance on the interval given by equation 4.53 and 4.54 to prevent ratcheting, vibrations and premature belt failure.

d_{w1} = 77.03 mm
d_{w2} = 346.62 mm

The acceptable drive centre distance interval with the intended pulley size was then calculated to be $226.83 < a < 847.30\,mm$.

4.12.3.2 Swing Arm Length

The swing arm lengths are limited by the nominal drive centre distance, a_{nom}. For the intended configuration the drive pulley will be concentric with the swing arm shaft in order to minimise the change in belt tension as the suspension moves. The driven pulley is concentric with the wheel axle. The number of teeth on the pulleys and the length of the belt itself is deciding factors in setting the nominal drive centre distance [28]. The length of a toothed belt must be a multiple of the tooth pitch and while custom lengths could be a possibility for larger production runs according to Gates [20] it was decided to only use standard lengths for this thesis work.

$$K = \frac{L_{wSt}}{4} - \frac{\pi}{8}(d_{wg} + d_{wk}) \tag{4.55}$$

$$a_{nom} = K + \sqrt{K^2 - \frac{(d_{wg} - d_{wk})^2}{8}} \tag{4.56}$$

L_{wSt} = Standard pitch length of the timing belt, mm

d_{wk} = Pitch diameter of the drive pulley, mm

d_{wg} = Pitch diameter of the driven pulley, mm

a_{nom} = Drive centre distance, calculated with a standard belt length, mm

The pitch diameters of the pulleys, d_{wk} and d_{wg} are dependent on the number of teeth on the pulley. The aim was to design a compact final drive where the diameter of the rear pulley should be as small as possible. The minimum recommended tooth count for a sprocket with an 11 mm pitch is 22, [20].

The pitch diameter for pulleys with 11 mm pitch can be calculated by:
Pitch diameter = $z_x \cdot 3.50125$

To obtain a speed ratio of 4.5:1, z_1 was set to 22 and z_2 to 99 and the desired drive centre distance was as close to 520 mm as possible. Calculations with the available standard belts were performed in order to find the closest match.

L_{wSt} = 1738 mm, the resulting number of teeth 158.

d_{wk} = 77.03 mm

d_{wg} = 346.62 mm

a_{nom} = 518.75 mm

A belt with 158 teeth was determined to be the best match with a resulting nominal drive centre distance, a_{nom} of 518.75 mm.

4.12.3.3 Wrap Angles, Span Length and Teeth in Engagement

The wrap angles and span length for the belt drive were calculated for further use in lifetime and vibration calculations. The number of teeth in engagement affects the stress in each tooth as well as the ratcheting resistance.

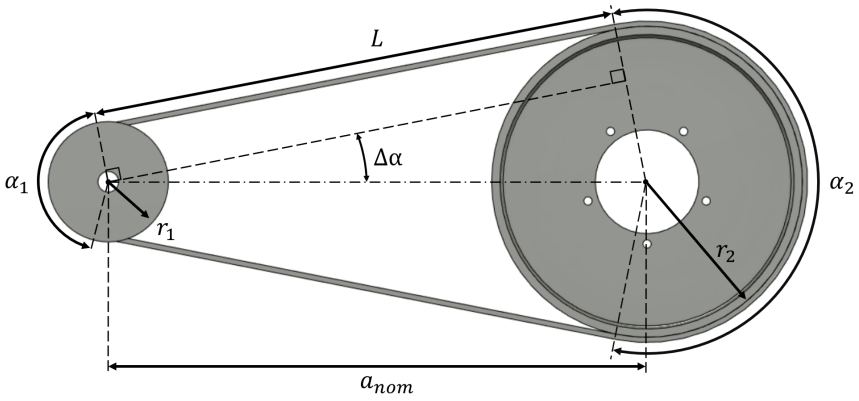

Figure 4.27: Wrap angles and span length

The wrap angles for the drive (α_1) and driven pulley (α_2), the span length (L) and the help angle ($\Delta\alpha$) can be seen in figure 4.27.

$$\Delta\alpha = \arcsin\left(\frac{r_2 - r_1}{a_{nom}}\right) \tag{4.57}$$

a_{nom} = Drive centre distance, calculated with a standard belt length, mm

$r_1 = \frac{d_{wk}}{2}$ = Pitch radius of the drive pulley, mm

$r_2 = \frac{d_{wg}}{2}$ = Pitch radius of the driven pulley, mm

The help angle $\Delta\alpha$ was first calculated to be 15.06° using equation 4.57.

$$\alpha_1 = \pi - 2\Delta\alpha^\circ \tag{4.58}$$

The wrap angle for the drive pulley was calculated using 4.58. The wrap angle for the drive pulley in this belt drive is 149.88°.

$$\alpha_2 = \pi + 2\Delta\alpha^\circ \tag{4.59}$$

The wrap angle on the driven pulley was calculated using equation 4.59. The wrap angle for the driven pulley is 210.12°.

$$z_e = \frac{z_k}{6}\left(3 - \frac{d_{wg} - d_{wk}}{a_{nom}}\right) \tag{4.60}$$

z_k =Number of tooth on the drive pulley

The number of engaged teeth on the drive pulley was calculated using equation 4.60. This was only done for the front pulley since the rear pulley has significantly more teeth engaged and therefore lower stresses and risk for ratcheting. The drive pulley in this belt drive has 9 teeth engaged with the belt.

$$L = a_{nom}\cos\left(\Delta\alpha\right)\ mm \tag{4.61}$$

The span length was determined using the following equation 4.61. The span length for this belt drive is 500.93 mm.

4.12.3.4 Belt Speed

The belt speed was calculated using the following equation. A max drive pulley speed of 6500 rpm was assumed.

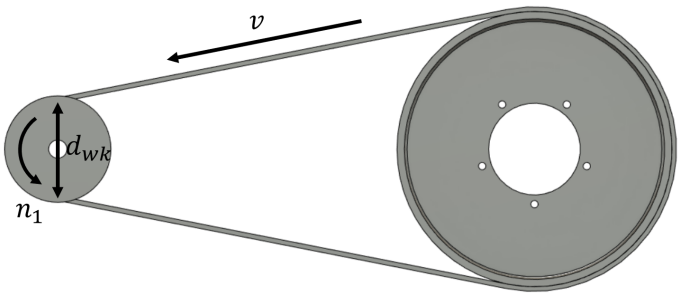

Figure 4.28: Belt speed

$$v = \frac{n_1}{60}\pi\frac{d_{wk}}{1000}\ m/s \tag{4.62}$$

n_1 = Max speed drive pulley, rpm
d_{wk} = pitch diameter drive pulley, mm

For this belt drive the belt max belt speed would be $v_{max,belt}$= 26.22 m/s.

4.12.3.5 Belt Tension and Tension System

Sufficient belt tension without significant change of tension during the suspension stroke is essential to ensure a long and reliable operating life and prevent ratcheting between the belt and sprockets. Different tension arrangements and configurations were evaluated.

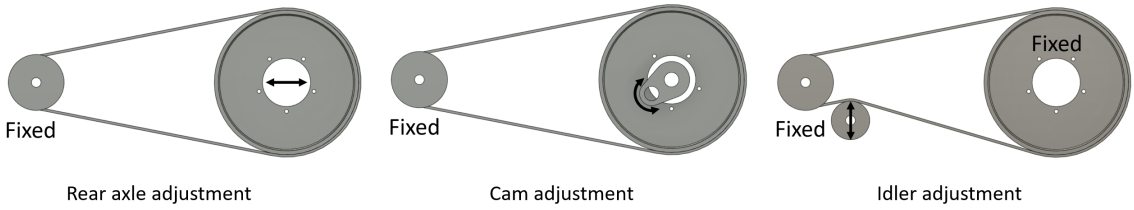

Figure 4.29: Belt tension systems

Three different belt tension systems were considered.

- Rear axle adjustments: This was the most simplistic tension system considered. This configuration is commonly used on ICE motorcycles with a roller chain final drive. The rear axle is moved using an adjustment screw on each side of the swing arm. This allows the pulley alignment to be adjusted.

- Cam adjustment: By mounting the wheel axle on an eccentric cam the belt system can be tensioned by rotating the lobe. This system can be implemented on a single-sided swing arm. A cam tension system adds an extra level of complexity since both the increased number of components and also due to the lack of adjustments for pulley alignment.

- Idler adjustment: A fixed or auto-adjusting idler pulley can be used on the slack side of the belt system. An idler pulley will improve the arc of contact for the dive and driven pulley but belt life may be reduced due to increased bending stress in the belt cord. The idler would also need to be designed in a way that would limit the change of tension as the rear suspension goes through its stroke length. Additionally, the pulley must be able to cope with negative torque during regenerative braking. According to Gates the belt width would have to be increased by 2-3 mm to have the same operating life if an idler is used.

The conclusion was that a traditional rear axle adjustment would be most suited for this vehicle, both due to the cost-effective design but also the possibility to adjust the belt alignment relatively easily.

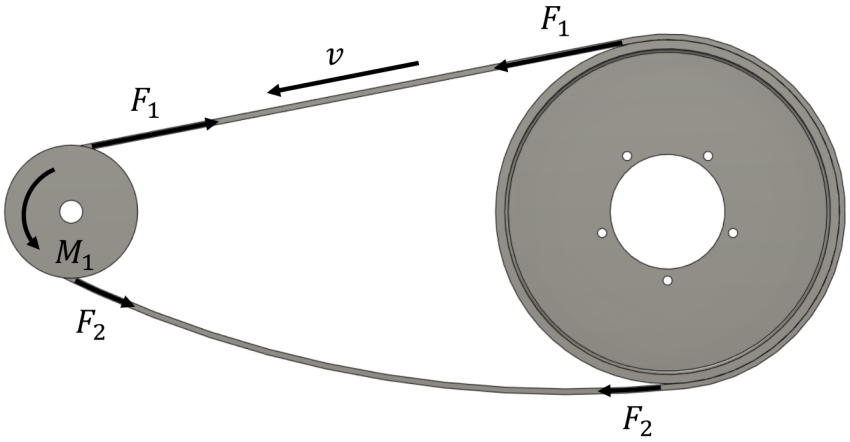

Figure 4.30: Belt forces

The static drive centre force was calculated using the following equation:

$$F_a = 1.4\frac{60 \cdot 10^6 P_N \sin\frac{\beta}{2}}{t\, z_k\, n_k}\ N \tag{4.63}$$

F_a =Static drive centre force, N

P_N = Rated power, kW

β = Arc of contact, degrees

t = Pitch, mm

z_k = Number of teeth of small pulley

n_k = Speed of small pulley, rpm

The static span force was calculated using the following equation:

$$F_T = \frac{F_a}{2\sin\frac{\beta}{2}}\ N \tag{4.64}$$

F_T = Static span force, N

The circumferential belt force was determined using the following equation.

$$F_U = \frac{P_N 1000}{V}\ N \tag{4.65}$$

F_u = Circumferential force, N

V = Circumferential speed, m/s
With the intended speed ratio and top speed, a circumferential belt speed of 26.2 m/s will be obtained at the top speed.
The belt should be tensioned to the frequency determined by the forces acting on the transmission. The appropriate frequency was determined using the following equation.

$$f = \sqrt{\frac{F_T 10^6}{4\, m_k\, L^2}}\ N \tag{4.66}$$

f = Frequency, Hz

m_k = Weight per metre, kg/m

L = Span length, mm

The static drive centre force, F_a for the belt drive was calculated to be 1190 N and the resulting static span force, F_T of 616 N.

The circumferential belt force, F_u is directly proportional to the belt velocity. At the intended top speed of the vehicle, a circumferential force of 6885 N will be present. A belt tension frequency of 61 Hz is recommended for the intended belt drive system.

4.12.3.6 Belt Width and Life Span

The belt width is largely dependent on how the motorcycle is used. To properly determine the lifespan and an appropriate belt width for this application further work has to be done.

Tooth shear life and cord fatigue calculations for the belt transmissions are typically conducted using duty cycle analysis. This was considered to be out of the scope of this thesis work, therefore the rest of the calculations assumed a belt width of 22 mm, as suggested by [20].

4.12.3.7 Belt Alignment and Pulley Flanges

The belt alignment and constraining method are essential aspects of the belt drive system. The belt manufacturers specify tolerances for the allowed misalignment.

Belt misalignment can be divided into parallel and angular misalignment or a combination of both. The allowed miss alignment of a belt and pulley system is dependent on several factors. The drive centre distance a_{nom} and the belt width are the most influential. A wider belt tolerates less angular misalignment than a narrow belt. Misalignment may result in increased wear and the risk of premature belt failure as well as increased frictional losses and sound emissions, as a result of uneven engagement and flange riding.

The belt must be constrained to the pulleys to ensure that the belt is kept in place. The flange arrangements can be configured in different ways depending on belt type, pulley manufacturing methods as well as design-related aspects.

- Front pulley with double flanges: By using two flanges on the front pulley a neater and less bulky rear pulley can be used. Standardized smaller pulleys with double flanges are available from the belt producers.
- Rear pulley with double flanges: Rear pulleys with two flanges tend to look heavy and bulky, additionally the manufacturing methods are more complex since one of the flanges must be fitted once the teeth have been machined.
- One flange on each pulley: Pulleys with one flange each can be more easily manufactured since they can be made from one pulley blank.
- Center track: Gates carbon drive can provide flange-less belts and pulleys that relay on a centre grove in the belt and a corresponding track in one or both pulleys. This system is compact and aesthetically pleasing. The system also has improved performance in muddy and dusty operating conditions and reduced sound emissions.

4.12.3.8 Noise and Frequency Calculations

Two main types of sound emissions are present in a belt drive system. Just as a roller chain final drive, the engagement between the toothed belt and the pulleys will cause a sound synchronous with the meshing frequency. Oscillations in the belt caused by harmonic span vibrations may also emit noise.

$$F = \frac{Z_1 \, N_1}{60} \, Hz \tag{4.67}$$

Z_1 = Number of teeth of the drive pulley
N_1 = Speed of drive pulley, rpm

According to [20] tooth meshing is generally the most significant contributor to sound emissions in a motorcycle belt drive. The meshing frequency was calculated using equation 4.67.

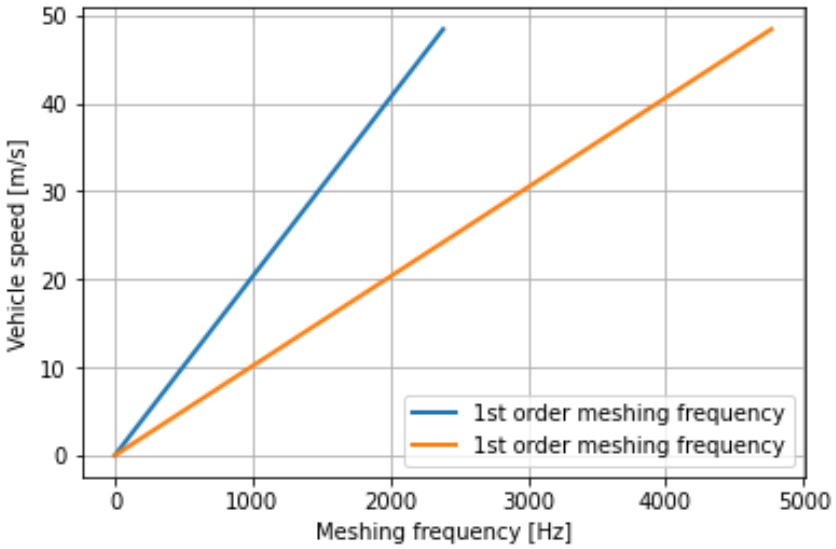

Figure 4.31: Meshing frequency

In figure 4.31 the first and second-order meshing frequency from standstill to 48 m/s can be seen. The first-order meshing frequency tends to be dominant. For a given speed ratio the meshing frequency can be changed by increasing or decreasing the diameter of both pulleys.

$$T = 4\,M\,W\,S^2\,f^2 \cdot 10^{-9}\;N \tag{4.68}$$

T =Belt span tension, N

M =Belt mass constant, g/m

W =Belt width, mm

S =Span length, mm

f= Natural frequency of the belt, Hz

The belt span tension for both the tight and slack sides of the belt was calculated using equation 4.68.

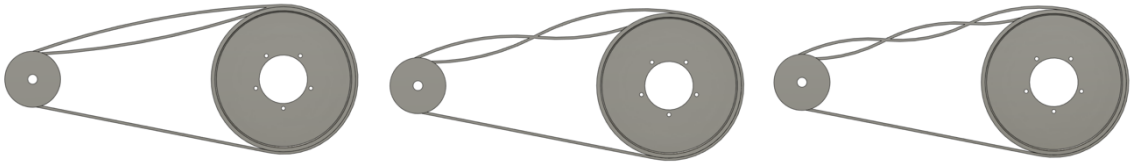

Figure 4.32: harmonics

Fundamental 1^{st} mode of span vibrations:

$$F = \sqrt{\frac{T}{4\,M\,W\,S^2 \cdot 10^{-9}}}\;Hz \tag{4.69}$$

2^{nd} harmonic of span vibration:

$$F = 2\sqrt{\frac{T}{4\,M\,W\,S^2 \cdot 10^{-9}}}\;Hz \tag{4.70}$$

3^{rd} harmonic of span vibration:

$$F = 3\sqrt{\frac{T}{4\,M\,W\,S^2 \cdot 10^{-9}}}\;Hz \tag{4.71}$$

4.12.4 Anti Squat and Swing Arm Pivot Location

With all the dimensions of the final drive known the location of the swing arm pivot that would give the best compromise in squat behaviour could be determined. The design target for anti-squat was set to be as close to 100% as possible throughout the suspension stroke. The software called Motorcycle Kinematic Setup was then used to determine the swing arm pivot location. All of the parameters used in the calculation setup can be seen in figure 4.33. A swing arm pivot height of 360 mm was found to be the best compromise giving an anti-squat percentage of 113% to 88% throughout the suspension travel of 135 mm. The resulting anti-squat percentage versus suspension travel can be seen in figure 4.34.

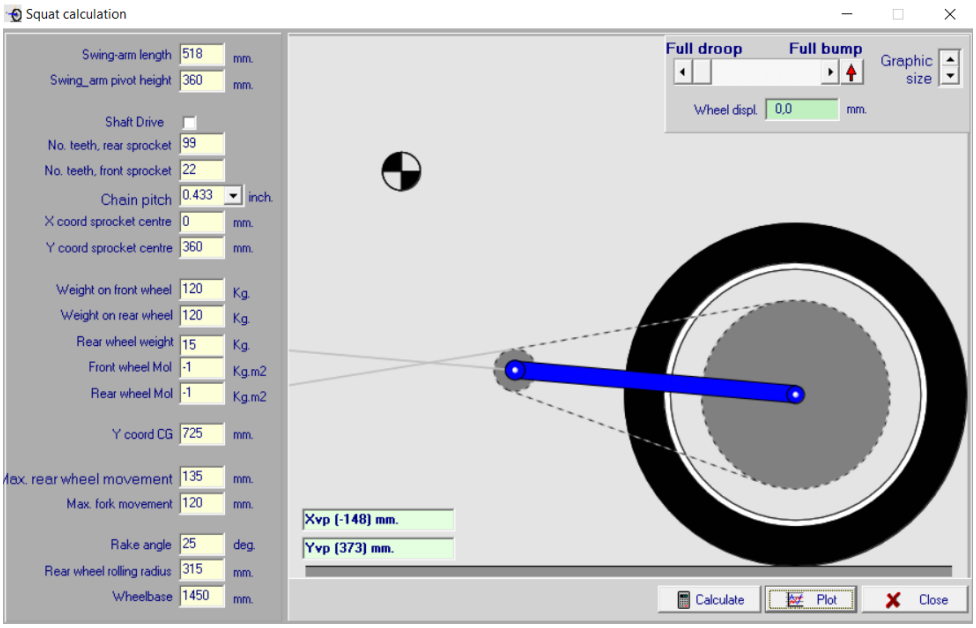

Figure 4.33: The setup used to find swing arm pivot height

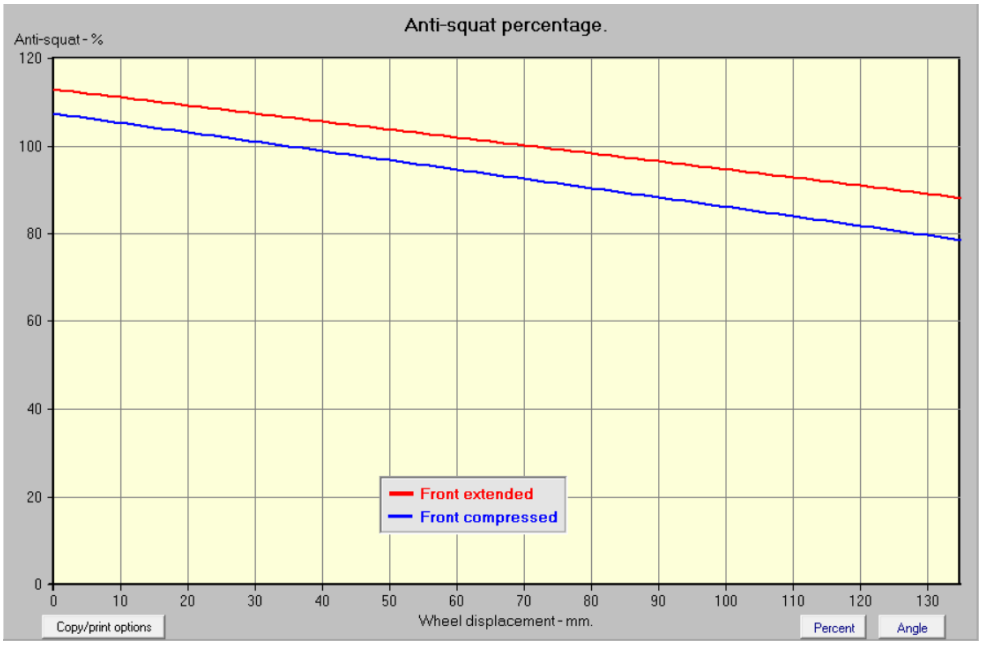

Figure 4.34: Resulting anti-squat percentage versus suspension travel

5
Final Concept and Initial Design

In this chapter, the final concept that was found to best fulfil the needs and requirements will be presented as well as the initial design work done on the final concept. Two alternative concepts that may be better suited depending on the choice of the motor will also be presented.

5.1 Final Concept

The final concept uses a PMSM axial flux motor mounted in the frame coaxially with the swing arm pivot and a synchronous belt is used as the final drive. The high torque density of a PMSM axial flux machine allows for a powertrain without a primary transmission which greatly reduces the overall complexity of the powertrain. By having the drive pulley co-axial with the swing arm pivot the difference in belt tension and anti-squat behaviour can be reduced, allowing for good handling and long belt life. A synchronous belt drive in this application allows for a speed ratio of up to 4.5:1, and the performance targets could be met with a motor torque of 215 Nm. The peak power of 80 kW that was found to be needed is also feasible since the torque density of the motor is the limitation. The efficient, silent operation and the relatively low cost of a belt drive make this transmission type well-suited for electric motorcycles.

In figure 5.1 the initial CAD model of the powertrain and swing arm can be seen. This cad model is still in an early conceptual stage and much design work is still required before prototypes and serial production can be considered.

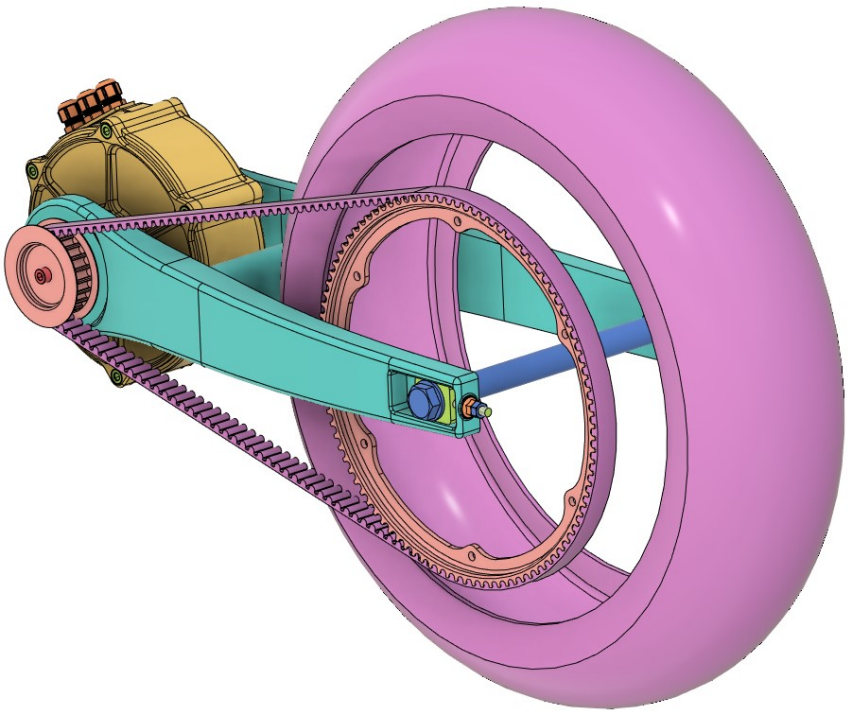

Figure 5.1: Motor, swing arm and final drive

5.2 Swing Arm and Final Drive

In figure 5.2 the swing arm, rear axle and drive belt system can be seen. Both sides of the swing arm are pivoting on deep groove ball bearings (other types of ball/roller bearings may also be used) that enable suspension movement with low resistance even with the high pretension and belt forces present in the system. The bearings also ensure a robust system with little deviation in pulley alignment over time.

Initially, a more conventional swing arm design with the drive pulley inside the swing arm was considered. This would have resulted in a significantly wider and more bulky design due to the width of the rear wheel, belt and belt to-tyre clearance. Additionally, much of the rear suspension would have to be disassembled to change the drive belt. The proposed design therefore allows the motor shaft and drive pulley to protrude through the swing arm bearing enabling easy access to the drive belt and a slimmer swing arm.

The swing arm pivot is located 360 mm above the ground with the suspension at full droop giving an anti-squat percentage as close to 100% as possible though out the suspension stroke.

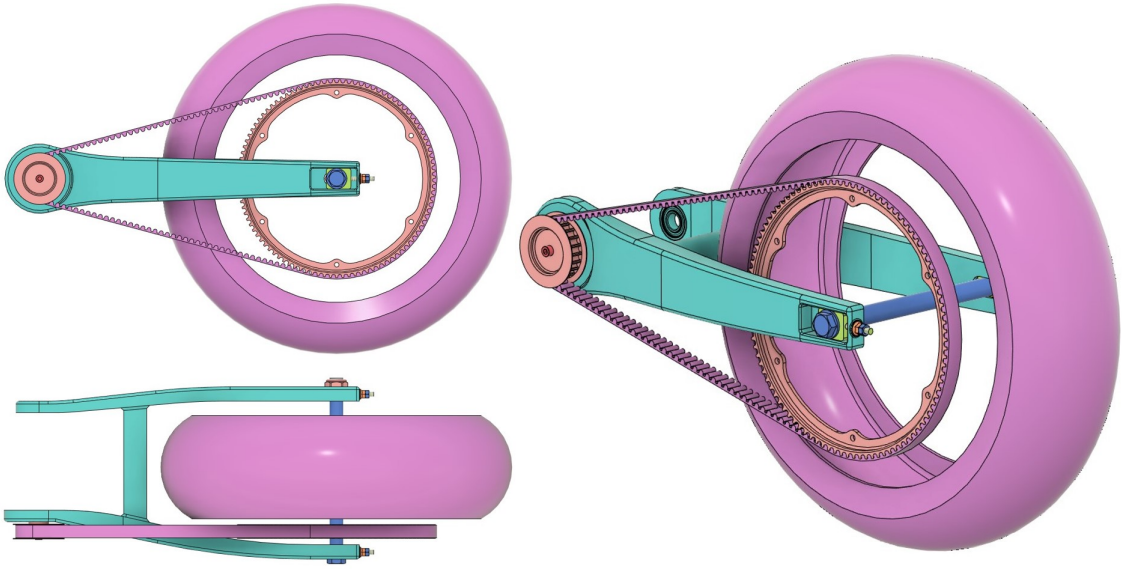

Figure 5.2: Swing arm and final drive

5.2.1 Belt Drive

The best flange options both from an aesthetical and mechanical perspective would be either the Gates Center track [20] or the configuration seen in figure 5.3. Having both of the flanges on the drive pulley reduces the manufacturing complexity of the driven pulley while the lack of flanges allows for a neater design. By using Gates Centre Track a system less sensitive to dust, mud and debris and with a slightly lower noise level could be expected.

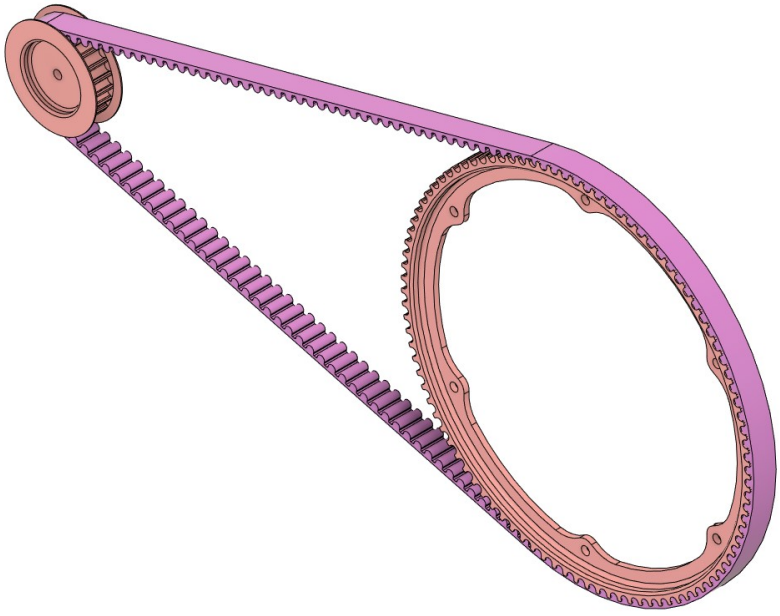

Figure 5.3: Final belt drive design

General specifications for the final belt drive system:

- Speed ratio: 4.5:1
- Drive pulley: 22 teeth, 77.03 mm pitch diameter
- Driven pulley: 99 teeth, 346.62 mm pitch diameter
- Belt: HTD profile, 11 mm Pitch, 22mm wide, 158 teeth.
- Nominal drive centre distance: 518.75 mm

The speed ratio of 4.5:1 used in this design was considered to be the highest speed ratio that could be used with the intended size of the rear wheel and belt pitch of 11 mm. The limiting factor is the rear pulley diameter as a result of the minimum allowed drive pulley diameter.

A smaller rear wheel pulley could be possible to use if an 8mm belt pitch is used instead of 11mm, this would however result in higher forces in the belt and worse resistance against ratcheting means that a wider belt must be used.

5.2.2 Belt tension and alignment

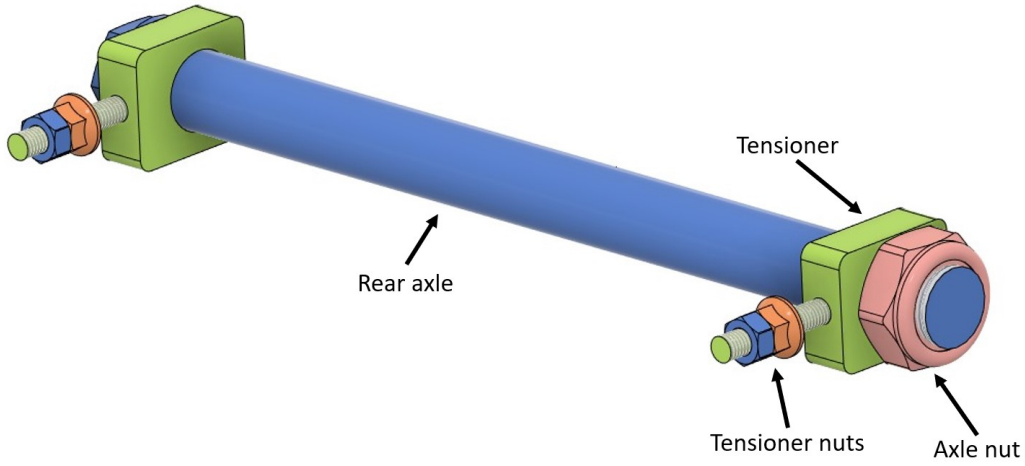

Figure 5.4: Rear axle and belt tension system

The most suitable belt tension system for the intended motorcycle with a double-sided swing arm was determined to be a rear axle with tensioner blocks. This rear axle and belt tension system can be seen in figure 5.4. The rear axle assembly can move in slots on the swing arm providing the required drive centre distance adjustment. The belt tension and angular alignment can be done by tightening or loosening the tension nuts.

Conventional ICE motorcycles with a chain drive traditionally use a similar arrangement but with adjustments screws in compression. Due to the high pretension required for a belt drive system, it was concluded that a design with adjustment screws in tension would be a better option. This will also make the adjustments nuts easier to access.

5.3 Alternative Concepts

Two other concepts that could be better suited for motors with less torque but higher maximum speeds are versions of the final concept using a primary reduction. These concepts might be options if a significantly cheaper motor and inverter combination could be sourced and/or higher production volumes are planned.

The preferred of the two uses a planetary gear set mounted co-axially with the motor shaft and swing arm pivot. This was found to be the best of the two because it would fit the overall packaging and off-the-shelf planetary gear sets are available. These would be relatively easy to integrate into a custom transmission housing. This concept makes for a compact package that could be mounted co-axially with the swing arm pivot.

In figure 5.5 a planetary reduction can be seen between the motor and swing arm. In this configuration the ring gear is held stationary, the sun gear is connected to the motor shaft and the output shaft (front pulley) is connected to the planet carrier.

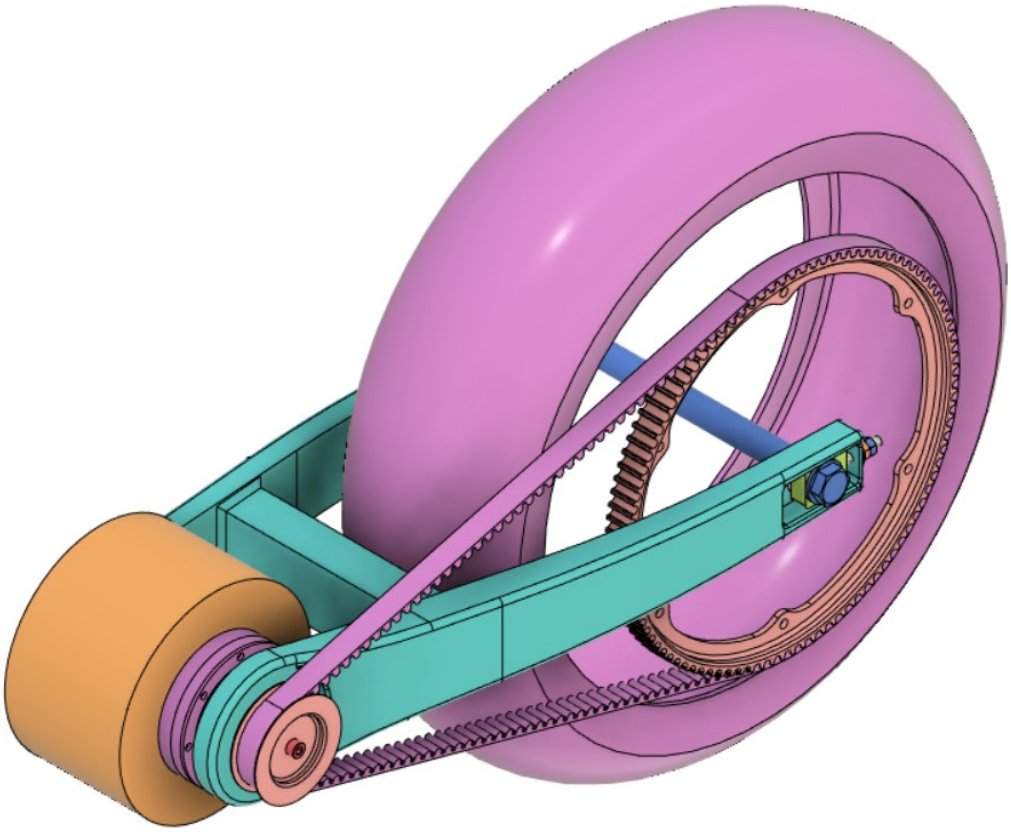

Figure 5.5: Planetary reduction

The last concept that uses spur gears as a primary transmission would be a good option if no motor could be found that will fit in the space between the swing arm bearings. By using spur gears the motor will be mounted with an offset to the output shaft allowing for a longer motor to be used. The drawback is the significantly higher complexity, cost and more design work. This concept would be a better option for larger production volumes.

In figure 5.6 the concept of using spur gears can be seen. By adding a third idler gear the distance between the input and output shafts can be increased without changing the overall speed ratio.

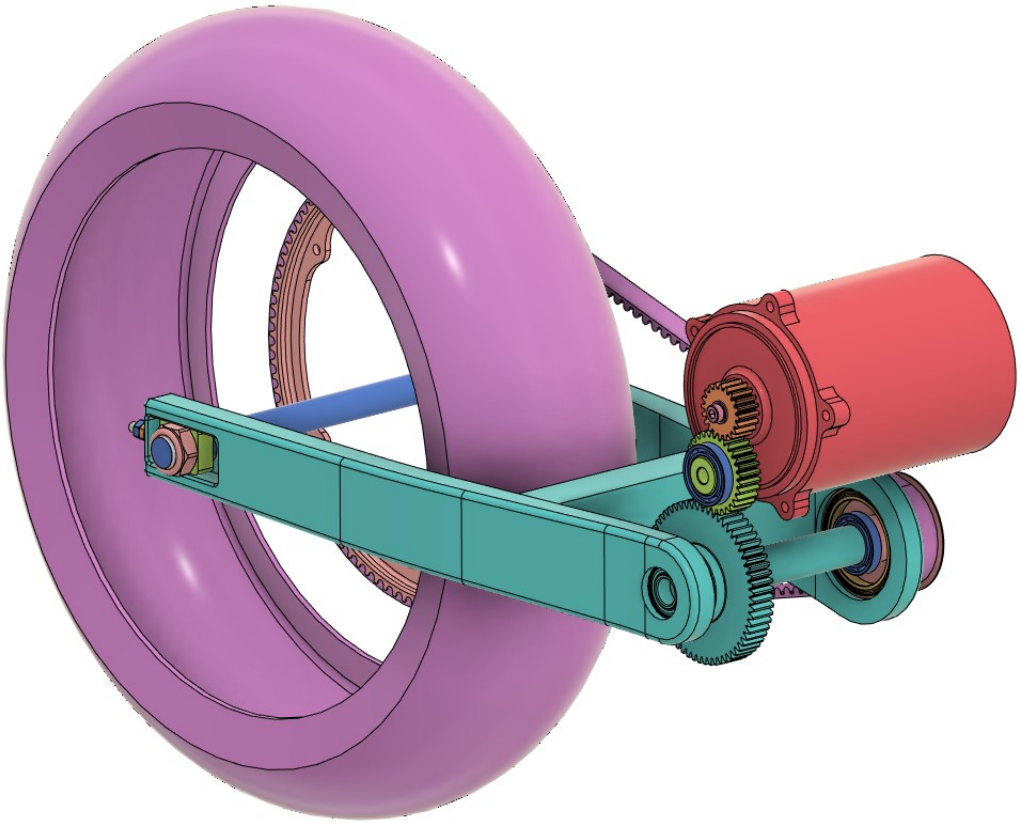

Figure 5.6: Spur gears with idler

6

Conclusions and Recommendations

In this chapter, the conclusions drawn from the results and ideas found during the project will be presented. Recommended further work will also be covered.

6.1 Performance Target

The acceleration and top-speed targets set at the beginning of the project are relatively high performance requirements especially when considering the allowed powertrain cost. Perhaps a better approach would be to optimize the performance based on a budget alternative and evaluate the resulting performance of the motorcycle.

The relation between top speed and acceleration performance could also be re-evaluated based on the intended end user and their riding style. More touring-focused models would need a higher top speed while urban motorcycles would benefit from more acceleration.

6.2 Motorcycle Dimensions

All of the motorcycle dimensions used in this project were set by using values found from existing motorcycles and guidelines found in the literature. This methodology was deemed adequate for the scope of this thesis focusing on the powertrain. For further development of the motorcycle setting the dimensions more thoroughly by using vehicle dynamics simulations and physical testing, is recommended.

6.3 Multistage Transmission

One alternative that would be interesting to evaluate further for higher production volumes would be to use a multistage transmission. This allows for smaller and cheaper motors and inverters to be used while maintaining good acceleration and top speed. Additionally, a multistage transmission in combination with a well-suited motor could improve the overall efficiency of the vehicle, allowing for better range or reduced battery capacity.

6.4 Motor and Inverter

Finding a motor and inverter combination that works well together and fits the overall package of the motorcycle requires a lot of research and supplier contacts. Continuing the work of finding a suitable motor is recommended since this largely determines the overall packaging of the motorcycle and the powertrain layout. Going for a standard or slightly modified existing motor rather than a clean sheet design is also recommended since the development cost for a new motor would be hard to cover with the planned production volumes.

6.5 Heat management and cooling

A well-designed cooling system can significantly affect the overall efficiency and performance of the powertrain. Especially battery heat management for markets with very high or very low ambient temperatures is challenging as well as motor and inverter cooling. CFD analysis would be the preferred way to ensure good heat management.

6.6 Mechanical Design

Continuing the work on the motorcycle by refining the final powertrain concept design is recommended as well as:

- Setting compliance and safety factor design targets that can be verified using structural analysis for stress and stiffness.
- The rear suspension and frame concepts will greatly affect the overall vehicle packaging as well as the aesthetics of the motorcycle. To continue the work by evaluating different rear suspension and frame designs.
- Using the battery container as a stressed member to increase frame stiffness and reduce the overall weight could be an interesting option to evaluate.

6.7 Prototype and Testing

Building a test motorcycle where different motor and inverter combinations could be tested is strongly recommended as well as testing different gear ratios and overall motorcycle dimensions. This would be the best way to evaluate noise emissions, performance, reliability and drivability of the powertrain concepts.

Bibliography

[1] Guzzella. L and Sciarretta.A, *Vehicle Propulsion Systems: Introduction to Modeling and Optimization*, ISBN: 978-3-642-35912-5, 2013

[2] Cossalter. V, *Motorcycle Dynamics*, ISBN: 978-1430308614, 2006

[3] The European Commission, *COMMISSION DELEGATED REGULATION (EU) No 134/2014*, 2013

[4] Jacobsson. B, *Vehicle Dynamics Compendium*, 2019

[5] Foyale.T, *Motorcycle Handling and Chassis Design*, ISBN: 9788493328610, 2005.

[6] Bradley. J, *The Racing Motorcycle*, ISBN: 9780951292952, 1996

[7] LiveWire, *Official Website*, URL: https://www.livewire.com

[8] Triumpth, *TE-1 Official Website*, URL: https://www.triumphmotorcycles.se/for-the-ride/brand/

[9] Gustafsson. G, Course material: PPU196/TME271 Produktutvecklingsprojekt, 2020

[10] Zero Motorcycles, *Official Website*, URL: https://zeromotorcycles.com/

[11] Energica, *Official Website*, URL: https://www.energicamotor.com/en/

[12] Factory, *Design for Manufacturing and Assembly*, URL: https://fractory.com/design-for-manufacturing-and-assembly-dfma/

[13] Six-sigma, *FMEA - Failure Mode and Effect Analysis*, URL: http://www.six-sigma.se/FMEA.html

[14] Mägi. M, Melkersson. K and Evertsson. M, *Maskinelement*, ISBN: 9789144109053, 2017

[15] Andersson. S, Dahlander. P, Hilmersson. M and Hedman. A, Course material: TME170 Powertrain Mechanics, 2022

[16] Tesla, *Tesla All Wheel Drive (Dual Motor) Power and Torque Specifications*, URL: https://www.tesla.com/blog/tesla-all-wheel-drive-dual-motor-power-and-torque-specificat

[17] Volvo, *Volvo Cars invests in designing and developing electric motors in-house*, URL: https://www.media.volvocars.com/global/en-gb/media/pressreleases/272958/volvo-cars-i

[18] Harley Davidson, *LIVEWIRE PARTS CATALOG: LIVEWIRE ONE™* , URL: https://www.livewire.com/resources

[19] SDP/SI, *HANDBOOK OF TIMING BELTS AND PULLYS*, URL: https://www.sdp-si.com/d265/pdf/d265t003.pdf

[20] Gates, *MOTORCYCLE & SCOOTER BELT DRIVE DESIGN GUIDE*, 2020

[21] Fuglede. N, Thomsen. J.J, *Kinematics of roller chain drives — Exact and approximate analysis*, URL: https://doi.org/10.1016/j.mechmachtheory.2016.01.009, 2016

[22] Ramsey Products Corporation, *Silent Chain Fundamentals*, URL: https://ramseychain.com/the-chain-doctor/silent-chain-basics/

[23] Ubydeal Transmission Solutions, *WHAT IS A BMW TRANSFER BOX – xDrive*, URL: https://cutietransfer.ro/en/articol/what-is-a-bmw-transfer-box-xdrive/
[24] National Geographic, *Noise Pollution*, URL: https://education.nationalgeographic.org/resource/noise-pollution/
[25] HP Wisard, *The Effects of Rotational Inertia on Automotive Acceleration*, URL: http://hpwizard.com/rotational-inertia.html
[26] Brock's Performance, *BST : The Effects of Inertia*, URL: https://blog.brocksperformance.com/bst-the-effects-of-inertia/
[27] Blissett. J, Degano. M, Gimeno-Fabra. M and Wheeler. P, *Design of Electrical System for Racing Electric Motorcycles*, 2016
[28] Optibelt, *TECHNICAL MANUAL optibelt DELTA Chain*, URL: https://www.optibelt.com/fileadmin/pdf/produkte/zahnriemen-pu/optibelt-DELTA-Chain-TM
[29] Guzzella. L, Amstutz. A, *The QSS-Toolbox Manual*, 2005
[30] Korobkov D.S, Ufimtseva O.V, *Choice of the Traction Motor for the Electric Racing Car "Formula Student"*, 2016
[31] Krajnik. P, Hashimoto. F, Karpuschewski. B, Jannone da Silva. E and Axinte. D, *Grinding and fine finishing of future automotive powertrain components*, 2021
[32] HUO ZHIMIN, YANG JIANFENG and HUANG JINXIANG, *Patent CN112455596A Transmission structure and electric motorcycle*, 2021
[33] LIN JUNFA, WU FANGZHEN, CHEN RONGYI, YE YUFAN and JIANG XINZHAN, *Patent CN213511940U Power transmission structure of electric motorcycle*, 2021

A

Vehicle Requirements

Requirement Specification						
ID	Criterion	Target	Priority 1=Requierment 2-5=Extras	Verification method	Stakeholder	Why?
Preformance						
1,1	Practical range	220-250 km @ 110km/h	1	Simulation/ calculation	RGNT R&D	Enable inter city travle
1,2	Top Speed	>180 km/h	3	Simulation/ calculation	RGNT R&D	Must be high enough to not feel as a low preformance bike
1,3	0-100km/h	<3.5 s	2	Simulation/ calculation	RGNT R&D	Most important preformance creterion for the end user
1,4	Capable of riding in the Alps (w/o passanger)	Continius riding at 100 km/h in 5.5° upphill and downhill gradients	2	Simulation/ calculation	RGNT R&D	Give reliability (not overheat) in all possible driving condistions
1,5	Continius cruising speed (w/o passanger)	140 km/h @ 30c ambient	1	Simulation/ calculation	RGNT R&D	Enable intercity tavel and is imorotant everyday riding performance
1,6	Power wheelie capable	0-72 km/h	4	Calculation	RGNT R&D	Good selling/marketing point
1,7	Regenerative braking tourqe rear wheel	325 Nm @ rear wheel, Calculated using script	2	Simulation/test/ design	RGNT Electrical R&D	Improve range and drivability, design requirement on negative tourqe
NVH & perceived quality						
2,1	Vibration level	Low	1	Engineering judgement	RGNT R&D	SP for electric motorcycle and RGNT brand
2,2	Noise	Low	1	Engineering judgement	RGNT R&D	SP for electric motorcycle and RGNT brand
2,3	Tier dimensions	180/55-17 (150-70-r18), RGTN input	1	-	RGNT R&D	Most common tyre size for A bikes
Vehicle dynamics and handling						
3,1	Percived mass	Normal	2	Simulation/test	RGNT R&D	Preformance and handling
3,2	Mass	<240kg	1	CAD/calculation-estimation	RGNT R&D	Preformance and handling
3,3	Wheelbase	1430-1460	1	CAD	RGNT R&D	Preformance and handling / packaging
3,4	weight distribution with 75 kg rider	50/50 front/rear	2	CAD/calculation-estimation	RGNT R&D	Preformance and handling
3,5	Combined Center of gravity height	<=50 % of Wheelbase	2	CAD/calculation-estimation	RGNT R&D	Handleing and precived weight
3,6	Seat hight	800 - 840 mm	2	CAD/calculation-estimation	RGNT R&D	Ergonomics and accesability form most riders
3,7	Unsprung mass	Low enough (find common values, try modeling)	3	CAD/calculation-estimation	RGNT R&D	Suspension quality and handling
3,8	Rear wheel Inertia	Low enough (find common values, try modeling)	3	CAD/calculation-estimation	RGNT R&D	Cornering and acceleration preformance
Battery and charging specifications						
5,1	Battery voltage	270v<nominal voltage<550v	1	Electrical design	RGNT Electrical R&D	Suitable current intervall in regards to the regulations/battery design and charing infrastructure
Manufacturing						
6.1	Cost of drivetrain	Classified	1	Supplier cost estimation	RGNT R&D	Classified
6,2	Complexity	Low (cost, DFMA, servisability)	2	Engineering judgement	RGNT R&D	To keep costs and assembly time low
6,3	Adaptability	Standard, Naked, sport-touring, scrambler(ligth adventure)	2	Engineering judgement	RGNT R&D	Possibility to adapt the powertrain to different categories of motorcycle
Reliability & maintenance						
7,1	Drive train service intervall	30k - 40k kilometer	3	Supplier data	RGNT R&D	SP for electric motorcycle and RGNT brand
7,2	Failure risk	Low	1	FMEA analys	RGNT R&D	Important for reliability and reputaion of brand
Lifecycle & sustainability						
8,1	Sustainable materials	Most components made of sustainable materials	3	Engineering judgement	RGNT R&D	Company goal of sustainable society
8,2	Recyclable	Most components made of recyclable materials	3	Engineering judgement	RGNT R&D	Company goal of sustainable society

B

Pre Study - Competing Models

General powertrain layouts and performance numbers for competing EV motorcycles													
Manufacturer	Model	Nominal voltage [V]	Battery capacity [kWh]	Motor type	Motor cooling	Power [kW]	Tourqe [Nm]	Primary transmission	Final drive	Total speed ratio	Top speed [km/h]	0-100 km/h time [s]	WMTC range [km]
Energica	Experia	306	Max: 22.5 Usable: 19.6	PM Assisted Synchronous Reluctance Motor (PMASynRM)	Water	Continuous: 60 @ 7000 rpm Peak: 75 @ 7500 rpm	Motor: 115 Wheel: 900	Helical gears	Chain	8:1	180	3.5	222
	Eva Ribelle RS	300	Max: 21.5 Usable: 18.9	Hybrid Synchronous Motor (HSM)	Water	Continuous: 110, Peak: 126 speed: 12.000 rpm	Motor: 222 Wheel: 1187	Helical gears	Chain	5.4:1	200	2.6	N/A
	Ego RS	300	Max: 21.5 Usable: 18.9	Hybrid Synchronous Motor (HSM)	Water	Continuous: 110, Peak: 126 speed: 12.000 rpm	Motor: 222 Wheel: 1187	Helical gears	Chain	5.4:1	240	2.6	N/A
LiveWire	ONE s1	254	Max: 15.5 Usable: 13.6	PMSM radial flux	Water	75 @10500 rpm, max speed 15000rpm	Motor: 117	Bevel gears	Belt	9.72:1	180	3.0	158
	DEL MAR s2		Max: 10.5	PMSM radial flux	Water	60	Motor: 250	Direct drive	Belt	N/A	180	3.1	N/A
Zero	SR	N/A	Max: 15.6 Usable: 13.7	PMSM radial flux	Air	52 @ 6255rpm	Motor: 166	Direct drive	Belt	4.5:1	167	N/A	183
	SR/F	N/A	Max: 17.3 Usable: 15.2	PMSM radial flux	Air	82 @ 5600 rpm	Motor: 190	Direct drive	Belt	4.5:1	200	N/A	183
	SR/S	N/A	Max: 17.3 Usable: 15.2	PMSM radial flux	Air	82 @ 5600 rpm	Motor: 190	Direct drive	Belt	4.5:1	200	N/A	180
	DSR	N/A	Max: 14.4 Usable: 12.6	PMSM radial flux	Air	52 @ 3500 rpm	Motor: 157	Direct drive	Belt	4.5:1	163	N/A	171
	DSR/X	N/A	Max: 17.3 Usable: 15.2	PMSM radial flux	Air	75 @3650 rpm	Motor: 225	Direct drive	Belt	4.01:1	180	N/A	172
	S	N/A	Max: 7.2 Usable: 6.3	PMSM radial flux	Air	34 @ 4300 rpm	Motor: 106	Direct drive	Belt	5:1	158	N/A	200
	FXE	N/A	Max: 7.2 Usable: 6.3	PMSM radial flux	Air	34 @ 4300 rpm	Motor: 106	Direct drive	Belt	5:1	137	N/A	106
Triumph	TE-1	360	15.0	PMSM radial flux	Water	130	Motor: 109	Helical gears	Belt	N/A	220	3.6	N/A
Verge	TS Ultra	N/A	21.8	PMSM radial flux	Air	150	Wheel: 1200	Hub motor	None	None	200	2.5	N/A
KTM	Freeride E-XC	260	3.9	PMSM axial flux	Water	Continious: 9 @4500 rpm Peak:18	Motor: 42	Spur gear	Chain	10.47:1	56	N/A	N/A
Stark	Varg	360	6.0	PMSM radial flux	Water	60	Wheel: 938	Gear train	Chain	11.19:1	N/A	N/A	N/A
SAVIC	Alpha	140	16.2	PMSM radial flux	Water	60	Motor: 200	Direct drive	Belt	4:1	N/A	3.5	N/A
	Delta	140	16.2	PMSM radial flux	Water	40	Motor: 140	Direct drive	Belt	4:1	N/A	4.5	N/A
BMW	CE04	148	8.9	PMSM radial flux	Water	31	Motor: 62	Helical gears	Belt	N/A	120	9.1	130
Damon	Hypersport	450	20	PMSM radial flux	Oil	Peak: 150 Max speed 15000 rpm	Motor: 235	Helical gears	Chain	N/A	322	3.0	N/A

B.1 Pre-study - belt drive layouts

Belt drive specifications for compeeting modells										
Manufacturer	Modell	Belt manufacturer	Belt model	Pitch [mm]	Width [mm]	Belt tooths	Pulley tooth count [Z2/Z1]	Speed ratio	Tensioning system	Flange arrangement
LiveWire	ONE S1	Gates Carbon Drive	Poly Chain® HTD® MOTO X9 Carbon™	11	25.4	174	84/28	3:1	fixed adjustable idler pulley	Drive pulley: 0 flanges Driven pulley: 1 flange Inside idler: 2 flanges Outside idler: 0 flanges
	DEL MAR S2	Gates Carbon Drive	Poly Chain® HTD® MOTO X9 Carbon™	11	22	N/A	84/(N/A)	N/A	rear axle	Drive pulley: 1 flange Driven pulley: 1 flange
ZERO	FXE	Gates Carbon Drive	Poly Chain® HTD® MOTO X9 Carbon™	11	17	158	90/18	5:1	rear axle	Drive pulley: 2 flanges Driven pulley: 1 flange
	s	Gates Carbon Drive	Poly Chain® HTD® MOTO X9 Carbon™	11	17	158	90/18	5:1	rear axle	Drive pulley: 2 flanges Driven pulley: 1 flange
	SR	Gates Carbon Drive	Poly Chain® HTD® MOTO X9 Carbon™	11	20	151	90/20	4.5:1	rear axle	Drive pulley: 2 flanges Driven pulley: 1 flange
	SR/F	Gates Carbon Drive	Poly Chain® HTD® MOTO X9 Carbon™	11	20	151	90/20	4.5:1	rear axle	Drive pulley: 2 flanges Driven pulley: 1 flange
	SR/S	Gates Carbon Drive	Poly Chain® HTD® MOTO X9 Carbon™	11	20	151	90/20	4.5:1	rear axle	Drive pulley: 2 flanges Driven pulley: 1 flange
	DSR	Gates Carbon Drive	Poly Chain® HTD® MOTO X9 Carbon™	11	17	158	90/20	4.5:1	rear axle	Drive pulley: 2 flanges Driven pulley: 1 flange
	DSR/X	Gates Carbon Drive	Poly Chain® HTD® MOTO X9 Carbon™	11	20	151	90/22	4.01:1	rear axle	Drive pulley: 2 flanges Driven pulley: 1 flange
SAVIC	Alpha	Optibelt	DELTA CHAIN 8MDC	8	36	N/A	N/A	4:1	cam adjustment, single sided swing arm	Drive pulley: 2 flanges Driven pulley: 1 flange
	Delta	Optibelt	DELTA CHAIN 8MDC	8	36	N/A	N/A	4:1	cam adjustment, single sided swing arm	Drive pulley: 2 flanges Driven pulley: 1 flange
BMW	CE04	Dayco	HT POWER PLUS	8	40	N/A	85/28	3.04:1	cam adjustment, single sided swing arm	Drive pulley: 2 flanges Driven pulley: 0 flanges
Triumph	TE-1	Gates Carbon Drive	Poly Chain® HTD® MOTO X9 Carbon™	11	N/A	N/A	N/A	N/A	cam adjustment, single sided swing arm	Centre track

C

Concept generation

C.1 Morphological matrix hub motors

Concept 1	
Motor type	PMSM radial flux
Motor placement	Wheel hub
Primary transmission	Direct drive
Secondary transmission	N/A

Concept 2	
Motor type	PMSM axial flux
Motor placement	Wheel hub
Primary transmission	Direct drive
Secondary transmission	N/A

Concept 3	
Motor type	Reluctance
Motor placement	Wheel hub
Primary transmission	Direct drive
Secondary transmission	N/A

C.2 Morphological matrix drive shaft

Concept 4	
Motor type	PMSM radial flux
Motor placement	Inboard
Primary transmission	Direct drive
Secondary transmission	Bevel

Concept 11	
Motor type	PMSM axial flux
Motor placement	Inboard
Primary transmission	Direct drive
Secondary transmission	Bevel

Concept 18	
Motor type	Reluctance
Motor placement	Inboard
Primary transmission	Direct drive
Secondary transmission	Bevel

Concept 5	
Motor type	PMSM radial flux
Motor placement	inboard
Primary transmission	Spur gear
Secondary transmission	Bevel

Concept 12	
Motor type	PMSM axial flux
Motor placement	Inboard
Primary transmission	Spur gear
Secondary transmission	Bevel

Concept 19	
Motor type	Reluctance
Motor placement	Inboard
Primary transmission	Spur gear
Secondary transmission	Bevel

Concept 6	
Motor type	PMSM radial flux
Motor placement	Inboard
Primary transmission	Planetary gear
Secondary transmission	Bevel

Concept 13	
Motor type	PMSM axial flux
Motor placement	inboard
Primary transmission	Planetary gear
Secondary transmission	Bevel

Concept 20	
Motor type	Reluctance
Motor placement	Inboard
Primary transmission	Planetary gear
Secondary transmission	Bevel

Concept 7	
Motor type	PMSM radial flux
Motor placement	Inboard
Primary transmission	Multi stage
Secondary transmission	Bevel

Concept 14	
Motor type	PMSM axial flux
Motor placement	Inboard
Primary transmission	Multi stage
Secondary transmission	Bevel

Concept 21	
Motor type	Reluctance
Motor placement	Inboard
Primary transmission	Multi stage
Secondary transmission	Bevel

Concept 8	
Motor type	PMSM radial flux
Motor placement	Inboard
Primary transmission	N/A
Secondary transmission	Bevel

Concept 15	
Motor type	PMSM axial flux
Motor placement	Inboard
Primary transmission	N/A
Secondary transmission	Bevel

Concept 22	
Motor type	Reluctance
Motor placement	Inboard
Primary transmission	N/A
Secondary transmission	Bevel

Concept 9	
Motor type	PMSM radial flux
Motor placement	inboard
Primary transmission	Belt
Secondary transmission	Bevel

Concept 16	
Motor type	PMSM axial flux
Motor placement	Inboard
Primary transmission	Belt
Secondary transmission	Bevel

Concept 23	
Motor type	Reluctance
Motor placement	Inboard
Primary transmission	Belt
Secondary transmission	Bevel

Concept 10	
Motor type	PMSM radial flux
Motor placement	Inboard
Primary transmission	Chain
Secondary transmission	Bevel

Concept 17	
Motor type	PMSM axial flux
Motor placement	inboard
Primary transmission	Chain
Secondary transmission	Bevel

Concept 24	
Motor type	Reluctance
Motor placement	Inboard
Primary transmission	Chain
Secondary transmission	Bevel

C.3 Morphological matrix tooth belt

Concept 25	
Motor type	PMSM radial flux
Motor placement	Inboard
Primary transmission	Direct drive
Secondary transmission	Tooth belt

Concept 32	
Motor type	PMSM axial flux
Motor placement	Inboard
Primary transmission	Direct drive
Secondary transmission	Tooth belt

Concept 39	
Motor type	Reluctance
Motor placement	inboard
Primary transmission	Direct drive
Secondary transmission	Tooth belt

Concept 26	
Motor type	PMSM radial flux
Motor placement	Inboard
Primary transmission	Spur gear
Secondary transmission	Tooth belt

Concept 33	
Motor type	PMSM axial flux
Motor placement	Inboard
Primary transmission	Spur gear
Secondary transmission	Tooth belt

Concept 40	
Motor type	Reluctance
Motor placement	Inboard
Primary transmission	Spur gear
Secondary transmission	Tooth belt

Concept 27	
Motor type	PMSM radial flux
Motor placement	Inboard
Primary transmission	Planetary gear
Secondary transmission	Tooth belt

Concept 34	
Motor type	PMSM axial flux
Motor placement	inboard
Primary transmission	Planetary gear
Secondary transmission	Tooth belt

Concept 41	
Motor type	Reluctance
Motor placement	Inboard
Primary transmission	Planetary gear
Secondary transmission	Tooth belt

Concept 28	
Motor type	PMSM radial flux
Motor placement	Inboard
Primary transmission	Multi stage
Secondary transmission	Tooth belt

Concept 35	
Motor type	PMSM axial flux
Motor placement	inboard
Primary transmission	Multi stage
Secondary transmission	Tooth belt

Concept 42	
Motor type	Reluctance
Motor placement	Inboard
Primary transmission	Multi stage
Secondary transmission	Tooth belt

Concept 29	
Motor type	PMSM radial flux
Motor placement	Inboard
Primary transmission	N/A
Secondary transmission	Tooth belt

Concept 36	
Motor type	PMSM axial flux
Motor placement	Inboard
Primary transmission	N/A
Secondary transmission	Tooth belt

Concept 43	
Motor type	Reluctance
Motor placement	Inboard
Primary transmission	N/A
Secondary transmission	Tooth belt

Concept 30	
Motor type	PMSM radial flux
Motor placement	Inboard
Primary transmission	Belt
Secondary transmission	Tooth belt

Concept 37	
Motor type	PMSM axial flux
Motor placement	Inboard
Primary transmission	Belt
Secondary transmission	Tooth belt

Concept 44	
Motor type	Reluctance
Motor placement	Inboard
Primary transmission	Belt
Secondary transmission	Tooth belt

Concept 31	
Motor type	PMSM radial flux
Motor placement	Inboard
Primary transmission	Chain
Secondary transmission	Tooth belt

Concept 38	
Motor type	PMSM axial flux
Motor placement	Inboard
Primary transmission	Chain
Secondary transmission	Tooth belt

Concept 45	
Motor type	Reluctance
Motor placement	Inboard
Primary transmission	Chain
Secondary transmission	Tooth belt

C.4 Morphological matrix chain

Concept 46	
Motor type	PMSM radial flux
Motor placement	Inboard
Primary transmission	Direct drive
Secondary transmission	Chain

Concept 47	
Motor type	PMSM radial flux
Motor placement	Inboard
Primary transmission	Spur gear
Secondary transmission	Chain

Concept 48	
Motor type	PMSM radial flux
Motor placement	Inboard
Primary transmission	Planetary gear
Secondary transmission	Chain

Concept 49	
Motor type	PMSM radial flux
Motor placement	Inboard
Primary transmission	Multi stage
Secondary transmission	Chain

Concept 50	
Motor type	PMSM radial flux
Motor placement	Inboard
Primary transmission	N/A
Secondary transmission	Chain

Concept 51	
Motor type	PMSM radial flux
Motor placement	Inboard
Primary transmission	Belt
Secondary transmission	Chain

Concept 52	
Motor type	PMSM radial flux
Motor placement	Inboard
Primary transmission	Chain
Secondary transmission	Chain

Concept 53	
Motor type	PMSM axial flux
Motor placement	Inboard
Primary transmission	Direct drive
Secondary transmission	Chain

Concept 54	
Motor type	PMSM axial flux
Motor placement	Inboard
Primary transmission	Spur gear
Secondary transmission	Chain

Concept 55	
Motor type	PMSM axial flux
Motor placement	Inboard
Primary transmission	Planetary gear
Secondary transmission	Chain

Concept 56	
Motor type	PMSM axial flux
Motor placement	inboard
Primary transmission	Multi stage
Secondary transmission	Chain

Concept 57	
Motor type	PMSM axial flux
Motor placement	Inboard
Primary transmission	N/A
Secondary transmission	Chain

Concept 58	
Motor type	PMSM axial flux
Motor placement	Inboard
Primary transmission	Belt
Secondary transmission	Chain

Concept 59	
Motor type	PMSM axial flux
Motor placement	Inboard
Primary transmission	Chain
Secondary transmission	Chain

Concept 60	
Motor type	Reluctance
Motor placement	inboard
Primary transmission	Direct drive
Secondary transmission	Chain

Concept 61	
Motor type	Reluctance
Motor placement	Inboard
Primary transmission	Spur gear
Secondary transmission	Chain

Concept 62	
Motor type	Reluctance
Motor placement	Inboard
Primary transmission	Planetary gear
Secondary transmission	Chain

Concept 63	
Motor type	Reluctance
Motor placement	Inboard
Primary transmission	Multi stage
Secondary transmission	Chain

Concept 64	
Motor type	Reluctance
Motor placement	Inboard
Primary transmission	N/A
Secondary transmission	Chain

Concept 65	
Motor type	Reluctance
Motor placement	Inboard
Primary transmission	Belt
Secondary transmission	Chain

Concept 66	
Motor type	Reluctance
Motor placement	Inboard
Primary transmission	Chain
Secondary transmission	Chain

D

Primary transmission complexity analysis

D.1 Spur gear transmission complexity

Spur gear transmission complexity					
N_p		N_op	N_c		complexity number
Drive gear	1	8	drive gear - drive gear bearings	2	9,78
Drive gear bearings	2		drive gear bearings - gearbox housing	2	
Driven gear	1		drive gear - driven gear	1	
Driven gear bearings	1		driven gear - driven gear bearings	2	
Geabox housing	1		driven gear bearings - gearbox housing	2	
Output seal	1		driven gear bearings - output seal	1	
Fill plug with breather	1		output seal - gearbox housing	1	
Drain plug	1		fill plug with breater - gearbox housing	1	
N_p sum	9		drain plug - gearbox housing	1	
			N_c sum	13	

D.2 Planetary transmission complexity analysis

Planetary transmission complexity					
N_p		N_op	N_c		complexity number
Sun gear	1	12	input shaft - sun gear	1	22,58
Planet gears	3		sun gear - planet gears	3	
Ring gear	1		planet gears - ring gear	3	
Planet carrier	1		ring gear - gearbox housing	1	
Gearbox housing	1		planet carrier - planet carrier bearings	2	
Pin shafts	3		planet carrier beaings - gearbox housing	2	
Thrust bearings	6		planet carrier - pin shafts	6	
Planet bearings	3		planet carrier - thrust bearings	6	
planet carrier bearings	2		thrust bearings - planet gears	6	
Drain plug	1		pin shafts - planet bearings	3	
Fill plug with breather	1		planet bearings - planet gears	3	
output seal	1		gearbox housing - drain plug	1	
N_p sum	24		gearbox housing - fill plug breather	1	
			gearbox housing - output seal	1	
			output seal - planet carrier	1	
			N_c sum	40	

D.3 tooth belt transmission complexity analysis

tooth belt complexity					
N_p		N_op	N_c		complexity number
Drive pulley	1	7	drive pulley - drive pulley bearings	2	9,11
Drive pulley bearings	2		drive pulley bearings - transmission housing	2	
Driven pulley	1		drive pulley - belt	1	
Driven pulley bearings	2		belt - driven pulley	1	
Belt	1		diven pulley - driven pulley bearings	2	
Idler tensioner	1		driven pulley bearings - transmission housing	2	
transmission housing	1		idler tensioner - belt	1	
N_p sum	9		idler tensioner - transmission housing	1	
			N_c sum	12	

D.4 Silent chain transmission complexity analysis

Silent chain transmission complexity					
N_p		N_op	N_c		complexity number
Drive sprocket	1	11	drive sprocket - drive sprocket bearings	2	13,70
Drive sprocket bearings	2		drive sprocket bearings - transmission housing	2	
Chain	1		drive sprocket - chain	1	
Driven sprocket	1		chain - driven sprocket	1	
Driven sprocket bearings	2		driven sprocket - driven sprocket bearings	2	
Guide rail	1		driven sprocket bearings - transmission housing	2	
Tensioner	1		chain - guide rail	1	
Transmission housing	1		guide rail - transmission housing	1	
Drain plug	1		guide rail - tensioner	1	
Fill plug with breather	1		tensioner - transmission housing	1	
output seal	1		transmission housing - output seal	1	
N_p sum	13		output seal - driven sprocket	1	
			fill plug with breather - transmission housing	1	
			drain plug - transmission housing	1	
			N_c sum	18	

E

Final drive complexity analysis

E.1 Driveshaft complexity analysis

Drive shaft complexity					
N_p		N_op	N_c		complexity number
Housing/swing arm	1	18	output shaft - front uv joint	1	20,72
front uv-joint	1		front uv-joint - front drive shaft	1	
front driveshaft	1		front driveshaft - rear driveshaft	1	
rear driveshaft	1		rear driveshaft - rear uv joint	1	
rear uv-joint	1		housing - pinion gasket - pinion gear	2	
pinion gasket	1		housing - pinion - bearings - spacer -shim	8	
pinion gear	1		pinion gear - crown gear	1	
pinion shim	1		housing - crown gear - bearings - shim - crown gear housing	5	
pinion bearings	2		housing - crown gear housing	1	
pinion bearing spacer	1		crown gear - crown gear gasket - crown gear housing	2	
crown gear	1		housing - fill plug	1	
outer crown gear bearing	1		housing - level plug	1	
inner crown gear bearing	1		crown gear - rim	1	
crown gear shim	1		N_c sum	26	
crown gear housing	1				
crown gear gasket	1				
fill plug	1				
level plug	1				
N_p sum	19				

E.2 Tooth belt complexity analysis

Belt drive complexity					
N_p		N_op	N_c		Complexity number
Front pully	1	4	output shaft -Front pully	1	4,58
Rear pully	1		front pully - belt	1	
Belt	1		belt - rear pully	1	
Tensioner	1		rear pully - rim	1	
N_p sum	4		tensioner - frame/swing	1	
			tensioner - belt	1	
			N_c sum	6	

E.3 Roller chain complexity analysis

chain complexity					
N_p		N_op	N_c		complexity number
front sprcket	1	5	output shaft - front sprocket	1	5,85
chain	1		front sprocket - chain	1	
rear sprocket	1		chain - rear sprocket	1	
tesnioner	2		rear sprocket - rim	1	
N_p sum	5		tesioners - swing	4	
			N_c sum	8	

E.4 Hub motor complexity analysis

Hub motor complexity					
N_p		N_op	N_c		Complexity number
motor	1	1	Motor-swing	2	1,44
			Motor-rim	1	
			N_c sum	3	

F

Elimination

F.1 Initial Elimination Matrix

RGNT	Elimination matrix						
Concept	Eliminating criterion						Decition
	Preformance	NVH & perceived quality	Vehicle dynamics and handling	Manufacturing	Reliability & maintenance	Lifecycle & sustainability	
1							Keep
2							Keep
3	Power/torque density						Discard
4				Complexity/manufacturing cost			Discard
5				Complexity/manufacturing cost			Discard
6				Complexity/manufacturing cost			Discard
7				Complexity/manufacturing cost			Discard
8				Complexity/manufacturing cost			Discard
9				Complexity/manufacturing cost			Discard
10				Complexity/manufacturing cost			Discard
11				Complexity/manufacturing cost			Discard
12				Complexity/manufacturing cost			Discard
13				Complexity/manufacturing cost			Discard
14				Complexity/manufacturing cost			Discard
15				Complexity/manufacturing cost			Discard
16				Complexity/manufacturing cost			Discard
17				Complexity/manufacturing cost			Discard
18	Power/torque density						Discard
19	Power/torque density						Discard
20	Power/torque density						Discard
21	Power/torque density						Discard
22	Power/torque density						Discard
23	Power/torque density						Discard
24	Power/torque density						Discard
25							Keep
26							Keep
27							Keep
28				Complexity/manufacturing cost			Discard
29	Similar to concept 25						Discard
30							Keep
31							Keep
32							Keep
33							Keep

F.2 Initial Elimination Matrix

RGNT	Elimination matrix						
Concept	Eliminating criterion						Decition
	Preformance	NVH & perceived quality	Vehicle dynamics and handling	Manufacturing	Reliability & maintenance	Lifecycle & sustainability	
34							Keep
35				Complexity/manufacturing cost			Discard
36	Similar to concept 32						Discard
37							Keep
38							Keep
39	Power/torque density						Discard
40	Power/torque density						Discard
41	Power/torque density						Discard
42	Power/torque density						Discard
43	Power/torque density						Discard
44	Power/torque density						Discard
45	Power/torque density						Discard
46		Chain noise/maintenance					Discard
47		Chain noise/maintenance					Discard
48		Chain noise/maintenance					Discard
49		Chain noise/maintenance					Discard
50		Chain noise/maintenance					Discard
51		Chain noise/maintenance					Discard
52		Chain noise/maintenance					Discard
53		Chain noise/maintenance					Discard
54		Chain noise/maintenance					Discard
55		Chain noise/maintenance					Discard
56		Chain noise/maintenance					Discard
57		Chain noise/maintenance					Discard
58		Chain noise/maintenance					Discard
59		Chain noise/maintenance					Discard
60	Power/torque density						Discard
61	Power/torque density						Discard
62	Power/torque density						Discard
63	Power/torque density						Discard
64	Power/torque density						Discard
65	Power/torque density						Discard
66	Power/torque density						Discard

RGNT	Weights							
0 = Less important 0,5 = equaly imporntant 1 = more important	Performance	NVH & Perceived Quality	VD & Handeling	Manufacturing	Reliability & Maintenance	Lifcycle & Sustainability	Sum	Relative Sum (weigth)
Performance		1	1	0,5	0,5	1	4	0,27
NVH & Perceived Quality	0		0,5	0,5	0,5	1	2,5	0,17
VD & Handeling	0	0,5		0,5	0,5	1	2,5	0,17
Manufacturing	0,5	0,5	0,5		0,5	1	3	0,20
Reliability & Maintenance	0,5	0,5	0,5	0,5		1	3	0,20
Lifcycle & Sustainability	0	0	0	0	0		0	0,00

RGNT	Kesselring matrix																									
	Solution alternative																									
Criterion	Weight	Ideal		1		2		25		26		27		30		31		32		33		34		37		38	
		v	t	v	t	v	t	v	t	v	t	v	t	v	t	v	t	v	t	v	t	v	t	v	t	v	t
Preformance	0,27	5	1,35	2	0,5	2	0,5	3	0,8	5	1,4	5	1,4	5	1,4	4	1,1	4,5	1,2	4	1,1	4	1,1	5	1,4	3	0,8
NVH & perceived quality	0,17	5	0,85	4,5	0,8	5	0,9	4,5	0,8	4	0,7	4	0,7	3	0,5	3	0,5	4,5	0,8	4	0,7	4	0,7	3	0,5	3	0,5
Vehicle dynamics and handling	0,17	5	0,85	4	0,7	2	0,3	3	0,5	5	0,9	5	0,9	5	0,9	4	0,7	4,5	0,8	4,5	0,8	4	0,7	5	0,9	4	0,7
Manufacturing	0,2	5	1	5	1	5	1	4	0,8	3	0,6	4	0,8	2	0,4	2	0,4	5	1	3	0,6	4	0,8	2	0,4	2	0,4
Reliability & maintenance	0,2	5	1	5	1	5	1	4	0,8	4	0,8	4	0,8	3	0,6	3	0,6	5	1	4	0,8	4	0,8	3	0,6	3	0,6
Lifecycle & sustainability	0	5	0	5	0	5	0	5	0	5	0	5	0	5	0	5	0	5	0	5	0	5	0	5	0	5	0
Total		5,05		3,985		3,73		3,685		4,28		4,48		3,71		3,27		4,745		3,925		4,04		3,71		3	
rank				5		7		9		3		2		8		10		1		6		4		8		11	
Decition				Discard		Discard		Discard		Keep		Keep		Discard		Discard		Keep		Discard		Discard		Discard		Discard	

DEPARTMENT OF INDUSTRIAL AND MATERIAL SCIENCE
CHALMERS UNIVERSITY OF TECHNOLOGY
Gothenburg, Sweden
www.chalmers.se

CHALMERS
UNIVERSITY OF TECHNOLOGY